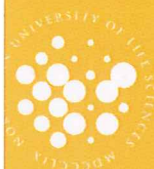


ACUTE TOXICITY EFFECT OF AMINES IN A NITRIFYING PROCESS

CAMILLA MARIA ORMSET

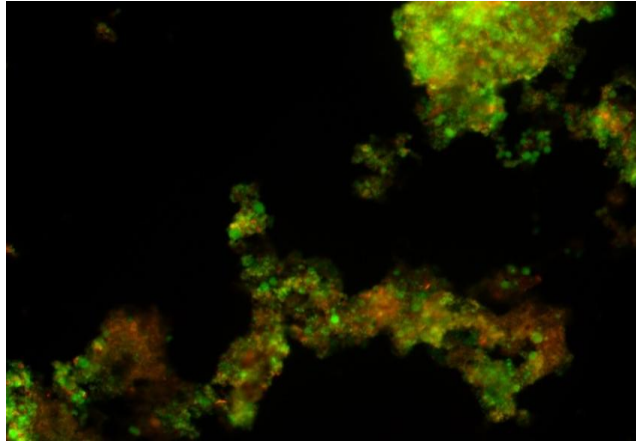
NORWEGIAN UNIVERSITY OF LIFE SCIENCES
DEPARTMENT OF CHEMISTRY AND BIOTECHNOLOGY
MASTER THESIS 30 CREDITS 2012



Acute toxicity effect of amines in a nitrifying process

Master thesis

Camilla Maria Ormset



Supervisors:

Ingrid Hauser

Prof. Kjetill Østgaard

Prof. Francisco J. Cervantes

Prof. Hallvard F. Svendsen

Prof. Roland Kallenborn

 **NTNU**
Norwegian University of
Science and Technology



Department of Biotechnology
Norwegian University for Science and Technology
Institute of Environmental Biotechnology
University of Life Sciences

Ås, May 2012

Declaration

I declare that I have authored this thesis independently, that I have not used other than the declared sources/resources, and that I have explicitly marked all material which has been quoted by content from the used sources.

Oslo, 05.14.2012

Camilla Maria Ormset

Acknowledgment

First of all, I would like to thank my supervisors at the Norwegian University for Science and Technology (NTNU) Professor Kjetill Østgaard, Professor Francisco J. Cervantes and Professor Hallvard F. Svendsen for giving me the opportunity to work on this project, and for their supportive guidance throughout this work. I am so grateful to PhD Ingrid Hauser, my daily supervisor, for good supervising with the experimental set up, planning the experiments, support and feedback. It was really a great experience working with such enthusiastic scientific dedication.

I also would like to thank the technicians Anita Storsve and Siri Stavrum at the department of Biotechnology for assistance in the laboratory.

At the Norwegian University of Life Science (UMB) I would like to thank Professor Roland Kallenborn for his assistance and feedback.

I would like to dedicate this master thesis to my mother.

Abstract

The longest continuous record of atmospheric CO₂ is found at the Mauna Loa observatory in Hawaii. Looking at the overall scenario the measurements show a steady increase in mean atmospheric CO₂ concentration from about 315 parts per million (ppm) in 1958 to 393,65 ppm in February 2012. The good news is that it is possible to reduce global emissions by as much as 85 percent by 2050; one of the measures to achieve this is the use of CO₂ capture and storage (CCS).

The principle of CCS is to capture the CO₂ from arising point sources and transport and store it safely in an underground geological formation. One of three main technologies of CCS is post-combustion capture, where the most commonly used method is absorption based on chemical solvents, such as amines and carbonates.

For post-combustion capture aqueous amines are the most common solvents and a solvent with 30 % of monoethanolamine (MEA) is the industry standard. Other commonly used amines are 2-amino-2-methyl-1-propanol (AMP, sterically hindered primary amine), methyldiethanolamine (MDEA, tertiary amine), diethanolamine (DEA, secondary amine) and cyclic piperazine.

To enable better solvent management and ultimately ensure that post-combustion capture of CO₂ power stations has a net positive human and environmental benefit it is important and necessary to prioritize waste monitoring and management, including liquid and solid waste, at the pilot scale.

The main purpose of this work was to investigate the feasibility of applying biological Nitrogen removal to remove the ammonia from the process water from a CO₂ capture plant based on amine absorption, where the main concern is the possible toxicity of the high amine content in the process water to the nitrifying bacteria culture.

In this work pilot studies were run in separate bench scale reactors both for nitrification and denitrification, exposing the nitrifying culture for MEA, AMP, DEA, MDEA and piperazine. By Hach-Lange assays and Fluorescamine assay the nitrification and denitrification process could be followed and the degradation of primary amines could be monitored.

The work was based on previous studies done by Colaço, Skjæran and Hauser (Colaço, 2009, Skjæran, 2010, Hauser, 2011) to try to reproduce the results gained from the acute toxicity of the amines MEA, AMP, DEA, MDEA and piperazine on a nitrifying biofilm previously exposed, versus a freshly developed nitrifying biofilm not previously exposed.

Experimental results indicated that the activity of the nitrifying culture stabilized around day 43 after the inoculation. The gained COD per Kaldnes K1 carrier in the nitrification culture could not be tracked because of interference on the Hach-Lange assay LCK 114 COD.

Comparing the acute toxicity of MEA unloaded with the acute toxicity of the MEA loaded (with 5 % CO₂ in air) the affect on the nitrifying culture was relative similar, except for when comparing the percentage recovery, which showed that the MEA unloaded recovers faster than the MEA loaded. The Fluorescamine assay gave a good correlation between the measured and the theoretical MEA concentration, indicating that there was no degradation of MEA during the time period of the acute toxicity test.

Overall, the EC₅₀ values for the ammonia oxidizing rate (AOR) were less than the EC₅₀ values for the nitrite oxidizing rate (NOR) (except for MDEA, which had a higher EC₅₀ value for the AOR), indicating that the AOR was more sensitive to lower concentrations during the acute toxicity than the NOR. The activity of the nitrifying process varied during the toxicity tests, but it did not stop. The tolerance in amine concentration represented by the EC₅₀ values for the AOR in ascending order: MEA unloaded (58 mM) < AMP (82 mM) < DEA (138 mM) < piperazine (190 mM) < MDEA (314 mM). The tolerance in amine concentration represented by the EC₅₀ values for the NOR in ascending order: MDEA (104 mM) < MEA unloaded (168 mM).

The EC₅₀ values can be used as an indication on how much the reclaimer waste has to be diluted when using biological degradation of the effluent from amine based CCS.

Abstract

Table of contents

List of figures

List of tables

Abbreviations

1. Introduction	1
1.1 Background	1
1.2 CO ₂ capture	3
1.3 Environmental impact	5
1.4 Biodegradation and ecotoxicity	7
1.4.1 Degradation mechanisms and pathways for amines	7
1.4.2 Biodegradation of monoethanolamine (MEA)	8
1.3 Nitrification	8
1.3.1 Basic process	9
1.3.2 Oxygen	10
1.3.3 pH	10
1.3.4 Temperature	11
1.3.5 Inhibiting substance	11
1.4 Denitrification	11
1.4.1 Basic process	11
1.4.2 Oxygen	12
1.4.3 Carbon source	13
1.4.4 Temperature	13
1.4.5 pH	13
1.5 Disadvantages and limitations of nitrification and denitrification	13
1.6 Moving bed biofilm reactors	14
1.7 Previous studies	15
1.8 Aims of the present work	17
Biofilm development	17
Acute toxicity of selected amines	17
2. Material and Methods	18
2.1 Chemical analysis	18

2.1.1 Hach-Lange assays	18
2.1.2 Fluorescamine assay	20
2.2 Biofilm development.....	20
2.2.1 Monitoring	20
2.3 Nitrification	21
2.3.1 Inoculum.....	21
2.3.2 Medium	21
2.3.3 Reactor	22
2.3.4 Monitoring	24
2.3.5 Acute Toxicity Test	24
2.4 Denitrification	26
2.4.1 Inoculum.....	26
2.4.2 Medium	26
2.4.3 Reactor	27
2.4.4 Monitoring	29
2.5 Waste handling	29
3. Results	30
3.1 Nitrification	30
3.1.1 Stabilization.....	30
3.1.2 Biofilm development.....	32
3.2 Inhibition of nitrification	33
3.2.1 Biofilm history	33
3.2.2 State of biofilm.....	33
3.2.3 Acute toxicity test on old biofilm.....	34
3.2.4 Acute toxicity test on the new biofilm.....	42
3.2 Denitrification	52
3.2.1 Stabilization.....	53
4. Discussion.....	55
4.1 Nitrification	55
4.1.1 Stabilization.....	55

4.1.2 Biofilm development.....	55
4.2 Inhibition of nitrification	55
4.2.1 State of biofilm	55
4.2.2 Acute toxicity.....	56
4.3 Denitrification	59
4.3.1 Stabilization.....	59
5. Conclusions.....	60
5.1 Nitrification	60
5.1.1 Stabilization.....	60
5.1.2 Biofilm development.....	60
5.2 Inhibition of nitrification	60
5.2.1 Acute toxicity.....	60
5.3 Future work	62
6. Bibliography	63
Appendix A.....	66
Appendix B.....	67
Appendix C.....	69
Appendix D.....	81
Appendix E.....	83

List of figures

Figure 1 World commercial energy demand by fuel from BP Energy Outlook 2030 (BP, 2011).	1
Figure 2 Atmospheric CO ₂ concentrations measured at Mauna Loa Observatory, Hawaii, presented as monthly mean (Department of Commerce, 2009).	2
Figure 3 CO ₂ capture and storage (CCS). CO ₂ is captured from the flue gas coming from a coal power plant and transported by a pipeline to a storage location where the CO ₂ is injected for safe storage typically more than 800 meters below the ground (Bellona, 2012).	3
Figure 4 Simplified flow process diagram for CO ₂ capture from flue gas using a chemical absorbent (Sintef, 2011).	4
Figure 5 The chemical reaction of CO ₂ by primary or secondary amine to form carbonate. For MEA, R ₁ = H and R ₂ =CH ₂ OH (Reynolds et al., 2012).	5
Figure 6 The chemical reaction of CO ₂ by tertiary and sterically hindered amine to form bicarbonate (Reynolds et al., 2012).	5
Figure 7 Estimated sinks of consumed MEA in a typical 420 MW natural gas combined cycle power with post combustion capture (Reynolds et al., 2012).	6
Figure 8 Reaction for the oxidative deamination of ethanolamine (MEA) by ethanolamine oxidase (Eide-Haugmo, 2011).	7
Figure 9 Relationship of free ammonia (NH ₃) and free nitrous acid (HNO ₂) inhibition to nitrifying organisms. The grey area represents total inhibition, and the dashed area marks partial inhibition (Henze et al., 2002).	11
Figure 10 The four models are representing the respiratory systems utilizing nitrate (a), nitrite (b), NO (c) and N ₂ O (d) carrying out the complete process of denitrification. When all four modules are activated complete denitrification is achieved. In a denitrification process pair wise overlaps (e to g) can naturally occur (Zumft, 1997).	12
Figure 11 The three phases of a biofilm life cycle; 1) Attachment, 2) Growth and 3) Dispersal (Rogne, 2010).	14
Figure 12 Enlarged Kaldnes K1 carrier with biofilm (left) and two clean Kaldnes K1 carriers in real size (right). The inside surface of the carrier is 500 cm ² /cm ³ (Hauser, 2011).	15
Figure 13 Ammonium-N recordings according to the LCK 303 Ammonium-Nitrogen assay as a function of ammonium-N concentration, while MEA concentration was kept constant at 0, 5, 10, 20, 30 and 40 mM (Colaço, 2009). Secondary lines, in grey provide guidance for linear interpolation.	19
Figure 14 The experimental set-up of the nitrification reactor (Hauser, 2011).	23

Figure 15 Flow schema of the acute toxicity assay, where E stands for empty and F stands for full (Hauser, 2011).	25
Figure 16 Set-up for the deaeration of the medium water (Hauser, 2011).	27
Figure 17 The experimental set-up of the denitrification reactor. (Hauser, 2011).....	28
Figure 18 The experimental timeline (in days) of the main nitrification reactor.....	30
Figure 19 Measured activity [mg/l] of ammonium ($\text{NH}_4^+\text{-N}$), nitrite ($\text{NO}_2\text{-N}$) and nitrate ($\text{NO}_3\text{-N}$), and monitored pH and dissolved oxygen (DO) concentration [%] in the nitrification reactor. The measurement started at day zero, when adding the Kaldnes K1 carriers, until day 88.	31
Figure 20 The production rate of the nitrifying activity represented as nitrate loading rate (NLR) and produced nitrate and nitrite, starting on day 29 after the up scaling to a 5 l glass reactor when the reactor were on a continuous flow mode with a flow rate of 100 ml/h until day 88.....	31
Figure 21 The nitrifying activity of the biofilm previously tested by Colaço, Skjæran, and Hauser before the acute toxicity of unloaded MEA on the nitrifying culture.	33
Figure 22 The nitrifying activity of the biofilm not previously tested, before the acute toxicity of AMP on the nitrifying culture.	34
Figure 23 The nitrification activity in terms of nitrite oxidized during acute toxicity of unloaded MEA on the nitrifying culture.	35
Figure 24 The nitrification activity in terms of ammonia oxidized during acute toxicity of unloaded MEA on the nitrifying culture.	35
Figure 25 The nitrification activity after 30 hours of recovery of the acute toxicity of unloaded MEA on the nitrifying culture.	36
Figure 26 The nitrification activity after 30 hours of recovery of the acute toxicity of unloaded MEA on the nitrifying culture.	36
Figure 27 The nitrification activity in terms of nitrite oxidized during acute toxicity of loaded MEA on the nitrifying culture.....	37
Figure 28 The nitrification activity in terms of ammonia oxidized during acute toxicity of loaded MEA on the nitrifying culture.	37
Figure 29 The nitrification activity in terms of ammonia oxidized after 30 hours of recovery of the acute toxicity of loaded MEA on the nitrifying culture.	38
Figure 30 The nitrification activity in terms of ammonia oxidized after 30 hours of recovery of the acute toxicity of loaded MEA on the nitrifying culture.	38
Figure 31 Acute toxicity of MEA unloaded and MEA loaded on the nitrifying culture. The nitrite oxidizing rate expressed in percent activity (%) is set relative to the slope of the initial activity without the test substance. The estimated EC_{50} of MEA unloaded and MEA loaded for the nitrite oxidizing	

rate was 168 mM and 210 mM respectively. All tests had a monitoring time range of 3 hours for each concentration.	39
Figure 32 Acute toxicity of MEA unloaded and MEA loaded on the nitrifying culture. The ammonia oxidizing rate expressed in percent activity (%) is set relative to the slope of the initial activity without the test substance. The estimated EC ₅₀ of MEA unloaded and MEA loaded for the ammonia oxidizing rate was 58 mM and 82 mM respectively. All tests had a monitoring time range of 3 hours for each concentration.	40
Figure 33 Measured values of MEA unloaded concentration [mM] by Fluorescamine assay as a function of theoretical MEA unloaded concentration [mM].	41
Figure 34 Measured values of MEA loaded concentration [mM] by Fluorescamine assay as a function of theoretical MEA loaded concentration [mM].	41
Figure 35 The nitrification activity in terms of nitrite oxidized during acute toxicity of AMP on the nitrifying culture.	42
Figure 36 The nitrification activity in terms of ammonia oxidized during acute toxicity of AMP on the nitrifying culture.	43
Figure 37 The nitrification activity after 30 hours of recovery of the acute toxicity of AMP on the nitrifying culture represented as nitrite oxidized.	43
Figure 38 The nitrification activity after 30 hours of recovery of the acute toxicity of AMP on the nitrifying culture represented as ammonia oxidized.	44
Figure 39 The nitrification activity in terms of nitrite oxidized during acute toxicity of DEA on the nitrifying culture.	44
Figure 40 The nitrification activity in terms of ammonia oxidized during acute toxicity of DEA on the nitrifying culture.	45
Figure 41 The nitrification activity after 30 hours of recovery of the acute toxicity of DEA on the nitrifying culture represented as nitrite oxidized.	45
Figure 42 The nitrification activity after 30 hours of recovery of the acute toxicity of DEA on the nitrifying culture represented as ammonia oxidized.	46
Figure 43 The nitrification activity in terms of nitrite oxidized during acute toxicity of MDEA on the nitrifying culture.	46
Figure 44 The nitrification activity in terms of ammonia oxidized during acute toxicity of MDEA on the nitrifying culture.	47
Figure 45 The nitrification activity after 30 hours of recovery of the acute toxicity of MDEA on the nitrifying culture represented as nitrite oxidized.	47
Figure 46 The nitrification activity after 30 hours of recovery of the acute toxicity of MDEA on the nitrifying culture represented as ammonia oxidized.	48

Figure 47 The nitrification activity in terms of nitrite oxidized during acute toxicity of piperazine on the nitrifying culture.....	48
Figure 48 The nitrification activity in terms of ammonia oxidized during acute toxicity of piperazine on the nitrifying culture.	49
Figure 49 The nitrification activity after 30 hours of recovery of the acute toxicity of piperazine on the nitrifying culture represented as nitrite oxidized.....	49
Figure 50 The nitrification activity after 30 hours of recovery of the acute toxicity of piperazine on the nitrifying culture represented as ammonia oxidized.	50
Figure 51 Acute toxicity of AMP, DEA, MDEA and piperazine on the nitrifying culture in terms of activity of the nitrite oxidizing rate. The estimated EC ₅₀ of MDEA was 80 mM, based on a logistic model. All tests had a monitoring time range of 3 hours for each concentration.....	51
Figure 52 Acute toxicity of AMP, DEA, MDEA and piperazine on the nitrifying culture in terms of activity of the ammonia oxidizing rate. The estimated EC ₅₀ of AMP, DEA, MDEA and piperazine was respectively 82 mM, 138 mM, 314 mM and 190 mM, based on a logistic model. All tests had a monitoring time range of 3 hours for each concentration.	51
Figure 53 Timeline (in days) of the denitrification reactor	52
Figure 54 Measured activity [mg/l] of ammonium (NH ₄ ⁺ -N), nitrite (NO ₂ -N) and nitrate (NO ₃ -N), and monitored pH in the denitrification reactor. The measurement started at day zero, when adding the Kaldnes K1 carriers, until day 67.	53
Figure 55 The reduction rate of the denitrifying activity represented as nitrate loading rate (NLR) and nitrate (NO ₃ -N) reduction rate, starting on day 31 after the up scaling to a 2 l glass reactor when the reactor were on a continuous flow mode with a flow rate of 60 ml/h until day 67.....	53

List of tables

Table 1 Reaction rate and yield constants for nitrifying bacteria at 20°C (Henze et al., 2002).	9
Table 2 Reaction rate constants for the denitrification process at 20°C (Henze et al., 2002).	12
Table 3 Summary of EC ₅₀ values from previous toxicity tests with the amines MEA, AMP, DEA, MDEA and piperazine on nitrifying culture tested by Colaço (twice) (Colaço, 2009), Skjæran (Skjæran, 2010) and Hauser (Hauser, 2011). Recovery values 30 hours after the acute toxicity gained from Skjæran (Skjæran, 2010) and Hauser (Hauser, 2011) is also given.	16
Table 4 Hach-Lange assays used for determining the concentration of ammonium, nitrate and nitrite.(Hach-Lange, 2011c, Hach-Lange, 2012, Hach-Lange, 2011d, Hach-Lange, 2011e)	18
Table 5 Hach-Lange assays used for determining the chemical oxygen demand.(Hach-Lange, 2011a, Hach-Lange, 2011b).....	19
Table 6 Composition of the medium supplied to the nitrification reactor.	21
Table 7 Composition of the trace metal stock solution, 100-fold.....	22
Table 8 Chemicals tested for acute toxicity on the nitrifying culture (Hauser, 2011).	24
Table 9 Medium composition for the denitrification reactor.	26
Table 10 Acute toxicity experiments on nitrifying culture.	33
Table 11 Summary of the acute toxicity of MEA unloaded and MEA loaded on the nitrifying culture in terms of activity for the nitrite oxidizing rate (NOR) and the ammonia oxidizing rate (AOR).	40
Table 12 Total dry weight of the old biofilm in terms of mg, before and after the acute toxicity test with MEA unloaded, given as the average and standard error of mean (SEM) of five and three parallels respectively.	42
Table 13 Summary of the acute toxicity of AMP, DEA, MDEA and piperazine on the nitrifying culture in terms of activity for the nitrite oxidizing rate (NOR) and the ammonia oxidizing rate (AOR).	52
Table 14 Total dry weight of the new biofilm in terms of mg, before and after the acute toxicity test with AMP, given as the average and standard error of mean of ten parallels.	52

Abbreviations

AMP	AMP Regular [2-amino-2-methylpropanol]
AOB	Ammonia oxidizing bacteria
AOR	Ammonia oxidizing rate ($\text{NH}_4^+ \rightarrow \text{NO}_2 \rightarrow \text{NO}_3$)
BP	Beyond Petroleum
CCS	CO ₂ capture and storage
COD	Chemical oxygen demand
DEA	Diethanolamine [2-(2-hydroxyethylamino) ethanol]
DO	Dissolved oxygen
EC ₅₀	Median effective concentration
EPS	Extracellular polymeric substances
HRT	Hydraulic Retention Time
IPCC	Intergovernmental Panel on Climate Change
MBBR	Moving bed biofilm reactor
MDEA	N-methyldiethanolamine [2-(2-hydroxyethyl (methyl) amino)ethanol]
MEA	Monethanolamine [2-ethanolamine]
MW	Molecular weight
NOB	Nitrite oxidizing bacteria
NOR	Nitrite oxidizing rate ($\text{NO}_2 \rightarrow \text{NO}_3$)
PCC	Post combustion capture
PPM	Parts per million
VSS	Volatile Suspended Solid

1. Introduction

1.1 Background

Over the past century the carbon dioxide (CO₂) concentrations in the atmosphere has been increasing compared to the rather steady level of the preindustrial era, when the CO₂ concentrations was about 280 parts per million (ppm) (for example a mole fraction of 0,000400 CO₂ is expresses as 400 ppm). The 2005 concentration of CO₂ (379 ppm) was about 35 % higher than in the mid-1800s, with the fastest growth occurring in the period 1995-2005 (IPCC, 2007). The increased concentrations of key greenhouse gases are a direct consequence of anthropogenic emissions. Since the anthropogenic greenhouse gases accumulate in the atmosphere, the result is produced net warming by strengthening of the natural “greenhouse effect”. Levels of other greenhouse gases, such as methane (CH₄) and nitrous oxide (N₂O), have also increased significantly. Fossil fuel is covering around 80 % of the total world energy demand and remains the dominant sources of primary energy (IEA, 2011). The world commercial energy demand sorted by fuel from the statistical review in BP Energy outlook 2030 is visualized in Figure 1.

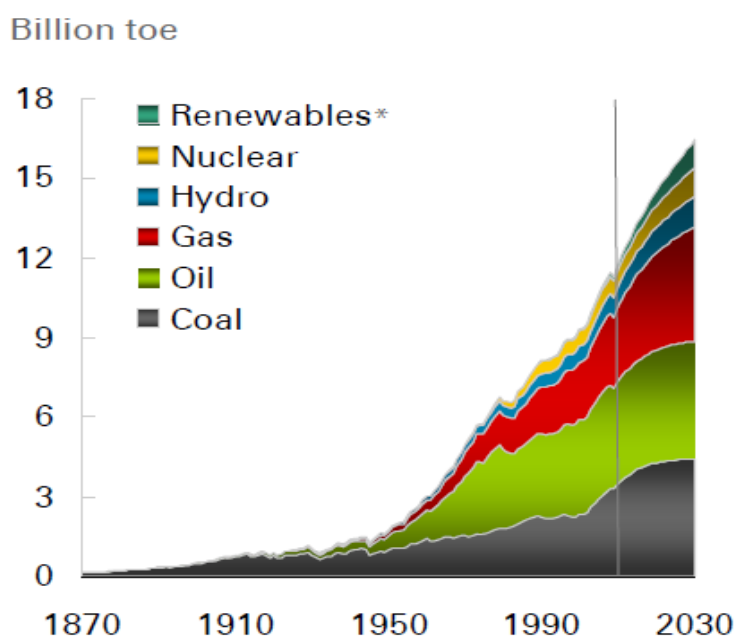


Figure 1 World commercial energy demand by fuel from BP Energy Outlook 2030 (BP, 2011).

The longest continuous record of direct atmospheric CO₂ measurements is found at the observatory Mauna Loa in Hawaii (Department of Commerce, 2009). The full history of atmospheric CO₂ concentrations from 1960 until 2010 measured at Mauna Loa observatory is visualized in Figure 2.

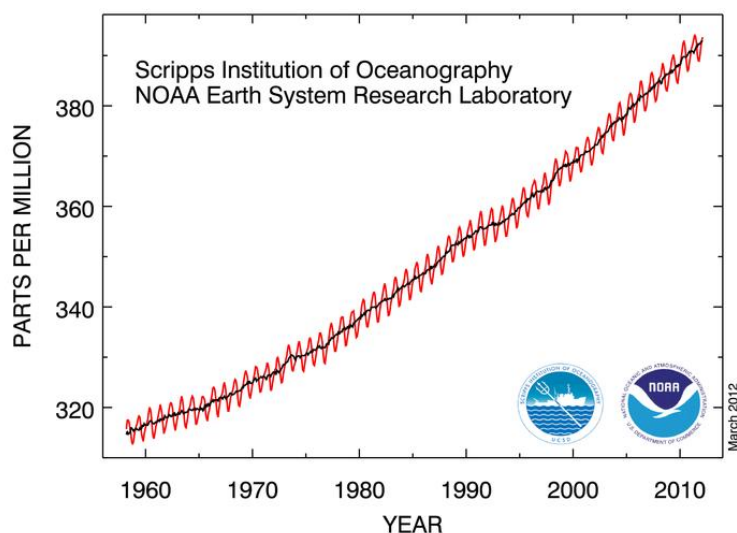


Figure 2 Atmospheric CO₂ concentrations measured at Mauna Loa Observatory, Hawaii, presented as monthly mean (Department of Commerce, 2009).

The red curve in Figure 2 shows the annual fluctuation in CO₂ and is caused by seasonal variations in CO₂ uptake by land and plants. The black curve represents the seasonally corrected data. Looking at the overall scenario the measurements collected at Mauna Loa Observatory show a steady increase in mean atmospheric CO₂ concentration from about 315 parts per million (ppm) in 1958 to 393,65 ppm in February 2012 (Department of Commerce, 2009).

According to the Fourth Assessment Report of the Intergovernmental Panel on Climate Change (IPCC), the anthropogenic greenhouse gas emissions will increase the average global temperature from 1,1 °C to 6,4 °C during the 21st century (IPCC, 2007). The global temperature is already 0,7 °C above the pre-industrial level, and a 2 °C increase is generally considered as the tipping point above which dramatic and irreversible impacts are expected to occur. Consequences of the increase in the average global temperature may be collapse of ecosystems and 15 to 40 percent of all species may become extinct. More draughts, floods and other extreme weather events will increase pressure on scarce food and water resources as the world population grows towards nine billion humans by 2050 (IPCC, 2007). According to the Snow, Water, Ice, Permafrost in the Arctic (SWIPA) report from the Arctic Monitoring and Assessment Programme (AMAP) the average Arctic autumn-winter temperatures are projected to increase by between 3 and 6 °C by 2080. The projections have taken into consideration scenarios in which greenhouse gas emissions are projected to be lower than they have been for the past ten years (AMAP, 2011).

To have a chance of avoiding such consequences of global warming, the IPCC has recommended a 50 to 85 percent reduction of global greenhouse gas emissions from 2000 to 2050 and a peak in emissions no later than 2015 (IPCC, 2007). The good news is that it is possible to reduce global emissions by as much as 85 percent by 2050: Energy can be generated from renewable sources and used more efficiently, fossil power can be de-carbonized by CO₂ capture and storage (CCS), and forestation management can be improved (Shao et al., 2009).

1.2 CO₂ capture

One of the methods for effective reduction of the greenhouse gas emissions to the atmosphere, under business as usual conditions is CCS. The principle of CCS is to capture the CO₂ from arising point sources, such as for example fossil fuel fire plants, and transport and store it safely in an underground geological formation, as visualized in Figure 3.

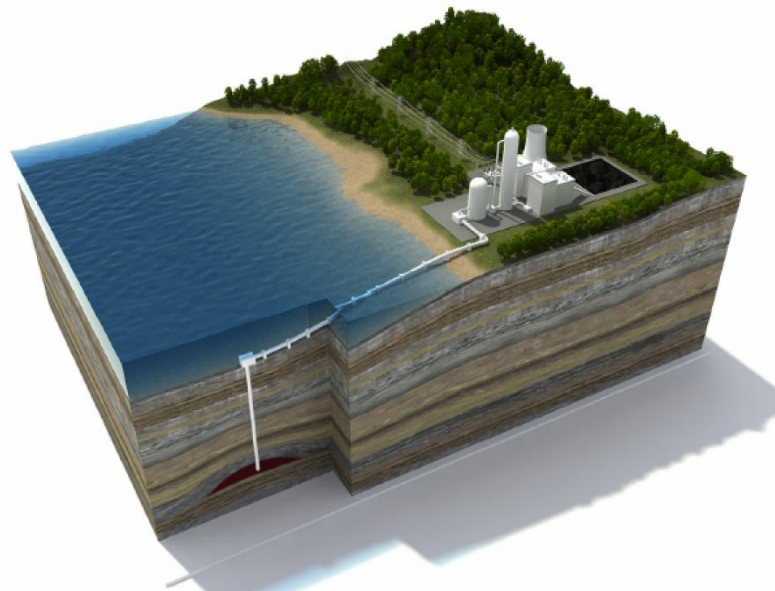


Figure 3 CO₂ capture and storage (CCS). CO₂ is captured from the flue gas coming from a coal power plant and transported by a pipeline to a storage location where the CO₂ is injected for safe storage typically more than 800 meters below the ground (Bellona, 2012).

For separation and capture of CO₂ from gas streams a wide range of technologies exist which are sorted in three main technologies: oxy-fuel combustion, pre-combustion and post-combustion. For separation of CO₂ there are several types of technologies including membrane separation, adsorption and absorption. For post-combustion capture the most commonly used method is absorption based on chemical solvents, where typical absorbents are amines and carbonates (Bellona, 2012). Chemical absorption, more specifically amine based processes, is currently the most popular way to remove

CO₂ in industry in Norway, and have been used commercially for removal of acid gas impurities from process gas stream for a long time (Eide-Haugmo, 2011). Figure 4 visualizes a simplified flow-sheet of the CO₂ capture process using a chemical absorbent.

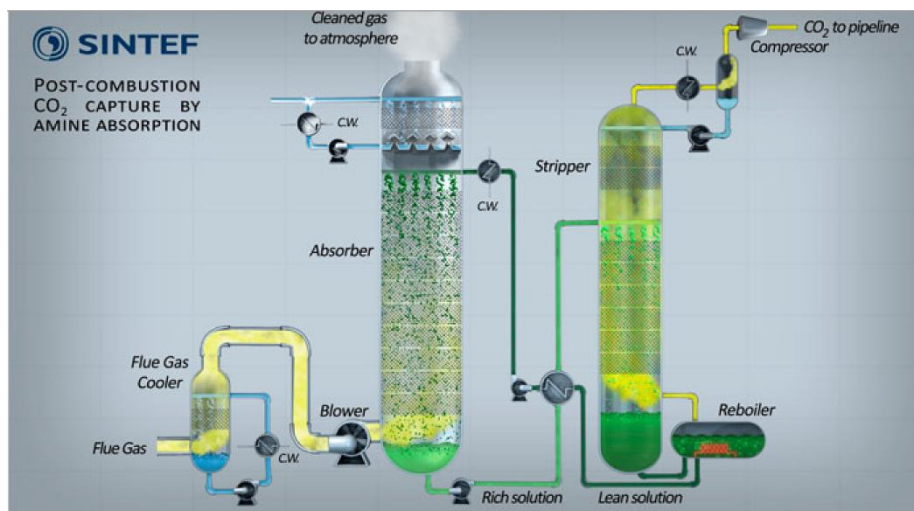


Figure 4 Simplified flow process diagram for CO₂ capture from flue gas using a chemical absorbent (Sintef, 2011).

In an amine based post-combustion CO₂ capture plant, the process gas is cooled down to a temperature between 40-60 °C, before entering the absorber bottom. Then the gas will contact the amine solution which flows down from the top of the absorber and CO₂ in the gas is absorbed into the solution where it reacts chemically with the amine. As the gas continues to pass up the absorber more of the CO₂ will be absorbed, resulting in a clean gas-stream with low CO₂ content. To make sure that no vaporized amine is discharged into the atmosphere a water wash can be used at the top of the absorber. To regenerate the CO₂-containing amine solvent, it is heated to reduce the absorbents ability to retain CO₂. Then the heated solution (rich on CO₂) goes to the top of the stripper which operates at a temperature typically between 100-125 °C, and flows down to the reboiler, releasing CO₂. In the top of the stripper a steam is used as a stripping gas. The stripping gas is recovered by a condenser and refeed to the stripper while a gas stream of high CO₂ purity leaves the column. About 80 to 90 % of the CO₂ can be removed from a power plant by post-combustion CO₂ capture. In order to regenerate solvent, maintain pumps, for the process gas blower and to compress CO₂ significant amounts of energy are needed (Eide-Haugmo, 2011).

For post-combustion capture aqueous amines are the most common solvents, and a solution with 30 % of monoethanolamine (MEA) is the industry standard. The process flow diagram in Figure 4 implies that in an ideal post-combustion system the solvent is continuously recycled and reused. However, during post-combustion capture both primary and secondary amines react with CO₂ to form a

carbonate and protonated amine, consuming approximately two mole of amine per mole of CO₂ as shown in Figure 5 (Reynolds et al., 2012).

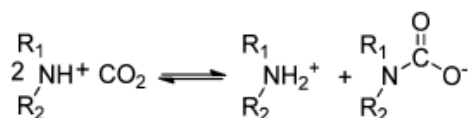


Figure 5 The chemical reaction of CO₂ by primary or secondary amine to form carbonate. For MEA, R₁= H and R₂=CH₂OH (Reynolds et al., 2012).

Sterically hindered and tertiary amines react with CO₂ to form bicarbonate, shown in Figure 6, and consume only one mole of protonated amine per mole of CO₂ absorbed (Reynolds et al., 2012).

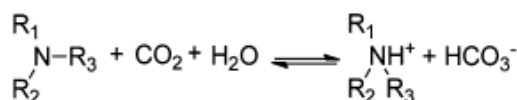


Figure 6 The chemical reaction of CO₂ by tertiary and sterically hindered amine to form bicarbonate (Reynolds et al., 2012).

Absorption of CO₂ by primary or secondary amine to form carbonate is generally more rapid than absorption of CO₂ by tertiary and sterically hindered amine to form bicarbonate (Reynolds et al., 2012). Primary or secondary amine is therefore commonly used for the pilot scale post-combustion capture despite their lower CO₂ capacity. 2-amino-2-methyl-1-propanol (AMP, sterically hindered primary amine), methyldiethanolamine (MDEA, tertiary amine) and diethanolamine (DEA, secondary amine) are other aqueous amines with similar CO₂ absorption rates but with lower CO₂ capacity than MEA. An aqueous amine which has higher CO₂ capacity and absorption rate than MEA is cyclic piperazine (Reynolds et al., 2012).

Development of solvents for chemical absorption post-combustion capture is a major area of research since absorption solvent is the key component. High CO₂ absorption capacity and rapidly and reversible reaction with CO₂ with minimal heat requirement is characteristics of an ideal solvent, together with good oxidative and thermal stability, low vapor pressure, low toxicity, low flammability and availability at low cost (Reynolds et al., 2012).

1.3 Environmental impact

For CO₂-capture processes based on absorption the focus have been on reducing the regeneration energy demand by developing new solvent systems. As mentioned above the main goal is to find solvents which have favorable characteristics for energy requirement, reaction rate and stability at process conditions. Another important concern if these processes are to be employed on a global

level, which will involve large scale use of solvents, is that emissions may occur through the cleaned exhaust gas, as degraded solvent and as accident spills. The absorbent also form degradation products, which needs to be handled. Therefore it is important that the chemical used have low or no negative environmental effects. In fact negative environmental effects of such processes could be a potential stopper for this technology (Eide-Haugmo, 2011).

Recent studies have demonstrated that both solvent degradation and corrosion rates are dependent on the dissolved oxygen (DO) concentration. During the post-combustion capture process there are many opportunities for solvent consumption by chemical degradation and physical processes such as evaporation and droplet carryover. The intimate mixing of the amine solvent with flue gas containing oxygen, SO_x and fly ash, during CO₂ absorption is known to accelerate oxidative degradation. Carbonate polymerization occurs during CO₂ desorption where the solvent experiences high temperature (100-150 °C) and high CO₂ partial pressure. The outlet of both the CO₂ absorber and CO₂ desorber are also sources of possible solvent loss as vapor or aerosols, but most of this solvent can be recovered by scrubbing the lean flue gas and CO₂ product streams with water. The main contributions of MEA consumption pathways for a natural gas power station are shown in Figure 7 (Reynolds et al., 2012).

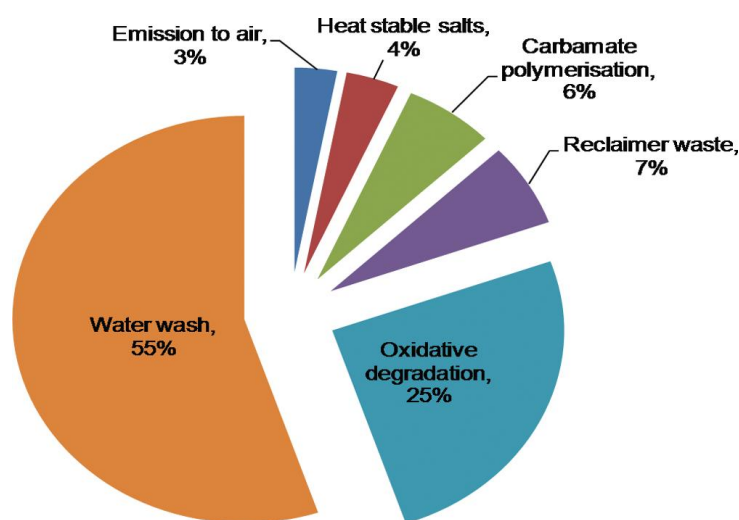


Figure 7 Estimated sinks of consumed MEA in a typical 420 MW natural gas combined cycle power with post combustion capture (Reynolds et al., 2012).

Evaporation from the absorber column is the most significant loss of MEA, but by washing the CO₂ lean flue gas with water may about 95 % of the evaporated solvent be recovered. Thermal degradation of MEA may occur at or above 200°C, but has not been observed during the release of

CO₂ in the post combustion capture process since the maximum temperature is about 150°C (Reynolds et al., 2012).

The biodegradability and ecotoxicity of amines used in post combustion capture vary (Eide-Haugmo et al., 2009). Recent studies of both factors in respect to the marine environment showed that AMP, MDEA and piperazine would have long persistence due to their low biodegradability, whereas DEA and MEA were found to be higher degradable (Eide-Haugmo et al., 2009). In terms of the ecotoxicity, all five amines were above the lowest acceptable value (10mg/l) for a chemical to be released in the marine environment with the following EC₅₀ values in ascending order: AMP (119mg/l) < MDEA (141mg/l) < MEA (198mg/l) < DEA (357mg/l) < piperazine (472mg/l) (Eide-Haugmo, 2011).

To enable better solvent management and ultimately ensure that post combustion capture of CO₂ power stations has a net positive human and environmental benefit it is important and necessary to prioritize waste monitoring and management, including liquid and solid waste, at the pilot scale.

1.4 Biodegradation and ecotoxicity

Biodegradation can be used to estimate the impact of contaminated effluents and accidental spills. Three factors can influence biodegradation: presence of micro-organisms capable of degrading the compound, environmental conditions allowing the organisms to grow and release the degradation enzymes, and good physical contact between the compound and the organism (Eide-Haugmo, 2011).

1.4.1 Degradation mechanisms and pathways for amines

The enzyme monoamine oxidase (MAO) can catalyze the oxidation of many primary, secondary and tertiary alkyl- and aryl alkyl amines. Ethanolamine oxidases catalyze the oxidative deamination of ethanolamine (MEA), the overall reaction is given in Figure 8.

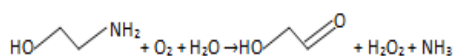


Figure 8 Reaction for the oxidative deamination of ethanolamine (MEA) by ethanolamine oxidase (Eide-Haugmo, 2011).

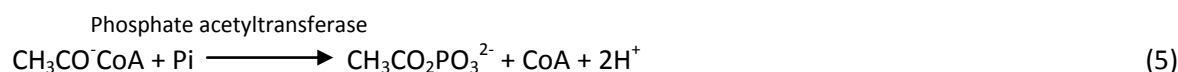
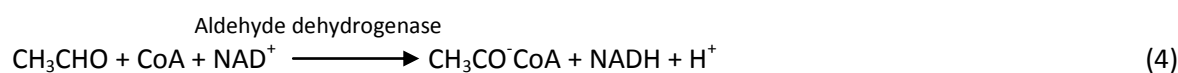
Degradation of primary amines can also be facilitated by copper-containing oxidases (CAO), which catalyze the oxidative deamination by dioxygen to form aldehydes, ammonia and hydrogen peroxide. The 2-step reaction is given in equation 1 and 2 (Eide-Haugmo, 2011).





1.4.2 Biodegradation of monoethanolamine (MEA)

In 1995 it was suggested to treat MEA in bioreactors with *Escherichia coli* K12 as a method for degrading waste amine solution Eide-Haugmo (Eide-Haugmo et al., 2009) concluded that the *Escherichia coli* culture could be effective for the continuous treatment of waste MEA. The proposed reaction mechanism for MEA is shown in equation 3-6, with the enzyme catalyzing each reaction given (Eide-Haugmo, 2011).



Xenobiotic compounds are man-made chemicals, but although foreign to the biosphere this does not necessarily mean that they form an environmental problem. The increase of xenobiotic amines in industrial applications encouraged researchers years ago to investigate their fate in the environment, mainly focusing on biological degradation.

1.3 Nitrification

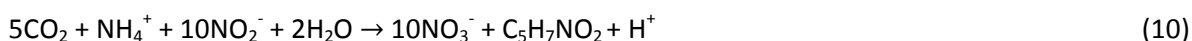
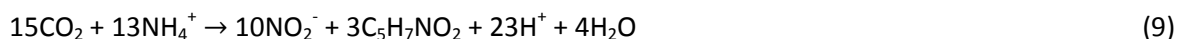
Ammonia exists in aqueous solution in two forms: NH_3 and NH_4^+ . Both forms may be toxic to aquatic species, but unionized ammonia (NH_3) is the more toxic form at low concentrations. The proportion of NH_3 relative to ionized ammonia (NH_4^+) in an aqueous solution depends on temperature, pH and salinity. At lower temperatures and pH the percentage of NH_4^+ increases on the expense of NH_3 (Chen et al., 2006). Because ammonia is toxic to aquatic species and causes eutrophication in natural water environments the removal of ammonia from wastewater has become a worldwide emerging concern. A biological approach is the only effective removal of nitrogen compounds in wastewater (Zhu et al., 2008).

1.3.1 Basic process

Nitrification of ammonia is a result of the sequential action of two separate groups of chemolithoautotrophic organisms, the ammonia oxidizing bacteria (AOB) and the nitrite oxidizing bacteria (NOB). In the first step of the nitrification process autotrophic bacteria, the most important being *Nitrosomonas*, oxidize ammonia into nitrite (NO_2^-). Nitrite is then oxidized to nitrate (NO_3^-) by several other genera of bacteria, the most important being *Nitrobacter*. NO_3^- is much less toxic than NH_4^+ . The basic chemical process for the AOB and the NOB are shown in equation 7 and 8 respectively (Chen et al., 2006).



Energy released from the above conversions is used to drive the life processes of the *Nitrosomonas* and the *Nitrobacter*. The reactions require oxygen as an electron acceptor, produce hydrogen ions (lowering pH) and produce nitrite as an intermediate product. CO_2 is used as a carbon source, but the CO_2 must be reduced before the carbon can form part of the cell mass. The reduction of CO_2 takes place through the oxidation of the nitrogen source of the organism concerned. In equation 9 and 10 have the bacterial biomass been assigned a typical composition where the formula $\text{C}_5\text{H}_7\text{O}_2\text{N}$ represent the chemical expression of the bacterial cell of *Nitrosomonas* and *Nitrobacter* (Colaço, 2009).



In wastewater are *Nitrosomonas* species and *Nitrobacter* species regarded as the respective typical dominating ammonia and nitrite oxidizers. But there have been other nitrifying species revealed such as *Nitrosococcus*, *Nitrosospira*, *Nitrosovibrio*, *Nitrospira*, *Nitrospina* and *Nitrococcus*. In Table 1 the reaction rate and yield constants of *Nitrosomonas* species and *Nitrobacter* species are shown.

Table 1 Reaction rate and yield constants for nitrifying bacteria at 20°C (Henze et al., 2002).

*Volatile suspended solids.

Reaction rate constants	AOB	NOB	Total process
Maximum specific growth rate (d^{-1})	0,6-0,8	0,6-1,0	0,6-0,8
Half-saturation constant ($\text{g NH}_4^+\text{-N/m}^3$)	0,3-0,7	0,8-1,2	0,3-0,7
Half-saturation constant ($\text{g O}_2/\text{m}^3$)	0,5-1,0	0,5-1,5	0,5-1,0
Maximum yield constant ($\text{g VSS}^*/\text{g NO}_3\text{-N}$)	0,10-0,12	0,05-0,07	0,15-0,20
Decay constant (d^{-1})	0,03-0,06	0,03-0,06	0,03-0,06

The low-energy Nitrogen substrates and the energy consuming CO_2 fixation of the nitrifiers result in poor growth yields and low growth rates (Colaço, 2009). The growth rate of the *Nitrobacter* (NOB) is greater than the growth rate of *Nitrosomonas* (AOB), and the oxidation of ammonia (equation 7) is usually the rate-limiting step in the conversion of ammonia to nitrate (Chen et al., 2006). Therefore, nitrite accumulation will only occur when oxidation of ammonium exceeds the velocity of the nitrite oxidation. The NOB is localized in the deeper parts of the oxic biofilm, and therefore oxygen diffusion can be a more limiting factor for the NOB compared to the AOB which has a homogeneous spatial distribution (Okabe et al., 2004).

The nitrification process is mainly influenced by DO concentration, pH, temperature, and inhibiting substances, besides substrate concentration.

1.3.2 Oxygen

Oxygen is a requirement in the ammonia oxidation and nitrite oxidation, as shown in equation 7 and 8. DO affects the growth rate of the AOB in a small degree at the level above 2 mg/l, but NOB is more sensitive to DO and will have a reduced growth rate with DO less than 4 mg/l. Also, nitrification ceases entirely below a DO concentration of 0,2 mg/l. Minimum oxygen level in nitrification biofilters is suggested to a DO of 2 mg/l. Within the biofilm DO drops rapidly, and is in fact the limiting factor. Since the nitrite oxidizers are strongly inhibited in a low DO environment, low DO concentrations can cause an accumulation of nitrite in the nitrification biofilters. The factors that affect the availability of oxygen to the nitrifiers at the surface of the biofilm are turbulence, organic loading, pH and temperature (Chen et al., 2006).

1.3.3 pH

The nitrification process is pH dependent. At higher pH the nitrifiers are inhibited by unionized ammonia (NH_3), and at lower pH inhibition is caused by nitrous acid (HNO_2) (Henze et al., 2002). The optimum pH for metabolism and growth of the autotrophic nitrifiers is in the range of pH 7,5-8. Dissociation equilibrium of both $\text{NH}_3 \leftrightarrow \text{NH}_4^+$ ($\text{pK}_a=9,3$) and $\text{HNO}_2 \leftrightarrow \text{NO}_2^-$ ($\text{pK}_a=3,4$) are a function of pH and therefore attribute to the pH dependent nitrification activity. Figure 9 shows the relationship of free NH_3 and free HNO_2 inhibition of nitrifying organisms (Henze et al., 2002).

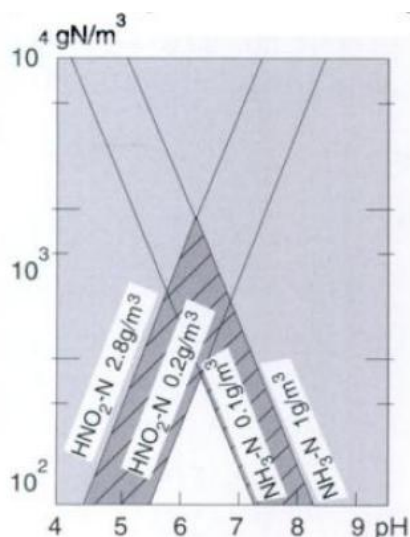


Figure 9 Relationship of free ammonia (NH_3) and free nitrous acid (HNO_2) inhibition to nitrifying organisms. The grey area represents total inhibition, and the dashed area marks partial inhibition (Henze et al., 2002).

Severe pH depression can occur when the alkalinity in the wastewater approaches depletion by the acid produced in the nitrification process, and therefore the appropriate range of pH must be stabilized by chemical addition, such as for example lime (Ahn, 2006).

1.3.4 Temperature

The optimum temperature for the nitrification process has been reported in the range of 20°C to 30°C , although the optimum temperature for the NOB might be lower (Chen et al., 2006).

1.3.5 Inhibiting substance

Nitrifiers can be inhibited by both substrate (NH_4^+ and NO_2^-) and product (NO_2^- and NO_3^-) if the concentration of either the substrate or the product is too high (Baribeau et al., 2006).

1.4 Denitrification

1.4.1 Basic process

In denitrification, nitrate and nitrite are converted into atmospheric nitrogen by heterogeneous mainly heterotrophic denitrifying bacteria through a series of intermediate gaseous nitrogen oxide products under anoxic conditions. The denitrification process carried out by heterotrophic bacteria is shown in equation 11, where the letters above the arrows correspond to the catalyzing enzymes, being a) Nitrate reductase, (b) Nitrite reductase, (c) NO reductase and (d) N_2O reductase (Rehm et al., 1999, Rittman and McCarty, 2001).



Of the enzymes in equation 11, Nitrite reductase is the key enzyme for denitrification because the enzyme catalyzes the first step which leads to a gaseous intermediate. The anoxic process is carried out by a diversity of bacteria belonging to the subclasses of *Proteobacteria*. The intermediates of the denitrification process, shown in equation 11, are toxic and should therefore be avoided. The enzymes are triggered in the cell by environmental factors as low oxygen tension and the availability of a Nitrogen oxide. As illustrated in Figure 10, only when all necessary enzymes are available for the bacteria, complete denitrification can occur (Zumft, 1997).

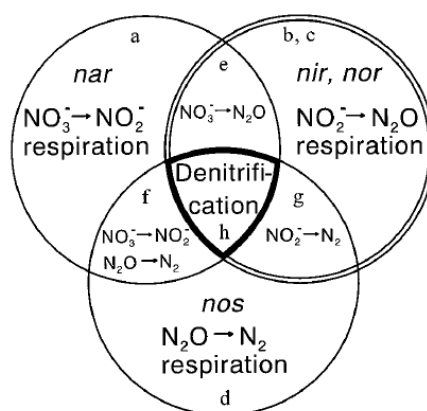


Figure 10 The four models are representing the respiratory systems utilizing nitrate (a), nitrite (b), NO (c) and N_2O (d) carrying out the complete process of denitrification. When all four modules are activated complete denitrification is achieved. In a denitrification process pair wise overlaps (e to g) can naturally occur (Zumft, 1997).

The reaction rate constants for the denitrifying bacteria are shown in Table 2.

Table 2 Reaction rate constants for the denitrification process at 20°C (Henze et al., 2002).

Reaction rate constants	Denitrification
Maximum specific growth rate (d^{-1})	3,0-6,0
Half-saturation constant ($g\ NO_3\text{-N}/m^3$)	0,2-0,5
Half-saturation constant ($g\ O_2/m^3$)	0,1-0,5
Half-saturation constant ($g\ COD/m^3$)	10,0-20,0
Maximum yield constant (COD/g COD)	0,4-0,6
Maximum yield constant (COD/g $NO_3\text{-N}$)	1,6-1,8
Decay constant (d^{-1})	0,05-0,10

The main factors that influence the denitrification, besides substrate concentration, are DO concentration, carbon source, temperature, pH and inhibiting substances.

1.4.2 Oxygen

The denitrification process is anaerobic as nitrate is used as an electron acceptor in the oxidation of organic matter to CO_2 and water. In nature, anywhere nitrate is present and oxygen is in very low

concentrations or nonexistent, denitrification will occur because denitrifiers are facultative and therefore when oxygen is available it is used as an oxidizing agent. The chosen pathway depends on the availability of a terminal electron acceptor. If oxygen is present, the bacterium will choose to respire aerobic, because the redoxpotential between the last cytochrome in the electron transport is higher for oxygen than for nitrate (Henze et al., 2002, Baribeau et al., 2006).

1.4.3 Carbon source

A carbon source is essential for the denitrification process. Without or if carbon is the limiting factor, denitrification will cease. Examples of commonly used external carbon sources are methanol, ethanol, acetic acid and wastewater from breweries and organic matter in wastewater. With the exception of the two latter examples, all the chemicals needed leads to an increased operational cost (Henze et al., 2002).

1.4.4 Temperature

As for the nitrification process, the denitrification process rate increases with increasing temperature until an optimum is reached at 40°C. At a higher temperature the denitrification rate is quickly reduces due to denaturation of enzymes (Lie, 1996).

1.4.5 pH

For denitrification process in activated sludge the optimum pH lies in the range 6,5-7,5 (Cherchi et al., 2009). At lower pH values denitrification rates decrease due to inhibition of nitrous oxide reductase, resulting in an accumulation of N₂O. Higher pH values favor N₂ gas production (Baribeau et al., 2006).

1.5 Disadvantages and limitations of nitrification and denitrification

Nitrification and denitrification are carried out by different microorganisms under different conditions, and for this reason the two processes should be designed and operated in separate time sequences or spaces. To accomplish complete nitrogen removal a long retention time or a large volume is required. For the nitrification process a high level of oxygen is required, set as 4,2 g O₂/g NH₄⁺-N, and a sufficient organic carbon source is required for denitrification, 2,86 g chemical oxygen demand (COD)/g NO₃⁻N. Normally, a high level of external carbon source is added in the denitrification process, for example methanol or acetate, and this increases the operational cost. The limitations of low removal efficiency, high oxygen requirement, long retention time and an external carbon source are the driving forces for developing new low-cost biological treatment processes for complete nitrogen removal (Zhu et al., 2008).

1.6 Moving bed biofilm reactors

When biota grows on the membrane surface it is called biofouling, producing a biofilm when bacteria attaches to the surface and begin to reproduce. A well functional and mature biofilm consists of living, growing and reproducing microorganisms. Components in a biofilm are high molecular weight extracellular polymeric substances (EPS), multivalent cations, biogenic, colloidal and inorganic particles and dissolved compounds. The complex structure of the biofilm protects and allows the microorganisms to grow. The EPS mainly consists of polysaccharides and proteins which holds the microbial cells in the biofilm together and provide a three-dimensional gel-like network enforced by divalent cations as for example Ca^{2+} . Other components which may contribute are DNA, lipids and humic substances (Rogne, 2010).

To understand the development of a biofilm, the life cycle of the biofilm can be divided into three phases. Phase one is the attachment, phase two is the growth and phase three is the dispersal.

Figure 11 illustrates the three phases of a biofilm life cycle.

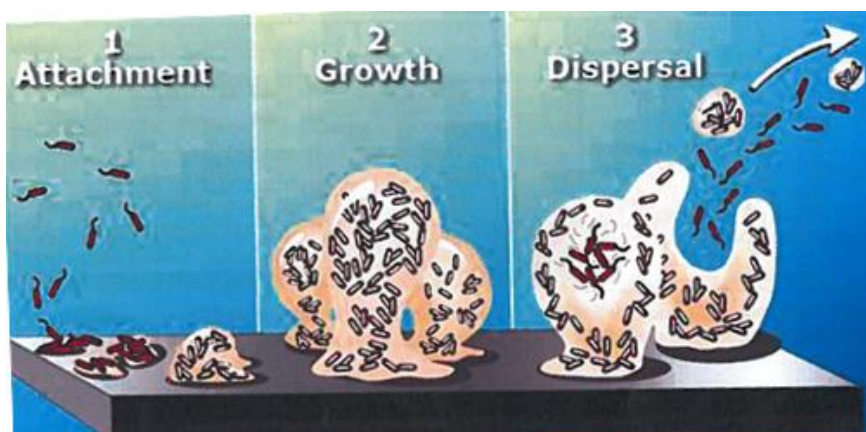


Figure 11 The three phases of a biofilm life cycle; 1) Attachment, 2) Growth and 3) Dispersal (Rogne, 2010).

In Figure 11 the attachment phase is when free-floating, or planktonic, bacteria encounters and attaches a surface. The amount of EPS is then increased when cells begin to divide as a result of production and dead-cell debris. In the second phase, the growth phase, the biofilm develop into a complex three dimensional structure. In the last phase, the dispersal, the biofilm starts to propagate by detachment of clumps of cells or individual cells. The biofilm can therefore reattach to a surface downstream of the original community (Rogne, 2010).

As biofilms are formed under a wide range and conditions by various organisms, there is no such thing as a general biofilm model. This is important to remember when comparing results amongst biofilms (Rogne, 2010).

Moving bed biofilm reactors (MBBR) systems involve biofilm growing on the inner surface of small plastic carriers, suspended within a liquid phase reactor. The carriers are kept inside the reactor by means of sieve or grill, which allows simple separation of the treated wastewater from biomass-containing carriers. Any excess biomass will be sloughed off the biofilm and leave the reactor with the effluent (Hauser, 2011).

The carriers used in this study were developed by AnoxKaldnes, now Krüger Kaldnes of Veolia Water and Solutions & Technologies (France), model Kaldnes K1. Kaldnes K1 carriers, shown in Figure 12, are made of polyethylene with a density of $0,95 \text{ g/cm}^3$, and a nominal dimension of 7 mm length and a diameter of 9 mm (Rusten et al., 2006).

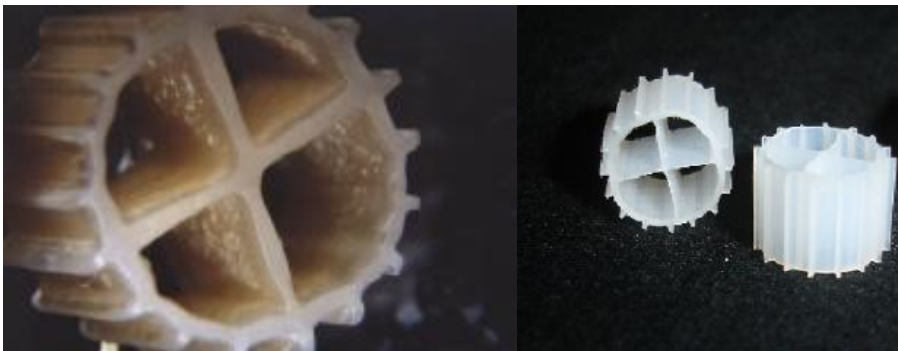


Figure 12 Enlarged Kaldnes K1 carrier with biofilm (left) and two clean Kaldnes K1 carriers in real size (right). The inside surface of the carrier is $500 \text{ cm}^2/\text{cm}^3$ (Hauser, 2011).

As shown in Figure 12, the biofilm grows mainly on the inside surface of the carrier ($500 \text{ cm}^2/\text{cm}^3$). For the carriers to move freely in the liquid suspension it is recommended that the filling fraction should be below 70 %. In every biofilm process the diffusion of compounds in and out of the biofilm is important and therefore is also the thickness of the effective biofilm (the depth of which the substrates have penetrated) of importance. The ideal biofilm in a MBBR system is thin and evenly distributed over the surface of the carrier. Normally the depth of the effective biofilm is less than $100 \mu\text{m}$. To be able to obtain an ideally depth of the biofilm the turbulence in the reactor is important for transporting the substrates (Rusten et al., 2006).

1.7 Previous studies

Pilot studies have been run since March 2009 by Master students Ana Borges Colaço, Julie Anita Skjæran and Ingrid Hauser. In summary, it has been shown that:

1. Suitable analytical methods for daily monitoring of the nitrogen balance (total nitrogen, ammonium, nitrite, nitrate and amine) are crucial. Analytical specificity and cross-interference has to be verified for each particular amine to establish proper calibration

routines. For primary amines, a fluorescence based assay has been successfully tested and applied.

2. Acute toxicity tests with a variety of amines have shown significant differences in response. Most striking, however, was the observed recovery kinetics when toxic load was removed, and the apparently irreversibly improved resistance developed by the adapted surviving ecosystem.
3. Studies with MEA have shown that efficient biological nitrogen removal can be obtained in the nitrification plus denitrification reactor sequence by adding ethanol as the necessary carbon source for the second step. When run in the recycled pre-denitrification configuration, all MEA was rapidly degraded and thereby serving as the carbon source for the anoxic respiration. Thus, no external addition of organic carbon is needed.
4. Studies with AMP show a completely different situation, where some biodegradation developed over months, but only at aerobic conditions and apparently with unknown toxic side products being formed. Anoxic utilization could not be observed.

Table 3 shows a summary of EC₅₀ values gained from previous toxicity tests with the amines MEA, AMP, DEA, MDEA and piperazine on nitrifying culture. Colaço tested the acute toxicity of MEA (twice) (Colaço, 2009), Skjæran tested the acute toxicity of AMP (Skjæran, 2010) and Hauser tested the acute toxicity of MEA, AMP, DEA, MDEA and piperazine (Hauser, 2011). Recovery values 30 h after the acute toxicity gained from Skjæran and Hauser is also given. In these previous acute toxicity tests performed by Colaço, Skjæran and Hauser only NO₃⁻-N (NOR) was measured.

Table 3 Summary of EC₅₀ values from previous toxicity tests with the amines MEA, AMP, DEA, MDEA and piperazine on nitrifying culture tested by Colaço (twice) (Colaço, 2009), Skjæran (Skjæran, 2010) and Hauser (Hauser, 2011). Recovery values 30 hours after the acute toxicity gained from Skjæran (Skjæran, 2010) and Hauser (Hauser, 2011) is also given.

Amine	Hauser 2011		Skjæran 2010		Colaço 2009 (I)	Colaço 2009 (II)
	EC _{50 (NOR)} [mM]	Recovery ~30h [%]	EC _{50 (NOR)} [mM]	Recovery ~30h [%]	EC _{50 (NOR)} [mM]	EC _{50 (NOR)} [mM]
MEA	86	109	-	-	100	10
AMP	30	41	32	100	-	-
DEA	18	27	-	-	-	-
MDEA	39	84	-	-	-	-
Piperazine	10	17	-	-	-	-

1.8 Aims of the present work

The objective of this master thesis was to test feasibility of biological treatment of selected, commonly used amines in an amine based CO₂ capture plant. The selected amines MEA, AMP, DEA, MDEA and piperazine were tested for acute toxicity on a nitrifying culture. All experiments were run on a lab bench scale. MEA were tested on an old nitrifying culture previously tested by Colaço, Skjæran and Hauser. The toxicity tests with MEA were run in two separate reactors with and without 5% CO₂ added to the air which was flushed through the reactors. The reactor where 5% CO₂ was added to the air flushed through the reactor will be referred to as MEA loaded. Meanwhile the reactor where pure air was flushed through the reactor will be referred to as MEA unloaded. The amines AMP, DEA, MDEA and piperazine were tested on a new nitrifying culture not previously tested.

The scope of this master thesis includes the following tasks:

Biofilm development

1. Set up a new bioreactor for biofilm development of nitrifying and denitrifying cultures on Kaldnes K1 carriers. The development of the nitrifying and the denitrifying cultures were monitored by measuring the activity for produced NH₄⁺-N, NO₂⁻-N and NO₃⁻-N.

Acute toxicity of selected amines

1. Selected amines are MEA, DEA, MDEA, AMP and piperazine.
2. Acute toxicity test of MEA unloaded and MEA loaded on an old nitrifying culture previously tested by Colaço, Skjæran and Hauser to estimate and compare the EC₅₀ and recovery ability 30 h after the acute toxicity with previous studies.
3. Acute toxicity test of AMP, DEA, MDEA and piperazine on a new nitrifying culture to estimate the EC₅₀ and recovery ability 30 h after the acute toxicity.

2. Material and Methods

2.1 Chemical analysis

The concentrations of ammonium, nitrate, nitrite and total nitrogen were analyzed throughout the experiments. At the start-up phase of the biofilm development in the nitrifying reactor, was the gained COD on the Kaldnes K1 carriers analyzed. Analyzes were done in an at-line reading mode by Hach-Lange assays. MEA was also determined by the use of fluorescamine assay in an at-line reading mode. The methods used including some previously observed interferences will be described in the following sections.

2.1.1 Hach-Lange assays

The concentrations of ammonium, nitrate, nitrite and total nitrogen concentration, as well as the COD were determined with assays from Hach-Lange for water quality. All assays used come in kits, which contain all the required reagents, whereas all procedures were carried out according to manufactures instruction. An overview of the assays is given in Table 4 and Table 5, with the article number, component measured, detection range and principle. All quantifications are based on colorimetric reactions, read by a Dr. Lange Lasa 100 mobile laboratory photometer. The photometer is able to recognize the different assays by reading a bar code on each cuvette being processed. For some assays when determining the COD (LCK 014, LCK 114 COD) the Dr. Lange Thermostat LT is required for thermal treatment at a specific temperature (148 °C) and time duration (2 h).

Table 4 Hach-Lange assays used for determining the concentration of ammonium, nitrate and nitrite. (Hach-Lange, 2011c, Hach-Lange, 2012, Hach-Lange, 2011d, Hach-Lange, 2011e)

Hach-Lange assay	Component measured	Range of detection [mg/l]	Principle
LCK 303 Ammonium-Nitrogen	NH_4^+ -N	2-47 mg/l	Reaction of ammonium ions at pH 12.6 with hypochlorite ions and salicylate ions in the presence of sodium nitroprusside as a catalyst to form indophenol blue.
LCK 339 Nitrate	NO_3 -N	0,23-13,5 mg/l	Nitrate ions in solutions containing sulphuric acid and phosphoric acids react with 2,6-dimethylphenol to form 4-nitro-2,6-dimethylphenol.
LCK 341 Nitrite	NO_2 -N	0,015-0,6 mg/l	Nitrites react with primary aromatic amines in acidic solution to form diazonium salts. These combine with aromatic compounds that contain an amino group or a hydroxyl group to form intensively colored azo dyes.
LCK 342 Nitrite	NO_2 -N	0,06-6 mg/l	Nitrites react with primary aromatic amines in acidic solution to form diazonium salts. These combine with aromatic compounds that contain an amino group or a hydroxyl group to form intensively colored azo dyes.

Table 5 Hach-Lange assays used for determining the chemical oxygen demand.(Hach-Lange, 2011a, Hach-Lange, 2011b)

Hach-Lange assay	Component measured	Range of detection [mg/l]	Principle
LCK 014 COD	Chemical Oxygen Demand	1000-10000	Oxidizable substances react with sulphuric acid-potassium dichromate solution in the presence of silver sulphate as a catalyst. Chloride is masked by mercury sulphate. The green coloration of Cr^{3+} is evaluated.
LCK 114 COD	Chemical Oxygen Demand	150-1000	Oxidizable substances react with sulphuric acid-potassium dichromate solution in the presence of silver sulphate as a catalyst. Chloride is masked by mercury sulphate. The Chloride is masked by mercury sulphate. The green coloration of Cr^{3+} is evaluated.

Previous studies by Colaço (Colaço, 2009) showed a clear underestimation of the ammonium concentration in the samples containing MEA providing a graph for quantitative correction, based on linear interpolation of recorded ammonium levels when the MEA concentration is known. Figure 13 shows Ammonium-N recordings according to the LCK 303 Ammonium-Nitrogen assay as a function of ammonium-N concentration, while MEA concentration was kept constant at 0, 5, 10, 20, 30 and 40 mM. This correction was applied for all samples with a MEA concentration higher than 10 mM/l.

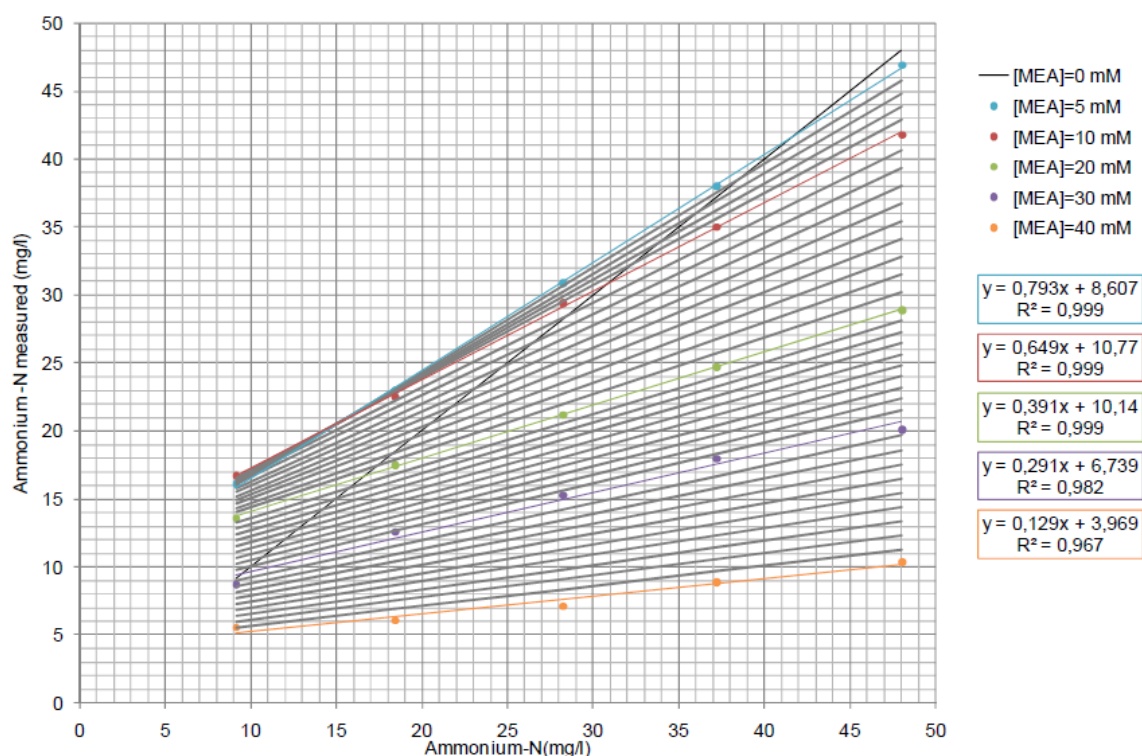


Figure 13 Ammonium-N recordings according to the LCK 303 Ammonium-Nitrogen assay as a function of ammonium-N concentration, while MEA concentration was kept constant at 0, 5, 10, 20, 30 and 40 mM (Colaço, 2009). Secondary lines, in grey provide guidance for linear interpolation.

2.1.2 Fluorescamine assay (Hauser, 2011)

Fluorescamine assays allow the detection of primary amines in the picomole range, whereas the reaction occurs almost instantaneously at room temperature in aqueous solutions. The products are stable highly fluorescent compounds with an excitation wavelength of 392 nm and an emission at 480 nm, whereas the reagent and its degradation products are non-fluorescent.

24 h before the assay a fluorescamine solution of 1 mg/ml was prepared, by dissolving 10 mg of Fluorescamine (Sigma-Aldrich) in 10 ml of acetone (BDH Prolabo), and kept in the dark.

An assay buffer was prepared in Milli-Q water consisting of 100 mM boric acid (analytical grade from Roth, 61,83 g/mol) with addition of NaOH (analytical grade from BDH Prolabo) until pH 7,0-9,5.

For each measurement series a calibration curve of fluorescamine, being 0, 0,2, 0,4, 0,6, 0,8 and 1,0 mM, was prepared to determine the concentration in the samples by interpolation.

When required, a dilution of the sample was made using Milli-Q water.

Right before the measurements 100 µl of each sample was diluted in 2,9 ml assay buffer and then 200 µl fluorescamine solution was rapidly added. Samples were then inverted 4-5 times and incubated in the dark for 20 min.

The fluorescence signal was measured in UV-grade polymethylmethacrylate disposable cuvettes from VWR, using a Perkin Elmer LS50B fluorimeter. The excitation wavelength was set to 392 nm and emission was measured at 480 nm, with 5-10 nm slit width.

2.2 Biofilm development

To track the development of the nitrifying biofilm on Kaldnes K1 carriers in the start-up phase, the gained COD was taken as measure. COD is the chemical oxygen demand and represents the total organic content which can be oxidized by sulphuric acid-potassium dichromate solution in the presence of silver sulphate as a catalyst.

2.2.1 Monitoring

The biofilm development on the Kaldnes K1 carriers was monitored in the start-up phase for the nitrifying reactor, analyzing the carriers for their COD with five replicates with Hach-Lange assay LCK014. Each carrier was rinsed with distilled water and cut into small pieces with a scalpel to fit into the opening of the test cuvette. Distilled water was added according to manufacturer's instruction. To monitor the nitrification and denitrification activity of the biofilm, samples of about 5 ml were taken from the reactors at least three times a week between day 1 and day 69 and 90 for the

denitrifying reactor and nitrifying reactor respectively. The samples were collected with a syringe from BD Plastipak and filtered with 0,45 µm filters from Sarstedt to remove suspended biomass. The filtrates were analyzed with Hach-Lange assay for ammonium, nitrate and nitrite concentration as described in section 2.1.1, and when necessary diluted with distilled water to fit in the detection range of each assay.

2.3 Nitrification

2.3.1 Inoculum

The nitrification reactor was inoculated on the 9th of January (day zero) in a 1 l reactor and immobilized on 300 ml Kaldnes K1 carriers. The medium had high ammonium content, 200 mg NH₄⁺-N/l. The inoculum was fresh sludge sewage from Ladehammeren domestic wastewater treatment plant in Trondheim, as well as enriched nitrifying sludge frozen from a previous lab course (TBT4130 Environmental Biotechnology at NTNU).

On the 23rd of January (day 14) the reactor was up scaled to a 2 l reactor adding 400 ml new Kaldnes K1 carriers, to the total of 700 ml carriers. On the 6th of February (day 28) the reactor was up scaled to a 5 l reactor with 700 ml Kaldnes K1 carriers.

2.3.2 Medium

The medium for the nitrification reactor is shown in Table 6 and Table 7. All components were dissolved in tap water and the pH was adjusted to 7,5 with 6 M HCl solution. A Media batch of 10 l was prepared at a time. All chemicals used in the medium were of analytical grade.

Table 6 Composition of the medium supplied to the nitrification reactor.

Compound	Distributor	Concentration
(NH ₄) ₂ SO ₄	Merck, Darmstadt, Germany	0,236 g/l [50 mg/l NH ₄ ⁺ -N]
(NH ₄) ₂ SO ₄	Merck, Darmstadt, Germany	0,472 g/l [100 mg/l NH ₄ ⁺ -N]
(NH ₄) ₂ SO ₄	Merck, Darmstadt, Germany	9,44 g/l [200 mg/l NH ₄ ⁺ -N]
(NH ₄) ₂ SO ₄	Merck, Darmstadt, Germany	11,8 g/l [250 mg/l NH ₄ ⁺ -N]
(NH ₄) ₂ SO ₄	Merck, Darmstadt, Germany	14,16 g/l [300 mg/l NH ₄ ⁺ -N]
K ₂ HPO ₄	(MV Laboratories) SDS, Zi de Valdonne, France	0,4 g/l
NaHCO ₃	Merck, Darmstadt, Germany	1,0 g/l
Trace metal solution		10 ml/l

Table 7 Composition of the trace metal stock solution, 100-fold.

Compound	Distributor	Concentration [mg/l]
$\text{MgSO}_4 \cdot 7\text{H}_2\text{O}$	Merck Darmstadt, Germany	25
$\text{CaCl}_2 \cdot 2\text{H}_2\text{O}$	Merck, Darmstadt, Germany	15
$\text{FeCl}_2 \cdot 4\text{H}_2\text{O}$	Merck Darmstadt, Germany	2.0
$\text{MnCl}_2 \cdot 2\text{H}_2\text{O}$	Merck Darmstadt, Germany	5,5
ZnCl_2	Merck Darmstadt, Germany	0,68
$\text{CoCl}_2 \cdot 6\text{H}_2\text{O}$	Merck Darmstadt, Germany	1,2
$\text{NiCl}_2 \cdot 6\text{H}_2\text{O}$	ACROS Organics	1,2
EDTA	Merck Darmstadt, Germany	2,8

Before inoculating the carriers, the enriched sludge culture was supplied with excess substrate (200 mg $\text{NH}_4^+\text{-N/l}$) and kept in batch over the weekend. After the inoculation of the carriers the $\text{NH}_4^+\text{-N}$ concentration in the medium was adjusted between 50 mg/l and 100 mg/l to establish a well developed biofilm, while preventing nitrite accumulation and subsequent inhibition of the nitrifying process.

2.3.3 Reactor

The reactor for the nitrification culture was set up as a standard 1 l glass reactor, and later carefully scaled up to 2 l and then 5 l with aeration. The experimental set-up of the nitrification reactor is shown in Figure 14.

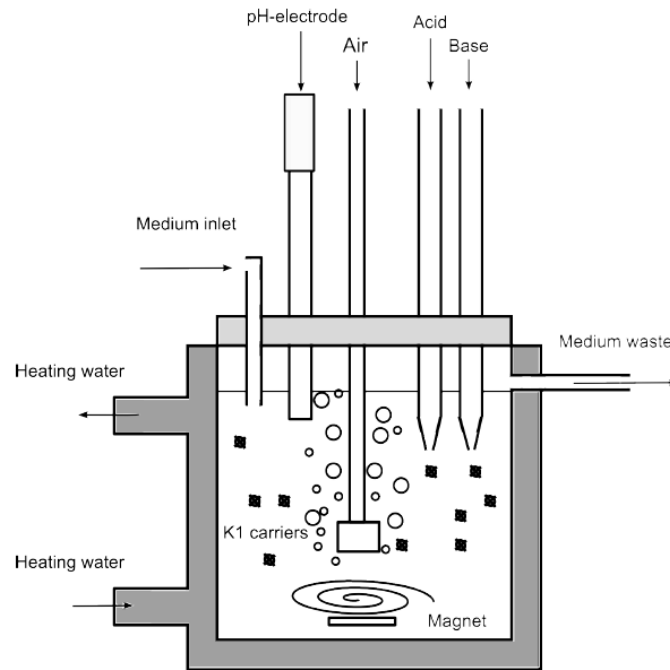


Figure 14 The experimental set-up of the nitrification reactor (Hauser, 2011).

The equipment used for the experimental set-up of the nitrification reactor was as follows:

- Outer glass jacket for temperature control.
- Water bath set to 25°C (Cole-Parmer polystat)
- pH-electrode and controller displaying pH and temperature (CONSORT CONTROLLER R301)
- Oxygen filter (Rexroth R412004418)
- Pump for medium supply (ISMATEC MCP, pump head type: ISM734B)
- Pumps for adding acid and base (Masterflex model 7014-20, Cole-Parmer Instrument Company)
- Magnetic stirrer at 300 rpm with 10 cm magnetic stirrer bar (Heidolph DREHZAHL No. 50300, type MRO)
- 700 ml biofilm carriers. (Added 300 ml Kaldnes K1 carriers on day zero, and 400 ml Kaldnes K1 carriers were added on day 14)

The range of pH was controlled by automatic addition of 0,5 M HCl or NaOH solutions and was set between 7,3 and 7,8. The wide pH range was chosen in order to avoid high salinity through increased addition of acid and base, even though the optimum pH for nitrification in biofilm is approximately 7,5. The reactor was covered with a black plastic bag and the medium container was kept in the fridge at 4°C to avoid unwanted algal growth in the system.

During the stabilization phase of the nitrification reactor, the reactor was operated in batch mode and fed with 200 mg/l $\text{NH}_4^+\text{-N}$ for two days and then 100 mg/l $\text{NH}_4^+\text{-N}$, see Table 6, until day four when the reactor was put on continuous flow mode with a flow rate of 100 ml/h and a $\text{NH}_4^+\text{-N}$ concentration of 100 mg/l. This was also done by Hauser (Hauser, 2011), but then the carriers were pre-inoculated in organic matter. A washout was observed when put on continuous flow with a flow rate of 100 ml/h, and therefore indicating that the flow rate should have been started at a lower level since the carriers were not pre-inoculated. The flow rate was adjusted to 50 ml/h until the up scaling to a 2 l glass reactor on day 14 after inoculation. After the up scaling the reactor was put on batch with a medium concentration of 250 mg $\text{NH}_4^+\text{-N/l}$, this was repeated three times. On day 28 the reactor was up scaled to a 5 l glass reactor and put in a continuous flow mode the next day with a flow rate of 100 ml/h and a $\text{NH}_4^+\text{-N}$ concentration of 250 mg/l. On day 52 the $\text{NH}_4^+\text{-N}$ concentration was raised to 300 mg/l.

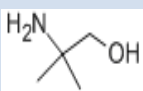
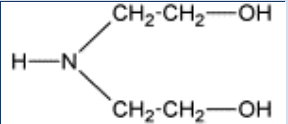
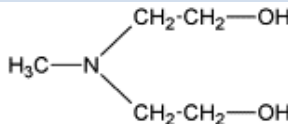
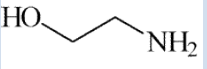
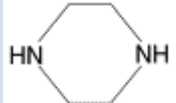
2.3.4 Monitoring

In addition to monitoring the nitrification activity of the biofilm, as described in section 2.2.1, the flow rate (ml/h), pH and DO (%) were also noted.

2.3.5 Acute Toxicity Test

Acute toxicity tests were carried out on the nitrifying culture to estimate the EC_{50} of five commonly used amines in CCS, which are MEA (loaded and unloaded), AMP, MDEA, DEA and piperazine. See Table 8 for a brief description of the investigated amines.

Table 8 Chemicals tested for acute toxicity on the nitrifying culture (Hauser, 2011).

	AMP	DEA	MDEA	MEA	Piperazine
Structure					
MW [g/mol]	89,14	105,14	119,16	61,08	86,14
MF	$\text{C}_{14}\text{H}_{11}\text{NO}$	$\text{C}_4\text{H}_{11}\text{NO}_2$	$\text{C}_5\text{H}_{13}\text{NO}_2$	$\text{C}_2\text{H}_7\text{NO}$	$\text{C}_4\text{H}_{10}\text{N}_2$
Density [g/ml]	0,934	1,097	1,038	1,012	1,1
CAS-Number	124-685	111-42-2	105-59-9	141-43-5	110-85-0
Distributor	Sigma-Aldrich Norway, Oslo	Fluka Norway, Oslo	Sigma-Aldrich Norway, Oslo	Sigma-Aldrich Norway, Oslo	Merck Darmstadt, Germany

Previously, the standardized assay was also done on MEA (Colaço, 2009), on AMP (Skjæran, 2010) and on AMP, DEA, MDEA, MEA and piperazine (Hauser, 2011) on a nitrifying culture.

MEA loaded and MEA unloaded were first tested for acute toxicity on the nitrifying culture previously tested by Colaço (Colaço, 2009), Skjæran (Skjæran, 2010) and Hauser (Hauser, 2011). 200 ml of carriers were transferred from the nitrifying reactor into two empty batch reactors, with the same set-up as shown in Figure 14, containing 100 ml of carriers each. Both reactors were filled with 500 ml medium as described in section 2.3.2 with an ammonium concentration of 50 mg $\text{NH}_4^+\text{-N}$ /l.

Over a total time range of 3 hours were samples of 5 ml taken every 30 minutes. The samples were collected with a syringe from BD Plastipak and filtered with 0,45 μm filters from Sarstedt to remove any suspended biomass. The filtrates were then analyzed with Hach-Lange assays, see section 2.1.1, for their $\text{NO}_3\text{-N}$, $\text{NO}_2\text{-N}$ and $\text{NH}_4^+\text{-N}$ concentrations, and when necessary diluted with distilled water to fit in the detection range of the assay.

After the 3 hours the reactors were drained and refilled with 500 ml media containing MEA. Following this procedure, the biofilm carriers were subsequently exposed to a series of logarithmic increasing concentrations of MEA ranging from 0, 3,16, 10, 31,6, 100 to 316 mM. The respective solutions were prepared in 500 ml medium, as described in section 2.3.2, with an ammonium concentration of 50 mg $\text{NH}_4^+\text{-N}$ /l and pH adjusted to 7,5 with 6 M HCl solution. Figure 15 show the flow diagram of the experiment.

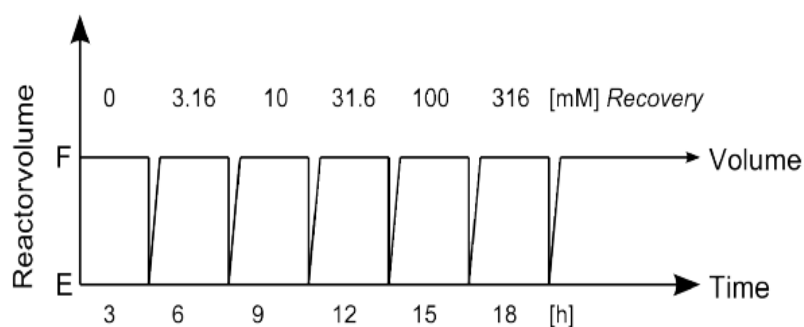


Figure 15 Flow schema of the acute toxicity assay, where E stands for empty and F stands for full (Hauser, 2011).

After monitoring the highest concentration, the biofilm was washed twice with tap water and left in medium (as described in section 2.3.2) with an ammonium concentration of 50 mg $\text{NH}_4^+\text{-N}$ /l for recovery and an activity monitoring over 3 hours was done after 30 hours. After the recovery the biofilm was frozen.

The four amines AMP, DEA, MDEA and piperazine were then tested on the new developed nitrifying culture, on day 85 after inoculation, using the same procedure. The four batch reactors had the same set-up as shown in Figure 14 and contained 100 ml carriers each. After monitoring the highest concentration, the biofilm was washed twice with tap water and left in medium (as described in section 2.3.2) with an ammonium concentration of 50 mg $\text{NH}_4^+\text{-N}$ /l for recovery and an activity monitoring over 3 hours was done after 30 hours. After the recovery the biofilm was frozen.

The results of the $\text{NO}_3\text{-N}$, $\text{NO}_2\text{-N}$ and $\text{NH}_4^+\text{-N}$ were used to calculate the respective effect of the nitrifying culture. EC_{50} , the effect concentration at which the activity reaches a level of 50 %, was found by plotting the produced amount of $\text{NO}_3\text{-N}$ and the sum of produced $\text{NO}_3\text{-N}$ and $\text{NO}_2\text{-N}$ as a function of time, the slope expresses the nitrification activity in (mg/h). The respective activity, and the recovery, was then normalized with the initial activity, expressed in percent, and plotted versus concentration in log-scale.

2.4 Denitrification

2.4.1 Inoculum

The denitrification reactor was inoculated on the 9th of January (day zero) in a 1 l reactor and immobilized on 300 ml Kaldnes K1 carriers. The medium had a nitrate content of 138 mg $\text{NO}_3\text{-N}$ /l. The inoculum was fresh sludge sewage from Ladehammeren domestic wastewater treatment plant in Trondheim. On day 18 the $\text{NO}_3\text{-N}$ content in the medium was adjusted to 553 mg/l.

On the 6th of February (day 28) the reactor was up scaled to a 2 l reactor.

2.4.2 Medium

The medium for the denitrification reactor is shown in Table 9. The same trace metal solution was used for both the nitrification reactor and the denitrification reactor, see Table 7. All components were dissolved in deaerated tap water and the pH was adjusted to 7,5 with 6 M HCl solution. A Media batch of 4 l was prepared at a time. All chemicals used in the medium were of analytical grade, except for the yeast extract and ethanol which were technical grade.

Table 9 Medium composition for the denitrification reactor.

Compound	Distributor	Concentration
K_2HPO_4	(MV Laboratories) SDS, Zi de Valdonne, France	0,533 g/l
NH_4Cl	Merck, Darmstadt, Germany	0,253 g/l
KNO_3	Merck, Darmstadt, Germany	4,0 g/l
Yeast extract	Oxoid	0,05 g/l
Ethanol	Kemetyl	1,0 g/l
Trace metal solution		10 ml/l

The deaeration of the tap water was done by connecting the water flask to a water suction pump, as the pressure reduction inside the flask makes the dissolved oxygen boil out. The set-up for the deaeration of the medium water is shown in Figure 16. In order to achieve complete removal of DO, the water was stirred over a time period of 2 hours for a volume of 4 l of tap water.

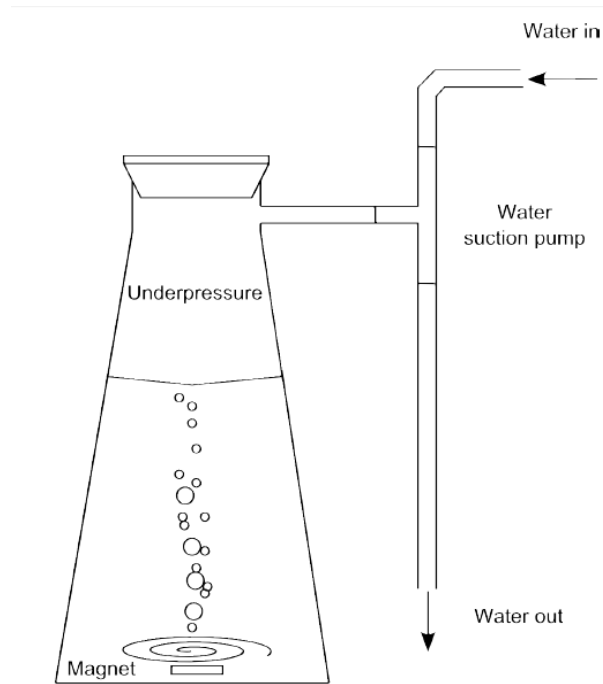


Figure 16 Set-up for the deaeration of the medium water (Hauser, 2011).

2.4.3 Reactor

The reactor for the denitrification culture was set up as a standard 1 l glass reactor, and later carefully scaled up to 2 l. The experimental set-up of the denitrification reactor is shown in Figure 17.

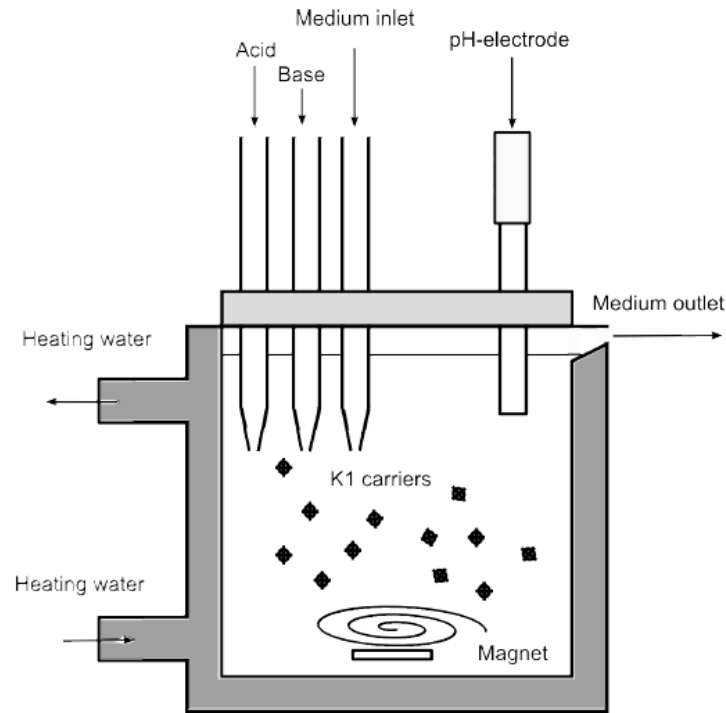


Figure 17 The experimental set-up of the denitrification reactor. (Hauser, 2011)

The equipment used for the experimental set-up of the nitrification reactor was as follows:

- Outer glass jacket for temperature control.
- Water bath set to 25°C (Cole-Parmer polystat)
- pH-electrode and controller displaying pH and temperature (CONSORT CONTROLLER R301)
- Pump for medium supply (Masterflex® model 7518-10, Cole-Parmer Instrument Company)
- Pumps for adding acid and base (Masterflex® model 7016-20 and model 7016-21, Cole-Parmer Instrument Company)
- Magnetic stirrer at 350 rpm with 8 cm magnetic stirrer bar (MINI MR1 basic, IKA Labortechnik)
- 300 ml biofilm carriers.

The range of pH was controlled by automatic addition of 0,5 M HCl or NaOH solutions and was set between 6,8 and 7,3. The wide pH range was chosen in order to avoid high salinity through increased addition of acid and base, even though the optimum pH for nitrification in biofilm is approximately 7. The reactor was covered with a black plastic bag and the medium container was kept in the fridge at 4°C to avoid unwanted algal growth in the system.

On day one the reactor was put on continuous flow mode with a flow rate of 36 ml/h and $\text{NO}_3\text{-N}$ content of 138 mg/l. On day 18 the $\text{NO}_3\text{-N}$ concentration in the medium was adjusted to 553 mg/l.

On day 30 the flow rate was adjusted to 60 ml/h, and on day 45 the flow rate was again adjusted to 90 ml/h.

2.4.4 Monitoring

In addition to monitoring the denitrification activity of the biofilm, as described in section 2.2.1, the flow rate (ml/h) and pH were also noted.

2.5 Waste handling

Throughout the experiments, the generated waste containing amines, was collected and disposed of the Department of Biotechnology, NTNU, and further processed according to regulations.

3. Results

3.1 Nitrification

Nitrification was promoted with excess $\text{NH}_4^+\text{-N}$ until a steady-state was reached. And then the acute toxicity of MEA, AMP, DEA, MDEA and piperazine was tested. Figure 18 shows the experimental timeline of the main nitrification reactor.

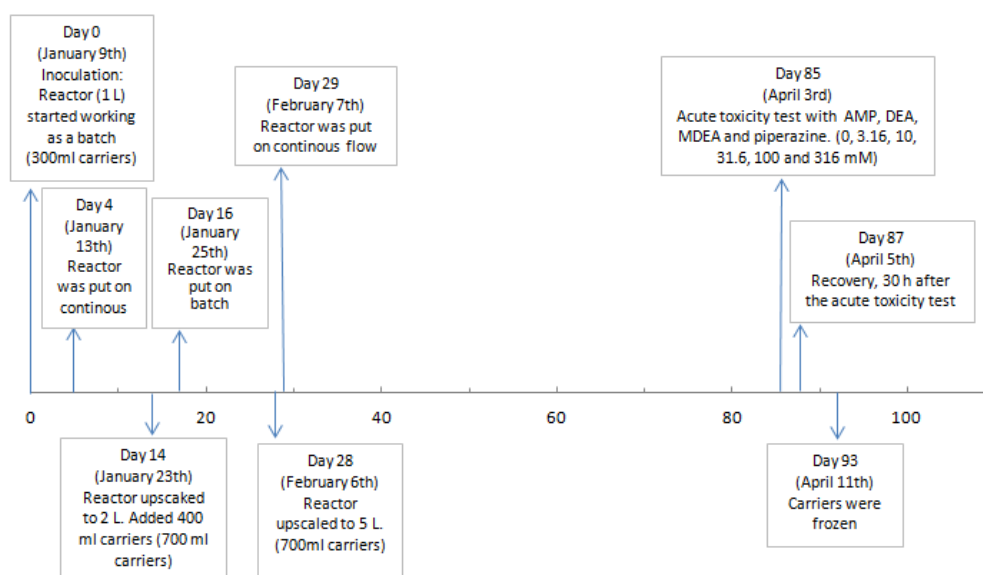


Figure 18 The experimental timeline (in days) of the main nitrification reactor.

3.1.1 Stabilization

The development and stabilization of the nitrification reactor is shown in Figure 19 and Figure 20.

Figure 19 shows the concentration of the components, $\text{NH}_4^+\text{-N}$, $\text{NO}_3\text{-N}$ and $\text{NO}_2\text{-N}$, in the nitrification process, from day zero, when the carriers were added to the reactor together with the nitrification medium, until day 88. Figure 20 shows the production rate of the nitrifying activity represented as nitrate loading rate (NLR) and produced nitrate and nitrite, for the time period after the up scaling to a 5 l glass reactor with a continuous flow mode with a flow rate of 100 ml/h (day 29) until day 88.

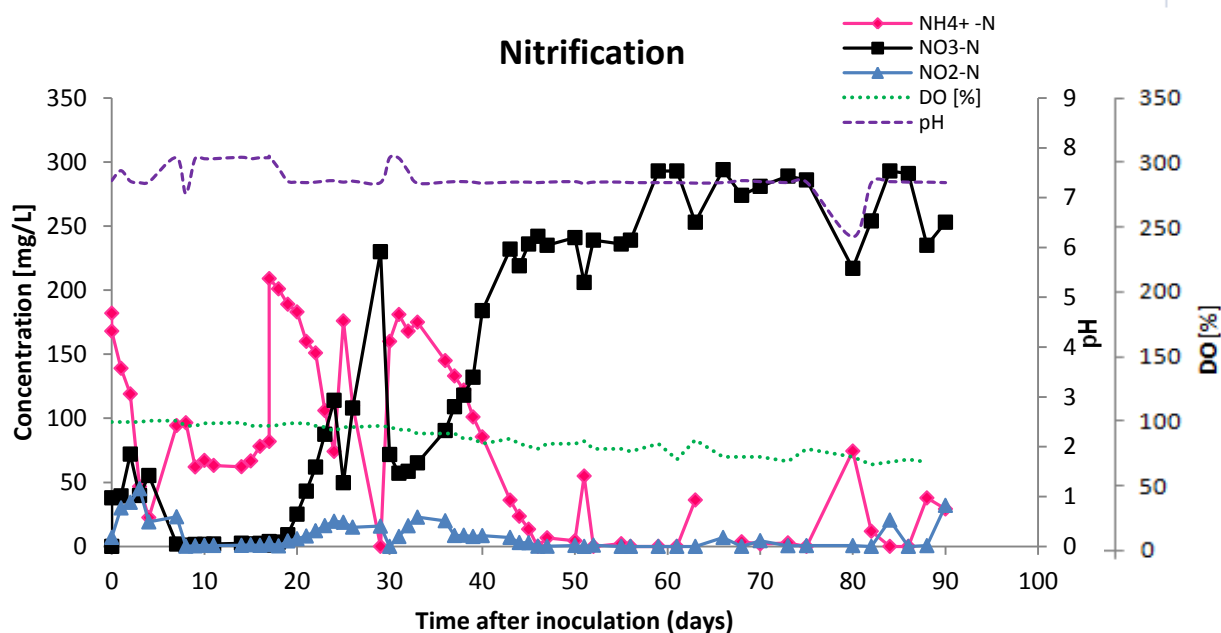


Figure 19 Measured activity [mg/l] of ammonium ($\text{NH}_4^+\text{-N}$), nitrite ($\text{NO}_2\text{-N}$) and nitrate ($\text{NO}_3\text{-N}$), and monitored pH and dissolved oxygen (DO) concentration [%] in the nitrification reactor. The measurement started at day zero, when adding the Kaldnes K1 carriers, until day 88.

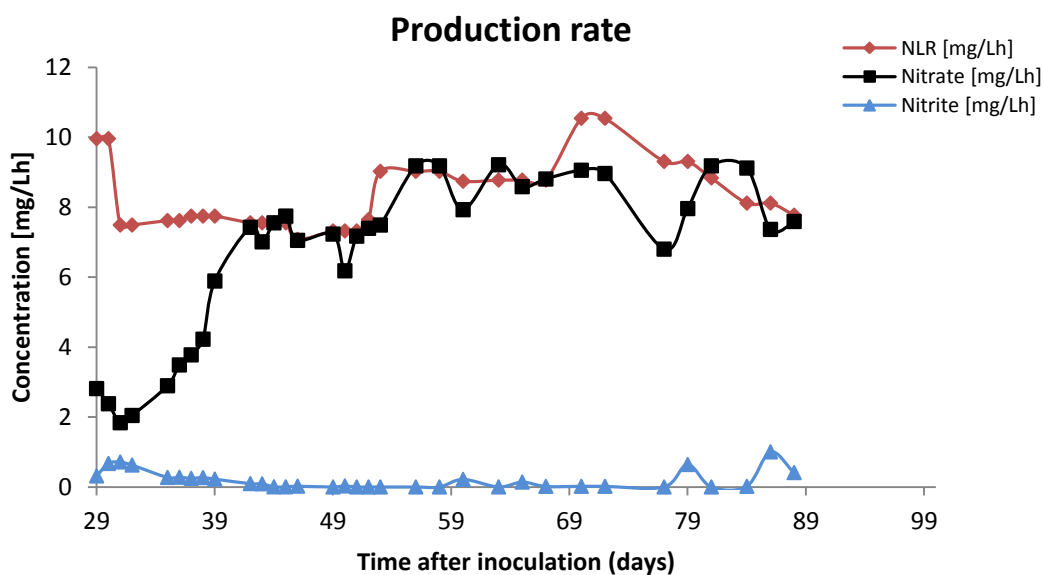


Figure 20 The production rate of the nitrifying activity represented as nitrate loading rate (NLR) and produced nitrate and nitrite, starting on day 29 after the up scaling to a 5 l glass reactor when the reactor were on a continuous flow mode with a flow rate of 100 ml/h until day 88.

During the stabilization phase of the nitrification reactor, the reactor was operated in batch mode and fed with 200 mg/l $\text{NH}_4^+\text{-N}$ for two days and then 100 mg/l $\text{NH}_4^+\text{-N}$, until day four when the

reactor was put on continuous flow mode with a flow rate of 100 ml/h and a NH_4^+ -N concentration of 100 mg/l. A washout was observed showing an increase in the NH_4^+ -N activity in Figure 19. After adjusting the flow rate to 50 ml/h and up scaling the reactor to a 2 l glass reactor on day 14, the NH_4^+ -N activity was still high. Therefore the reactor was put on batch with a medium concentration of 250 mg NH_4^+ -N/l; this was performed three times, as shown in Figure 19. After the procedure of feeding the nitrifying culture three times with a high ammonium concentration (250 mg/l) in batch, the nitrification activity increased, as shown in Figure 19. After the last up scaling to a 5 l reactor on day 28 and the continuous flow mode the following day with a flow rate of 100 ml/h the nitrifiers had to adapt, but around day 43 after the inoculation the nitrification activity stabilized and a well adjusted nitrifying culture was obtained, as shown in Figure 19, indicating that the AOB and the NOB were equally developed and that the nitrifying biofilm was robust and well established.

On day 77 the pump which adjusted the 0,5 M NaOH had stopped and therefore showing a decrease in pH concentration in Figure 19, showing that a drop in pH influenced the nitrification activity by decreasing the NO_3 -N produced and increasing the NH_4^+ -N activity. Along the process there were some operational problems with pumps which were replaced.

On the 85th day after inoculation 500 ml of carriers were taken out to five new reactors with 100 ml of carriers in each reactor, so the acute toxicity of AMP, DEA, MDEA and piperazine could be tested. After the removal of the carriers there was observed a loss in activity and accumulation of nitrite and ammonium, as was expected.

3.1.2 Biofilm development

To find the gained COD per Kaldnes K1 carrier in the nitrification culture the measured COD value per Kaldnes K1 carrier had to be found. This was done by the geometric mean of three replicates. The results of measured COD [mg/l] per empty Kaldnes K1 carrier, see appendix A, gave a COD per Kaldnes K1 carrier of (5182±238) mg/l. Compared to previous measurement done by Hauser (Hauser, 2011) ((748±75) mg/l) this was a significant increase, and therefore the measurement was repeated with different treatment of the empty carrier before measuring the COD value. The carriers were incubated over night in different solutions; nitrification media (see section 2.3.2), Milli-Q water, Milli-Q water with 1 % trace metal stock solution (see section 2.3.2) and ethanol (EtOH). The affect of rinsing the empty carrier with distilled water before measuring the COD value was also investigated, but neither of the experiments resulted in decrease in the COD value of the Kaldnes K1 carrier, see appendix A. Because the COD value of the empty Kaldnes K1 carrier were on the level of the Kaldnes K1 carrier with biofilm on, being (5246±225) mg/l on day 7 after inoculation following the procedure

described in section 2.2.1, the gained COD per Kaldnes K1 carrier in the nitrification culture could not be followed.

3.2 Inhibition of nitrification

3.2.1 Biofilm history

The acute toxicity of five different amines was tested in six independent experiments. Table 10 gives an overview of the chronological order and which amines were tested on which biofilm. The results will be organized according to this experimental outline in the following section.

Table 10 Acute toxicity experiments on nitrifying culture.

Experiment	Date	Tested amine	Biofilm origin	Previous exposure
1 - 2	7.3.2012	MEA unloaded and MEA loaded	Nitrification (section 2.3)	MEA, AMP, DEA, MDEA and Piperazine
3 - 6	3.4.2012	AMP, DEA, MDEA, Piperazine	Nitrification (section 2.3)	None

3.2.2 State of biofilm

Previous experiments have indicated diversity between tested-biofilms, it is therefore important to take into consideration the state of the biofilm before carrying out an acute toxicity test. The nitrifying activity of the old and the new biofilm is given in Figure 21 and Figure 22 where time (h) is plotted against measured concentration (mg/l) of NO_3^- -N, NO_2^- -N and NH_4^+ -N before adding the test substances to the media. The nitrifying activity of the old biofilm before the acute toxicity of MEA loaded and the nitrifying activity of the biofilm in the four reactors were DEA, MDEA and piperazine were tested are given in appendix B.

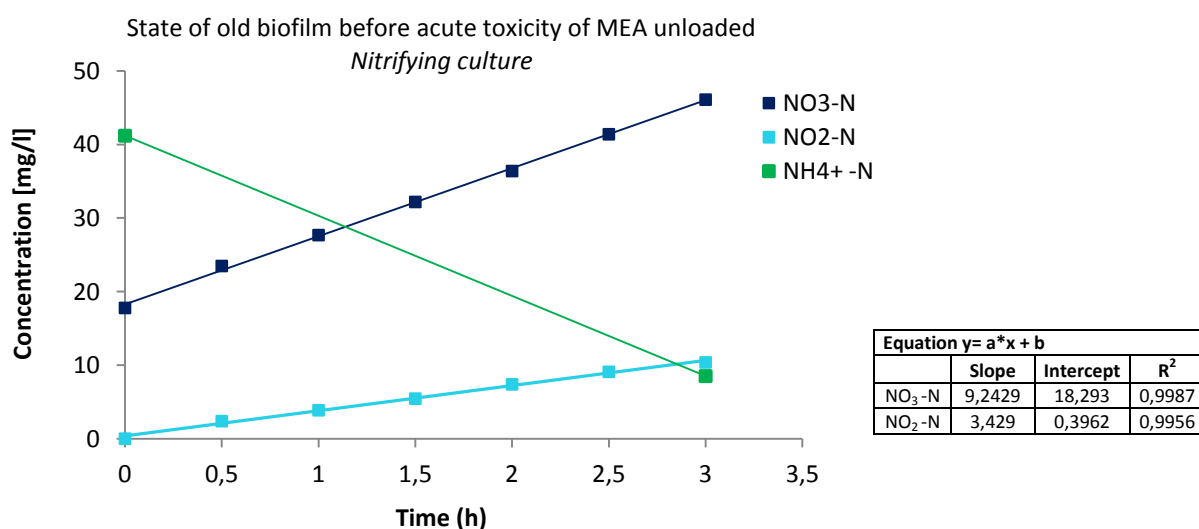


Figure 21 The nitrifying activity of the biofilm previously tested by Colaço, Skjæran, and Hauser before the acute toxicity of unloaded MEA on the nitrifying culture.

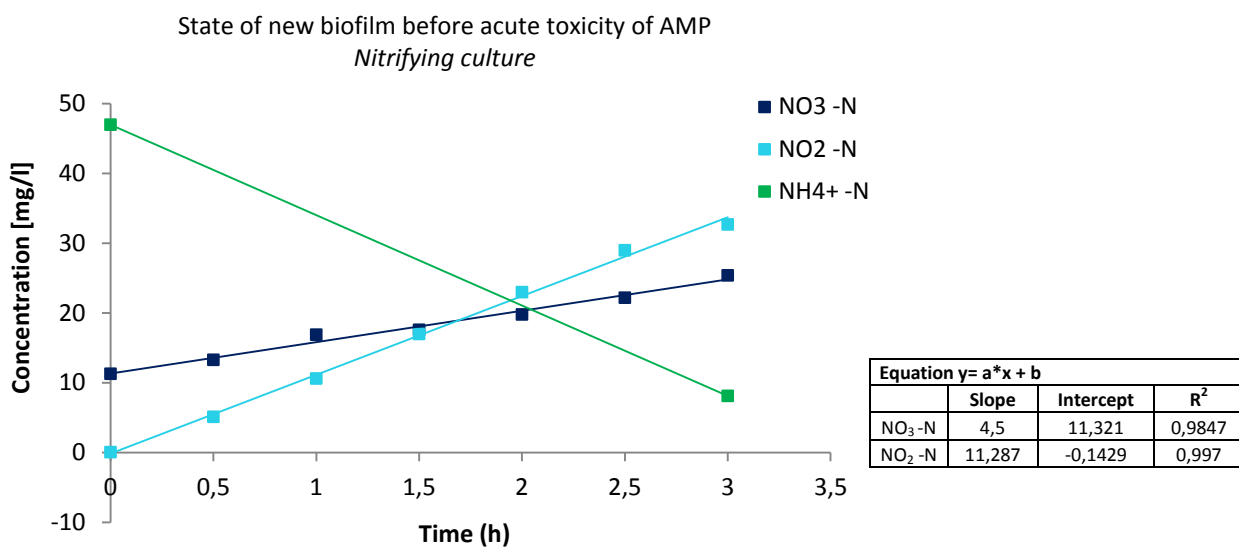


Figure 22 The nitrifying activity of the biofilm not previously tested, before the acute toxicity of AMP on the nitrifying culture.

3.2.3 Acute toxicity test on old biofilm

The results of experiment 1 and 2 are given in Figure 23-30 as the nitrification activity in terms of nitrite oxidizing rate and ammonia oxidizing rate during the acute toxicity test of MEA unloaded and MEA loaded on the nitrifying culture and the corresponding recovery 30 hours after the acute toxicity test as a function of time. The nitrification activity in terms of nitrite (NO₂-N) and ammonium (NH₄⁺-N) concentrations during the acute toxicity test of MEA unloaded and MEA loaded on the nitrifying culture and the corresponding recovery 30 hours after the acute toxicity test as a function of time are given in appendix C.

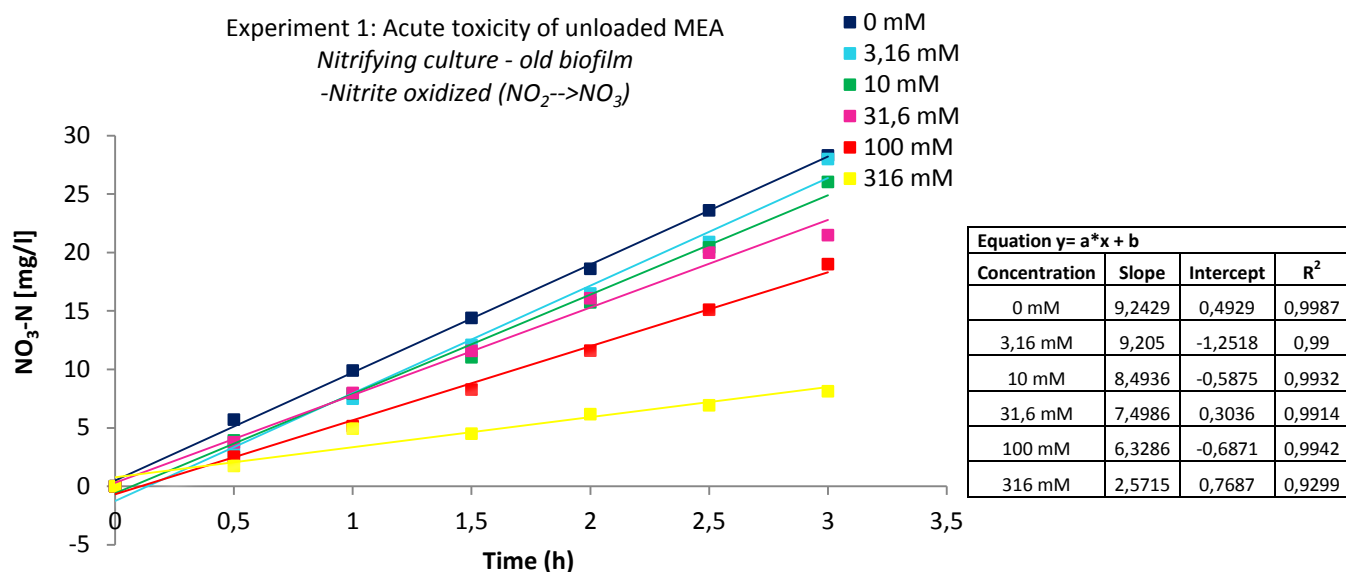


Figure 23 The nitrification activity in terms of nitrite oxidized during acute toxicity of unloaded MEA on the nitrifying culture.

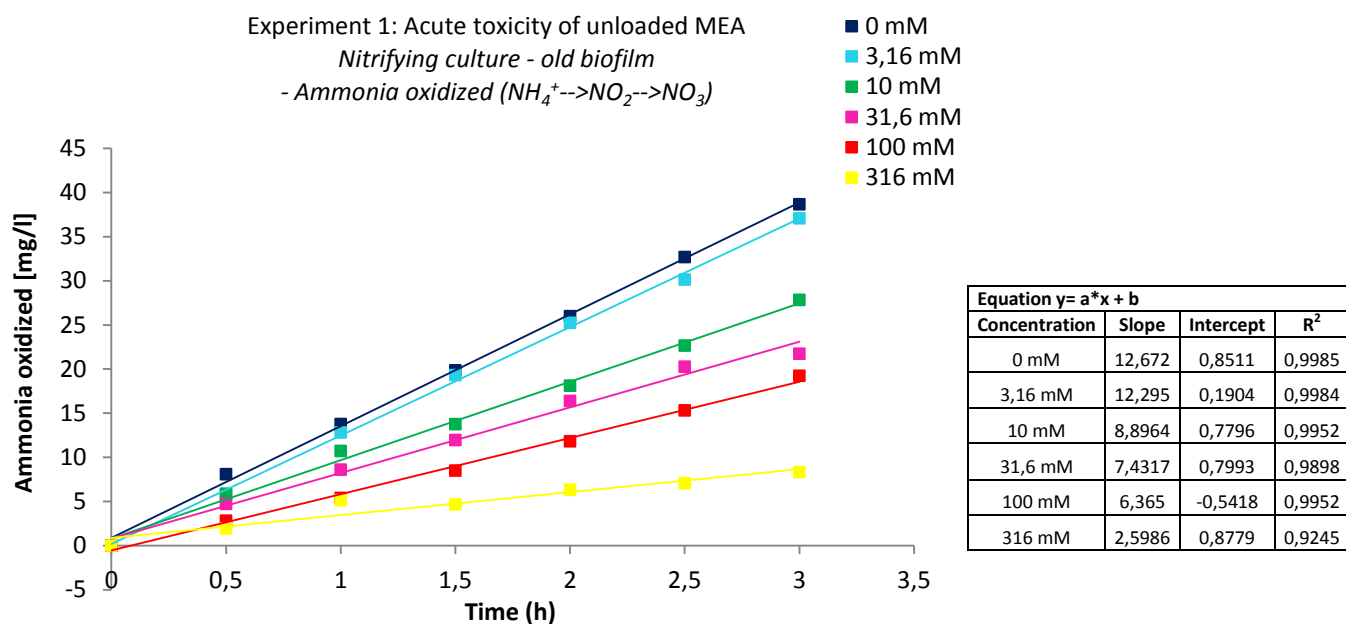


Figure 24 The nitrification activity in terms of ammonia oxidized during acute toxicity of unloaded MEA on the nitrifying culture.

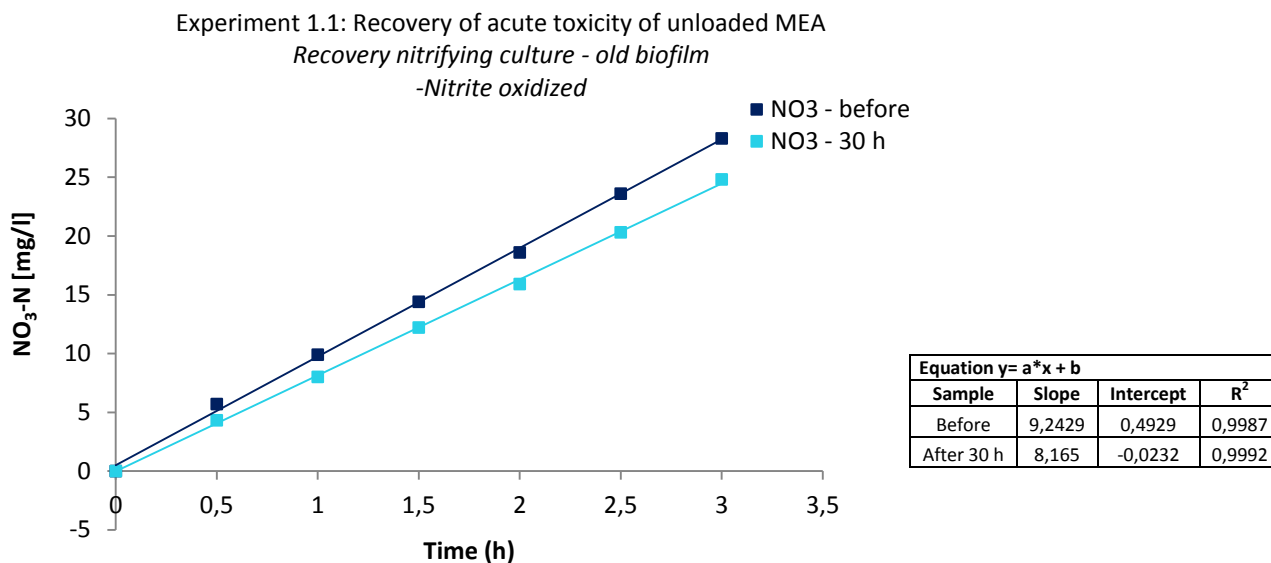


Figure 25 The nitrification activity after 30 hours of recovery of the acute toxicity of unloaded MEA on the nitrifying culture.

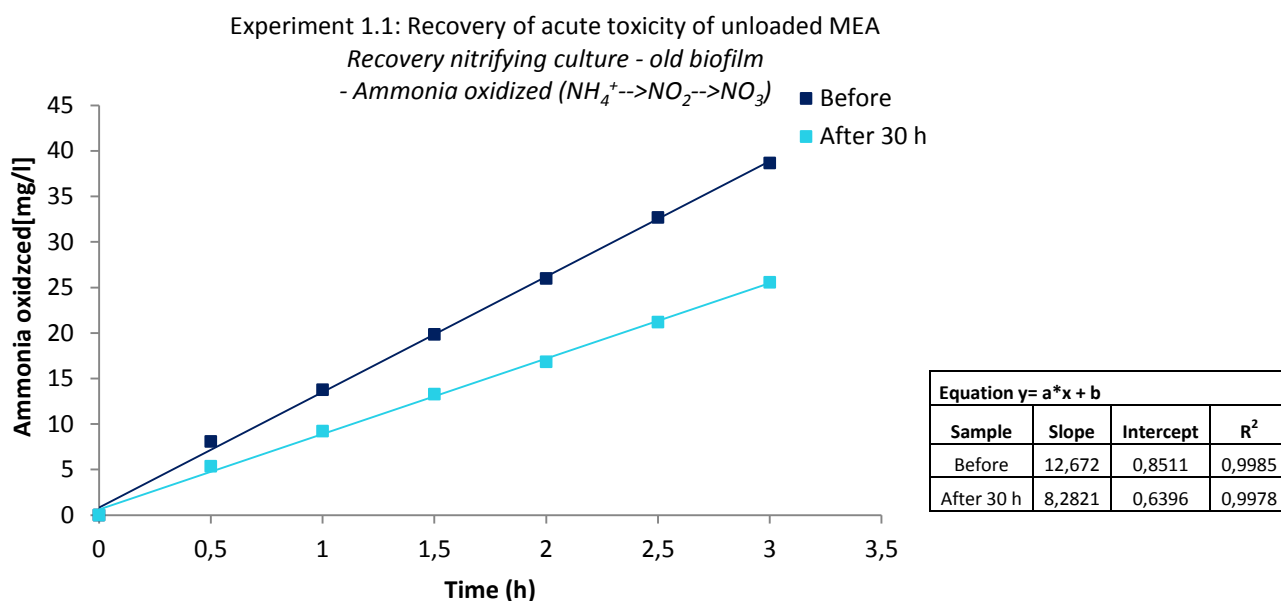


Figure 26 The nitrification activity after 30 hours of recovery of the acute toxicity of unloaded MEA on the nitrifying culture.

The activity during the acute toxicity test with MEA unloaded decreased with increased concentration of MEA unloaded, but the nitrification process never stopped. The recovery in respect to the initial activity was 65 % after 30 hours.

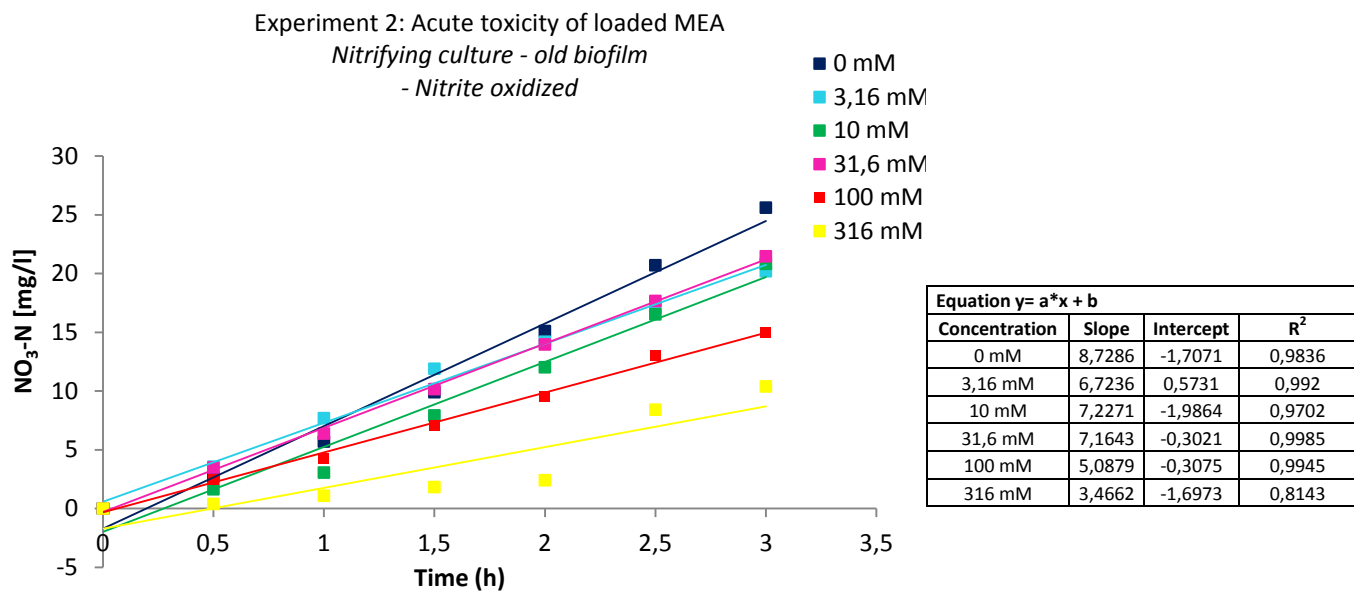


Figure 27 The nitrification activity in terms of nitrite oxidized during acute toxicity of loaded MEA on the nitrifying culture.

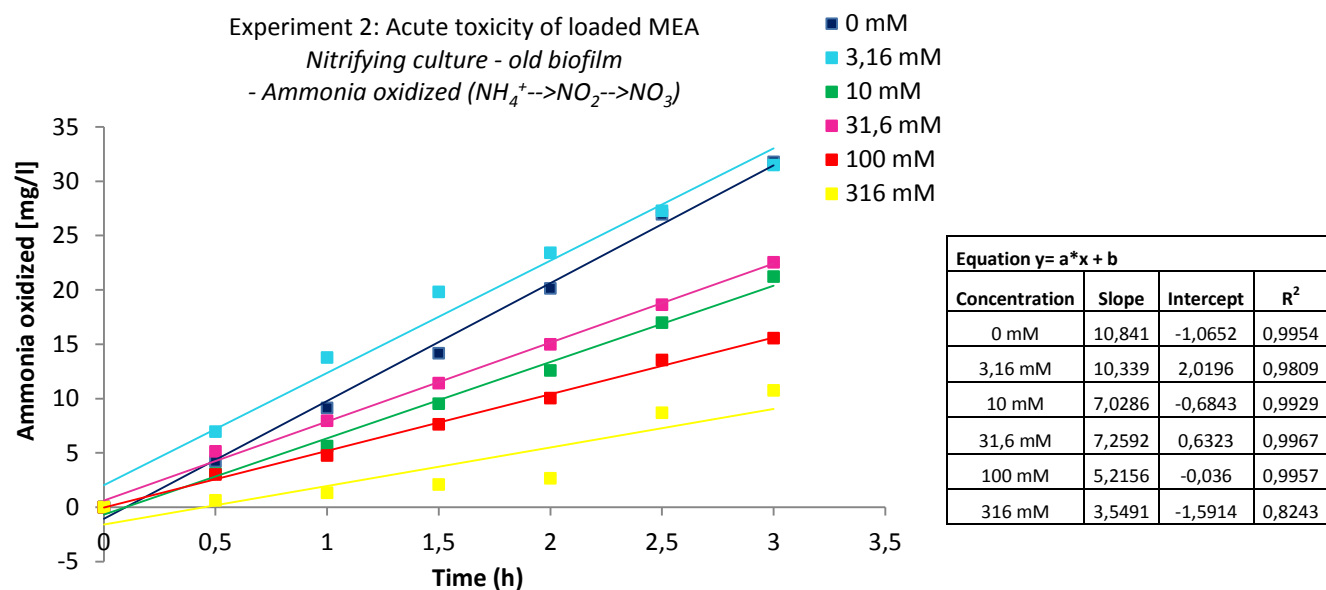


Figure 28 The nitrification activity in terms of ammonia oxidized during acute toxicity of loaded MEA on the nitrifying culture.

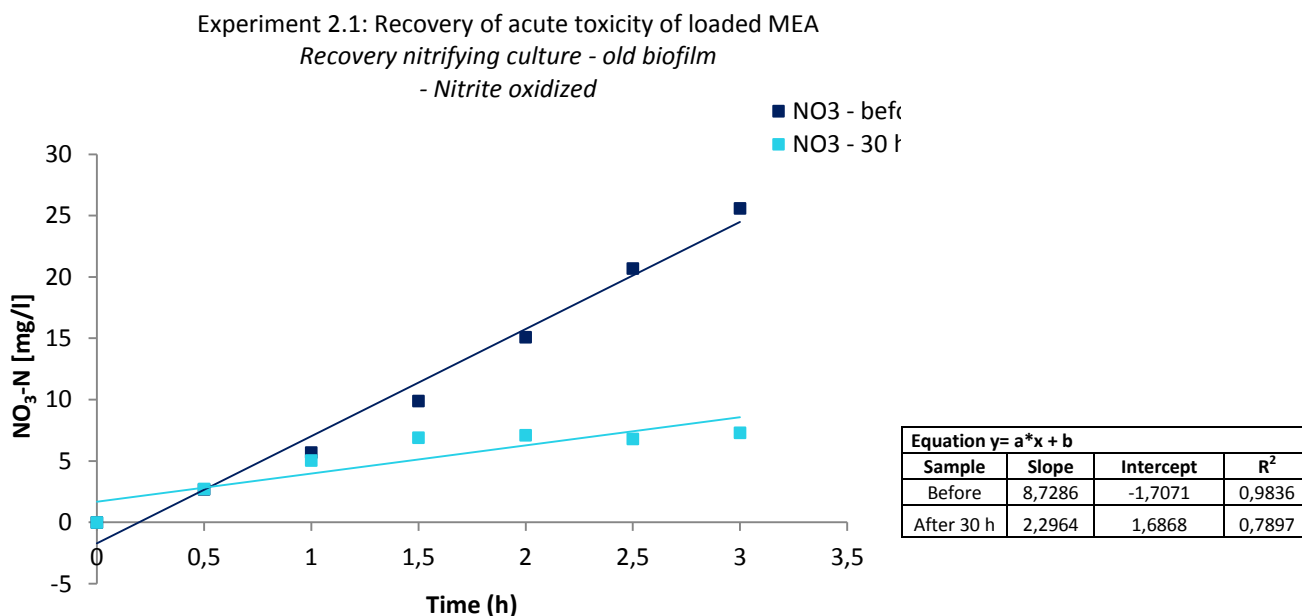


Figure 29 The nitrification activity in terms of ammonia oxidized after 30 hours of recovery of the acute toxicity of loaded MEA on the nitrifying culture.

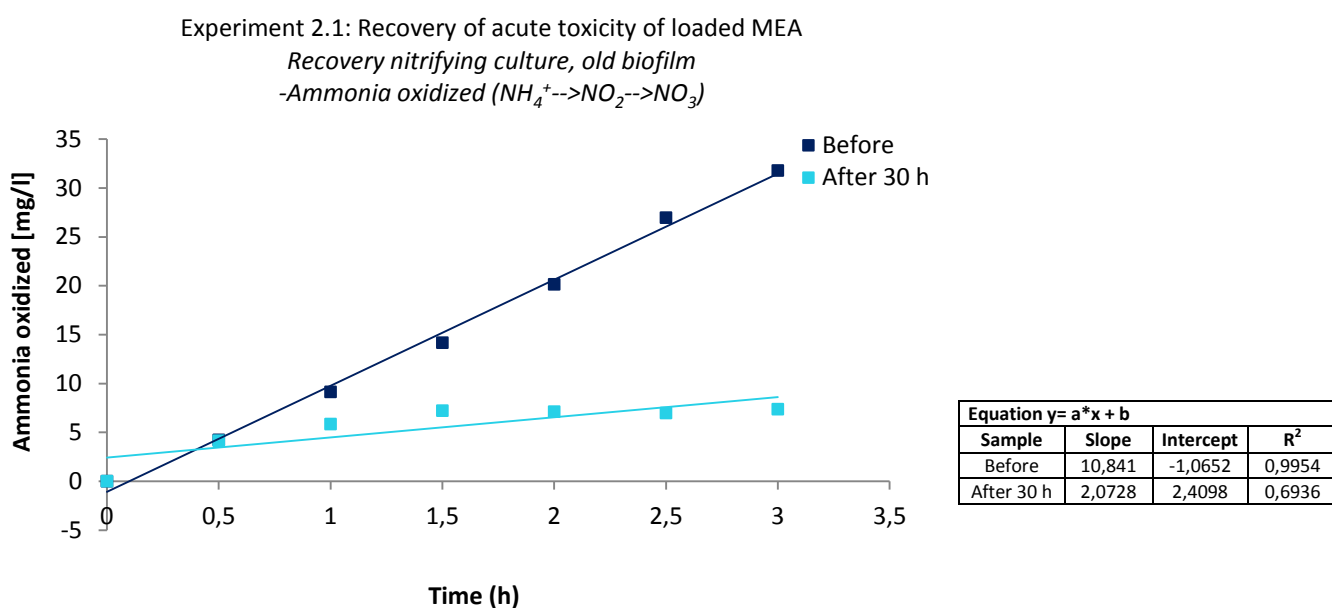


Figure 30 The nitrification activity in terms of ammonia oxidized after 30 hours of recovery of the acute toxicity of loaded MEA on the nitrifying culture.

The activity during the acute toxicity test with MEA loaded decreased with increased concentration of MEA loaded, but the nitrification process never stopped. The recovery in respect to the initial activity was 19 % after 30 hours.

For estimating the EC₅₀, the calculated slope of each concentration is set relative to the slope of the initial activity without the test substance. Based on the calculated activity (%), a linear regression in Excel was applied to interpolate the concentration at 50 % activity for the nitrite oxidizing rate and the ammonia oxidizing rate. Figure 31 and Figure 32 shows the relative activity as a function of the logarithmic dose with the fitted curves and the estimated EC₅₀ for MEA unloaded and MEA loaded for the nitrite oxidizing rate and the ammonia oxidizing rate respectively. The values for EC₅₀ and recovery kinetics are summarized in Table 11. The mass balance from the acute toxicity tests are shown in appendix D.

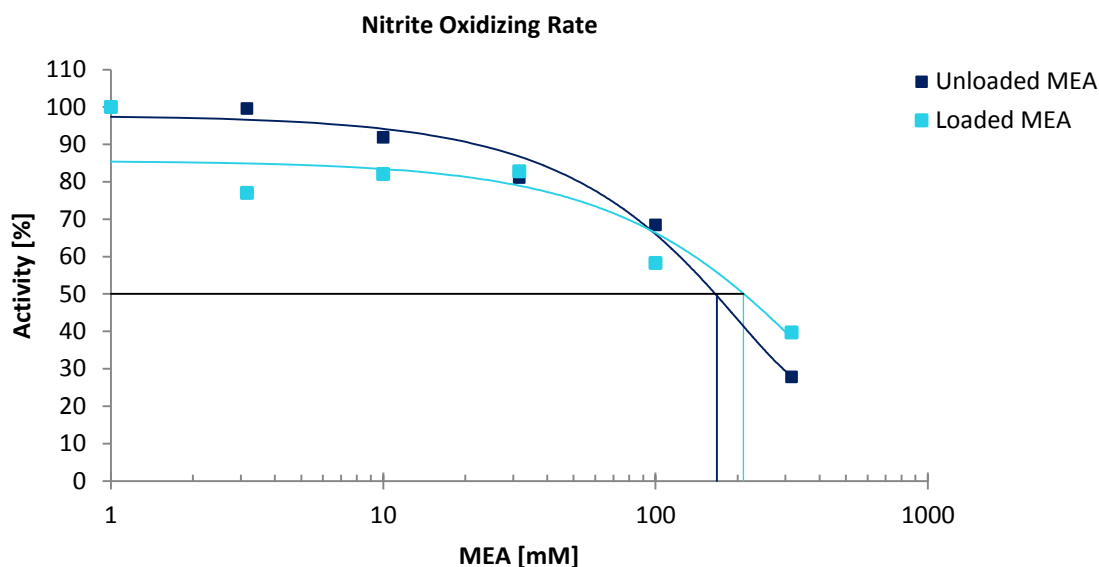


Figure 31 Acute toxicity of MEA unloaded and MEA loaded on the nitrifying culture. The nitrite oxidizing rate expressed in percent activity (%) is set relative to the slope of the initial activity without the test substance. The estimated EC₅₀ of MEA unloaded and MEA loaded for the nitrite oxidizing rate was 168 mM and 210 mM respectively. All tests had a monitoring time range of 3 hours for each concentration.

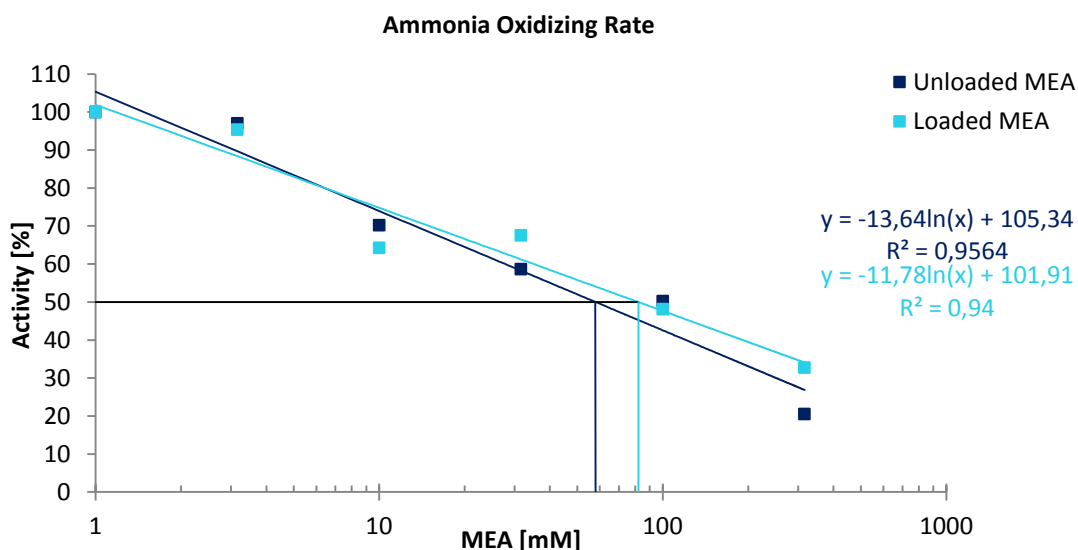


Figure 32 Acute toxicity of MEA unloaded and MEA loaded on the nitrifying culture. The ammonia oxidizing rate expressed in percent activity (%) is set relative to the slope of the initial activity without the test substance. The estimated EC_{50} of MEA unloaded and MEA loaded for the ammonia oxidizing rate was 58 mM and 82 mM respectively. All tests had a monitoring time range of 3 hours for each concentration.

Table 11 Summary of the acute toxicity of MEA unloaded and MEA loaded on the nitrifying culture in terms of activity for the nitrite oxidizing rate (NOR) and the ammonia oxidizing rate (AOR).

Experiment	Amine	EC_{50} [mM]		Recovery 30 h [%]	
		NOR	AOR	NOR	AOR
1	MEA unloaded	168	58	88	65
2	MEA loaded	210	82	26	19

3.2.3.1 Quantification of MEA with fluorescamine assay

The Fluorescamine assay was performed as described in section 2.1.2, to quantify the concentration of MEA during the time course of the acute toxicity test with MEA unloaded and MEA loaded. A calibration curve was prepared to determine the concentration in the samples by interpolation, see appendix E. Emission intensity of a series of samples with different MEA concentration recorded at excitation and emission wavelengths of 392 nm and 480 nm respectively. In Figure 33 and Figure 34 the measured values of MEA unloaded and MEA loaded [mM] by Fluorescamine assay was plotted as a function of the theoretical MEA unloaded and MEA loaded concentration [mM]. The R^2 values being 0,9982 and 0,997 respectively for MEA unloaded and MEA loaded gave a good correlation between the theoretical and measured MEA unloaded and loaded concentration, R^2 equal to 1 being the best correlation. The good correlation between the theoretical and measured MEA unloaded and

loaded concentration indicates that there is no degradation of MEA during the time course of the acute toxicity test.

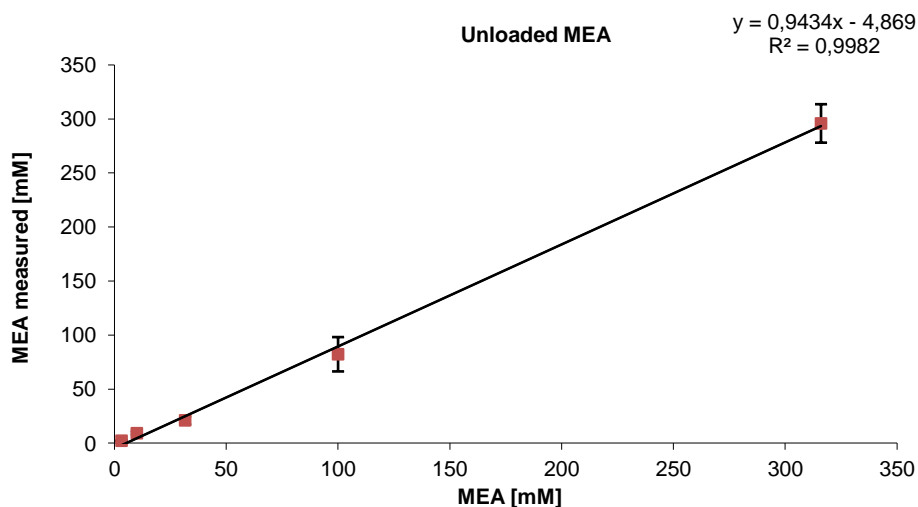


Figure 33 Measured values of MEA unloaded concentration [mM] by Fluorescamine assay as a function of theoretical MEA unloaded concentration [mM].

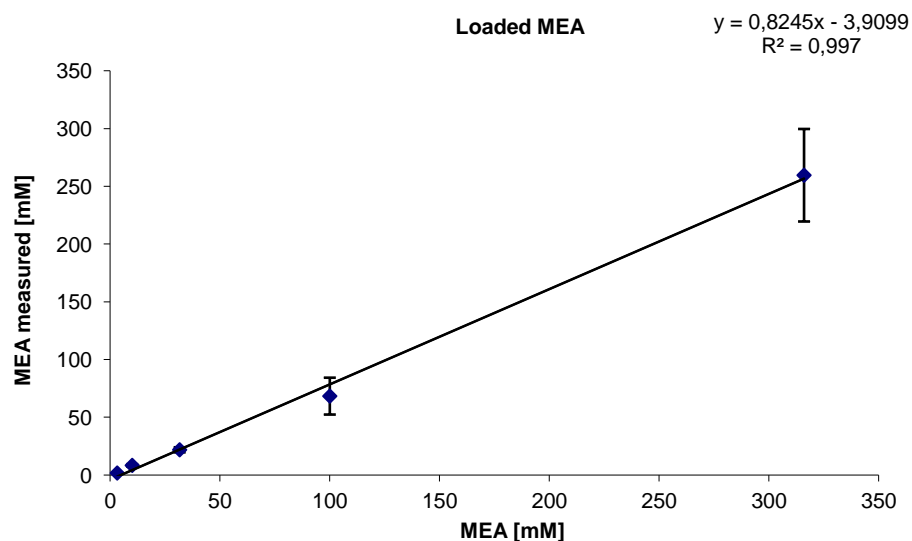


Figure 34 Measured values of MEA loaded concentration [mM] by Fluorescamine assay as a function of theoretical MEA loaded concentration [mM].

3.2.3.2 Total dry weight

Based on the average weight and SEM for 49 empty Kaldnes K1 carriers, being 153 ± 1 mg, the total dry weight of the old biofilm, in terms of mg, before and after the acute toxicity of MEA unloaded were found. Table 12 shows the average and SEM of five parallels before and three parallels after the acute toxicity of MEA unloaded.

Table 12 Total dry weight of the old biofilm in terms of mg, before and after the acute toxicity test with MEA unloaded, given as the average and standard error of mean (SEM) of five and three parallels respectively.

	Before	After
Amine	Average (mg)	Average (mg)
MEA unloaded	14,5±6,4	21,9±11,8

3.2.4 Acute toxicity test on the new biofilm

The results of experiment 3 - 6 (see Table 10) are given in Figure 35-50 as the nitrification activity in terms of the nitrite oxidizing rate and the ammonia oxidizing rate during the acute toxicity test of AMP, DEA, MDEA and piperazine on the nitrifying culture and the corresponding recovery 30 hours after the acute toxicity test as a function of time. The nitrification activity in terms of nitrite ($\text{NO}_2\text{-N}$) and ammonium ($\text{NH}_4^+\text{-N}$) concentrations during the acute toxicity test of AMP, DEA, MDEA and piperazine on the nitrifying culture and the corresponding recovery 30 hours after the acute toxicity test as a function of time are given in appendix C.

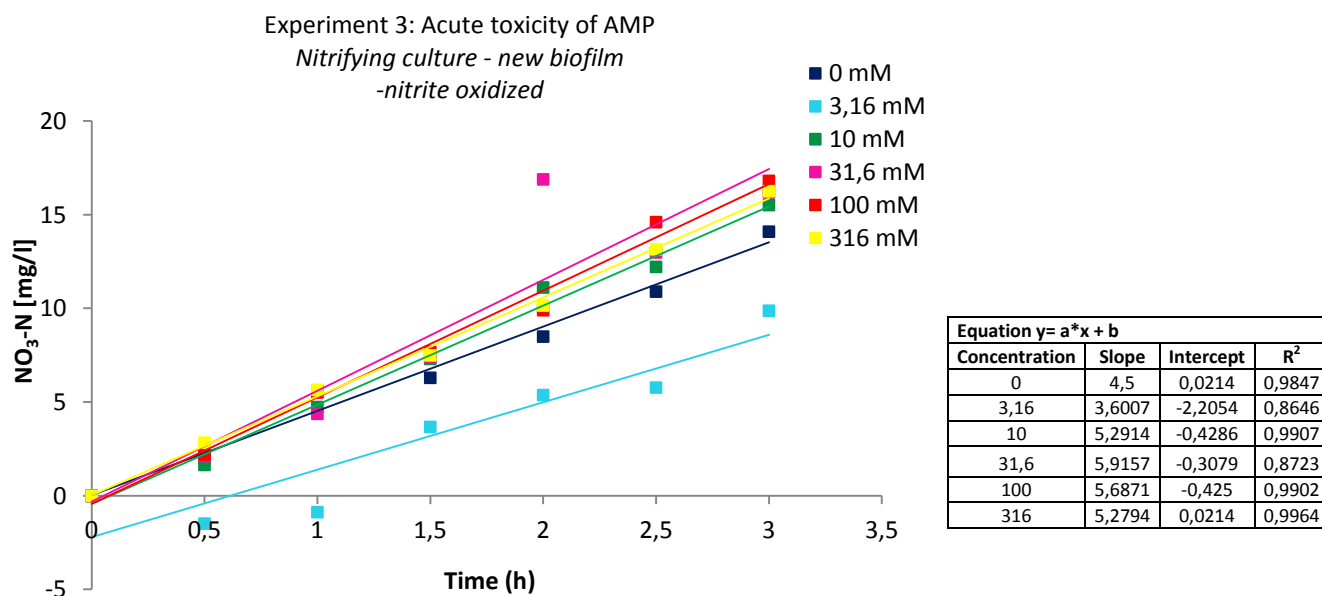


Figure 35 The nitrification activity in terms of nitrite oxidized during acute toxicity of AMP on the nitrifying culture.

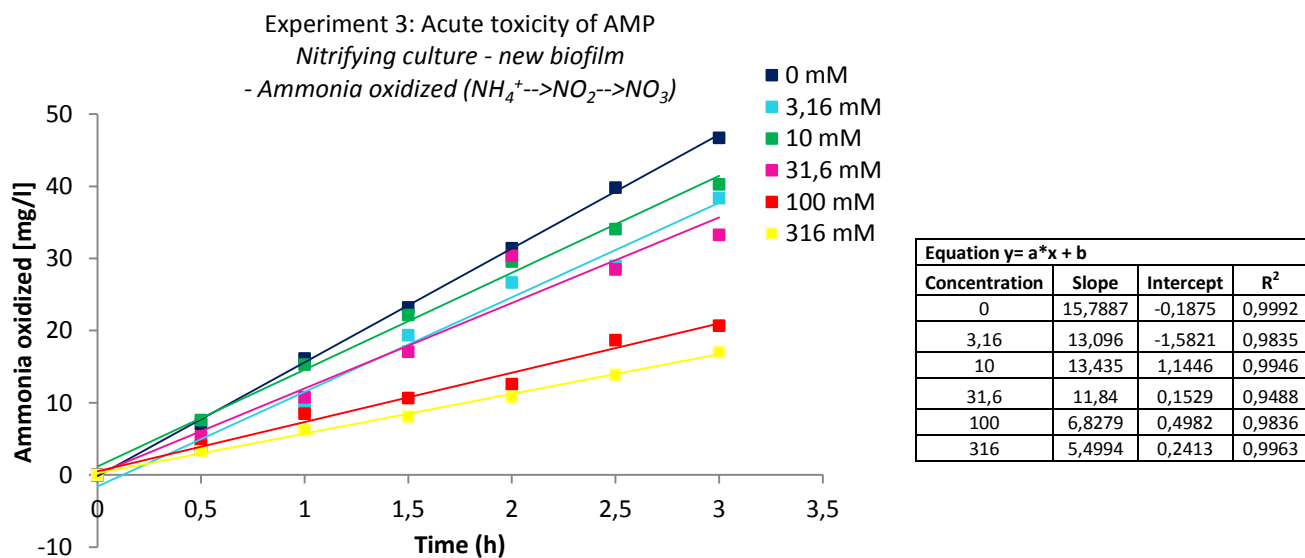


Figure 36 The nitrification activity in terms of ammonia oxidized during acute toxicity of AMP on the nitrifying culture.

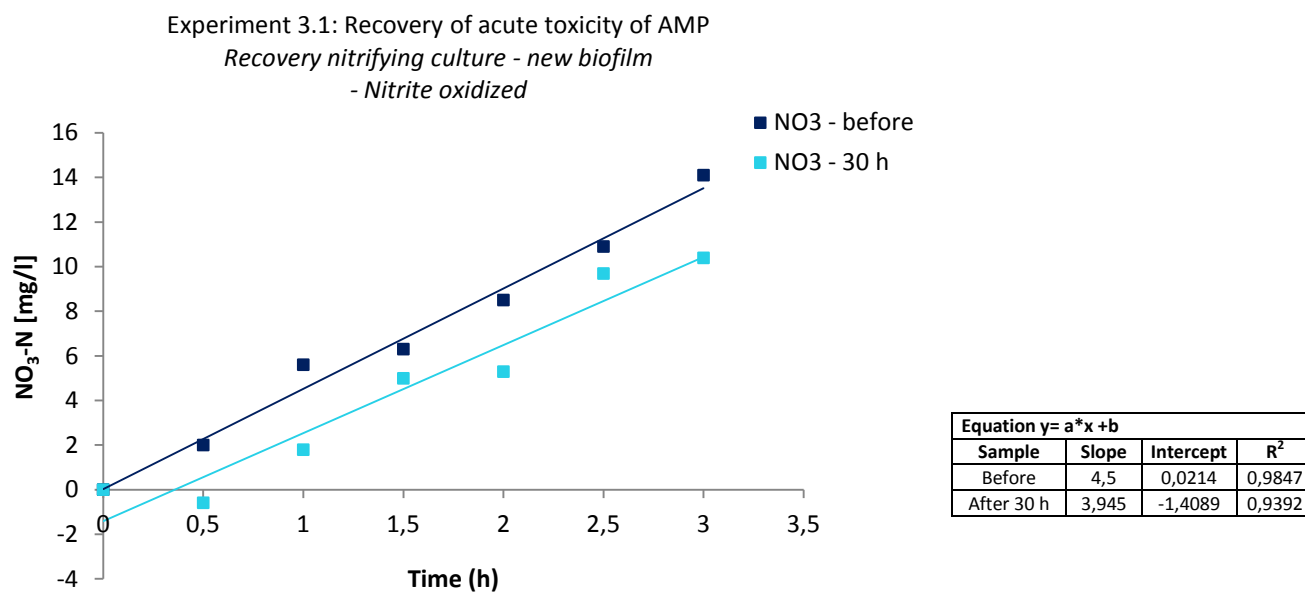


Figure 37 The nitrification activity after 30 hours of recovery of the acute toxicity of AMP on the nitrifying culture represented as nitrite oxidized.

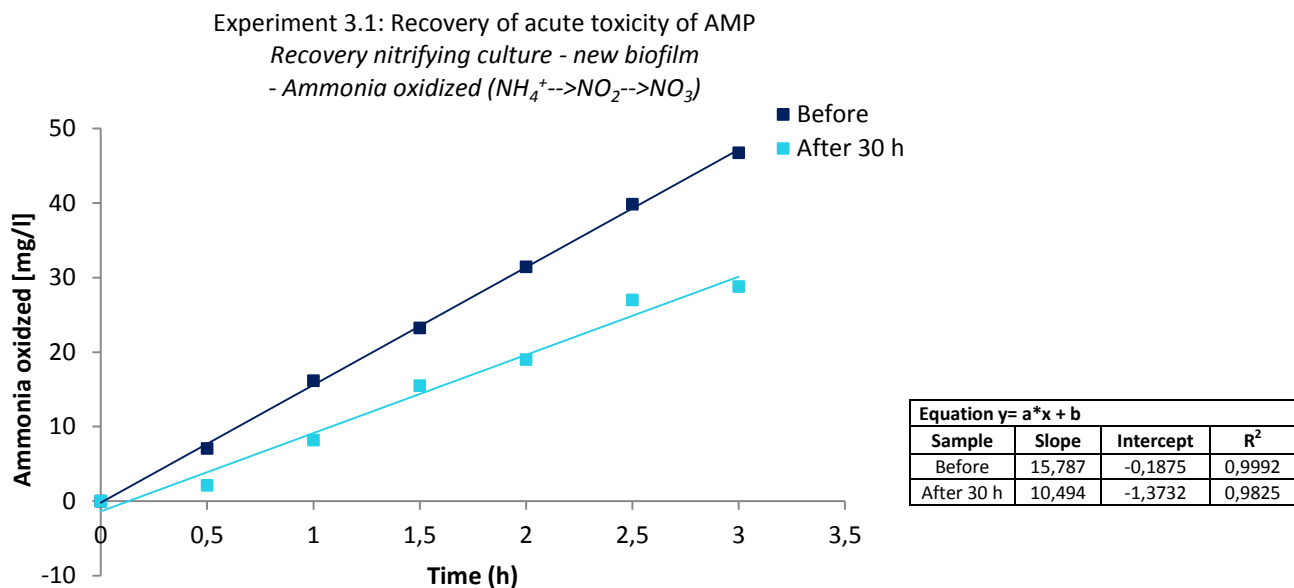


Figure 38 The nitrification activity after 30 hours of recovery of the acute toxicity of AMP on the nitrifying culture represented as ammonia oxidized.

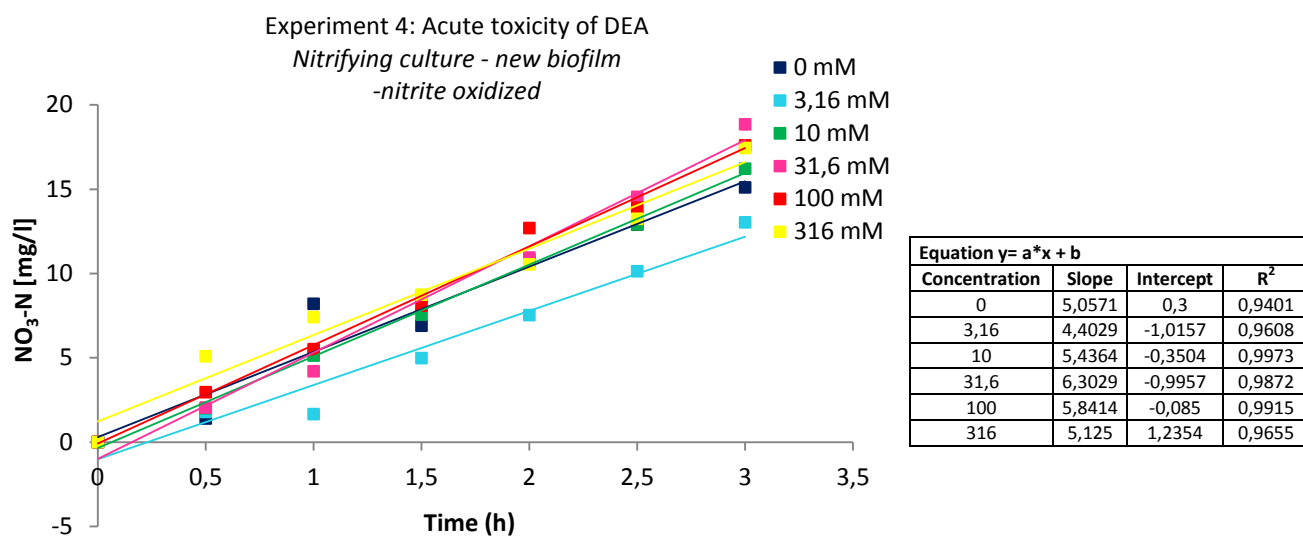


Figure 39 The nitrification activity in terms of nitrite oxidized during acute toxicity of DEA on the nitrifying culture.

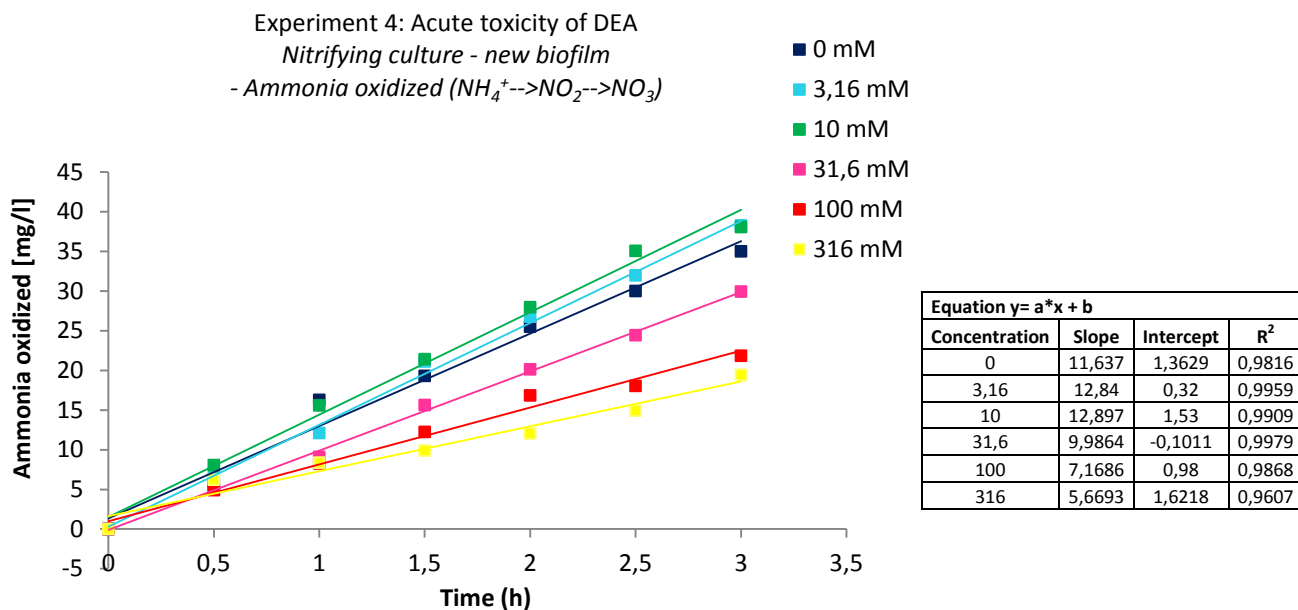


Figure 40 The nitrification activity in terms of ammonia oxidized during acute toxicity of DEA on the nitrifying culture.

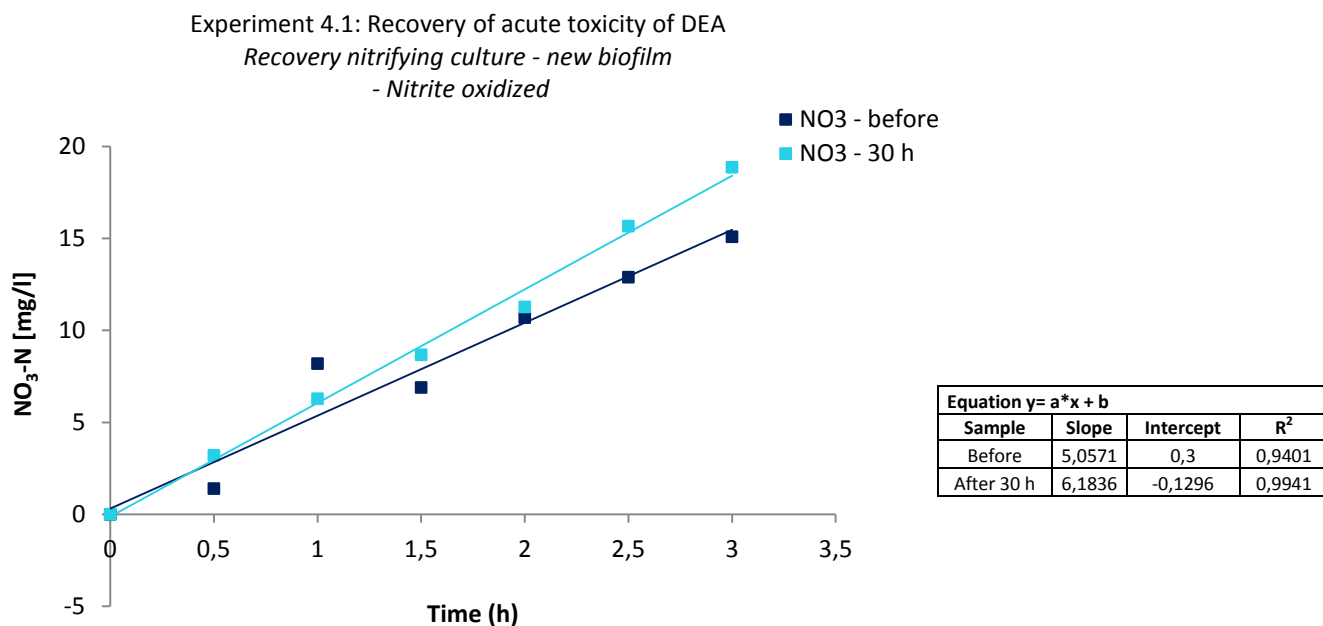


Figure 41 The nitrification activity after 30 hours of recovery of the acute toxicity of DEA on the nitrifying culture represented as nitrite oxidized.

Experiment 4.1: Recovery of acute toxicity of DEA
 Recovery nitrifying culture - new biofilm
 - Ammonia oxidized ($NH_4^+ \rightarrow NO_2^- \rightarrow NO_3^-$)

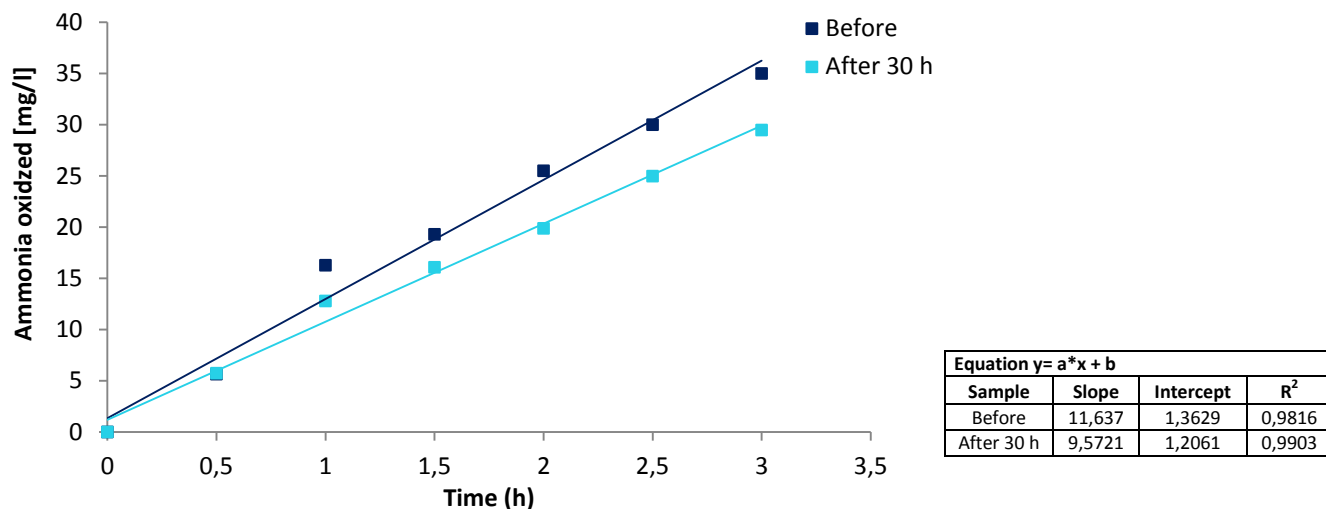


Figure 42 The nitrification activity after 30 hours of recovery of the acute toxicity of DEA on the nitrifying culture represented as ammonia oxidized.

Experiment 5: Acute toxicity of MDEA
 Nitrifying culture - new biofilm
 - nitrite oxidized

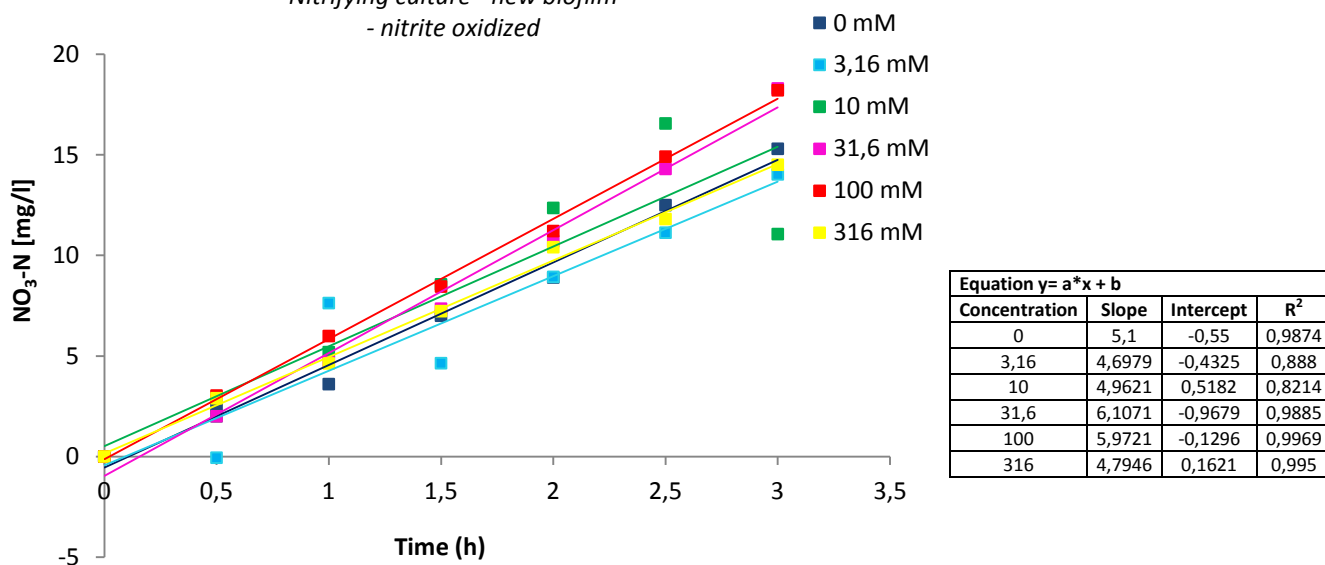


Figure 43 The nitrification activity in terms of nitrite oxidized during acute toxicity of MDEA on the nitrifying culture.

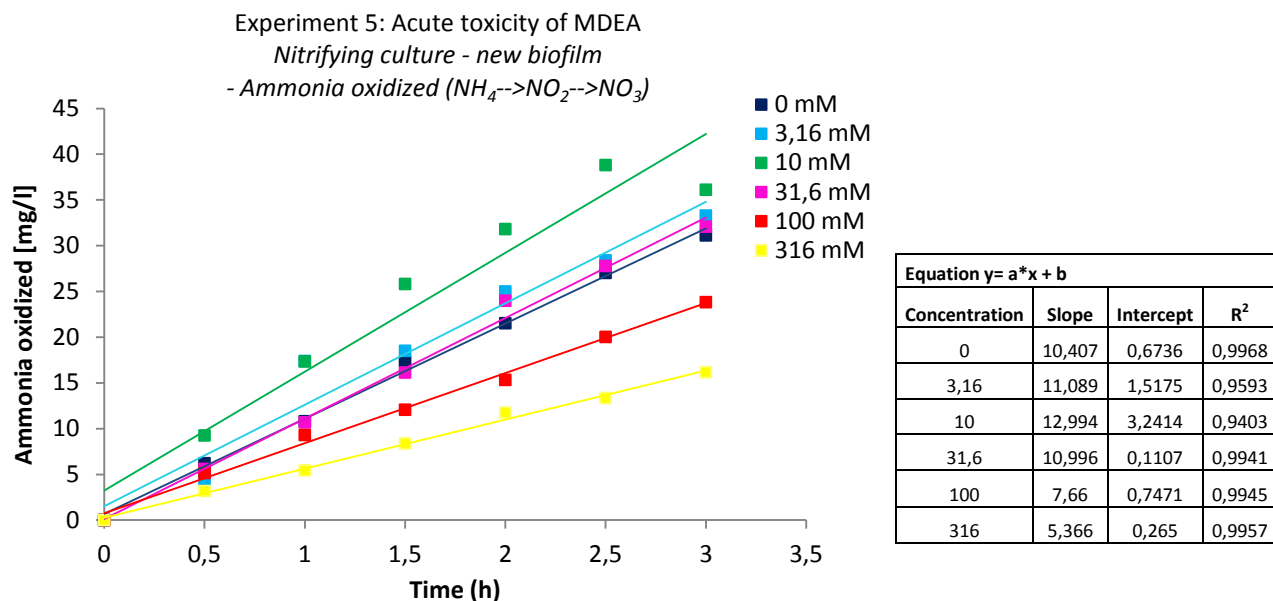


Figure 44 The nitrification activity in terms of ammonia oxidized during acute toxicity of MDEA on the nitrifying culture.

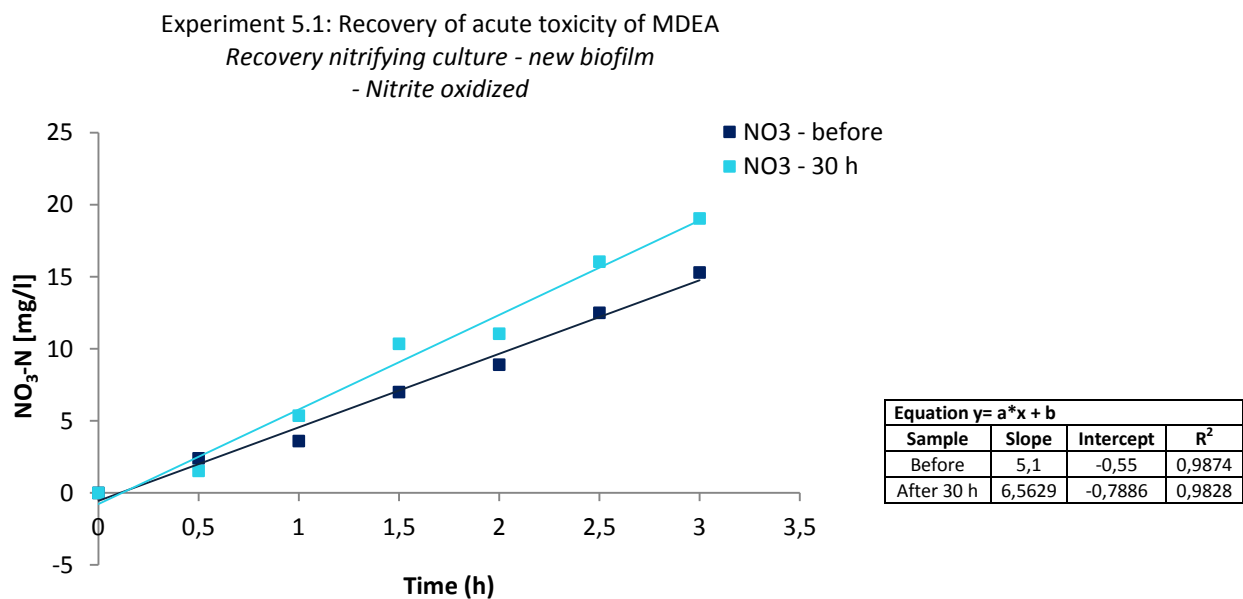


Figure 45 The nitrification activity after 30 hours of recovery of the acute toxicity of MDEA on the nitrifying culture represented as nitrite oxidized.

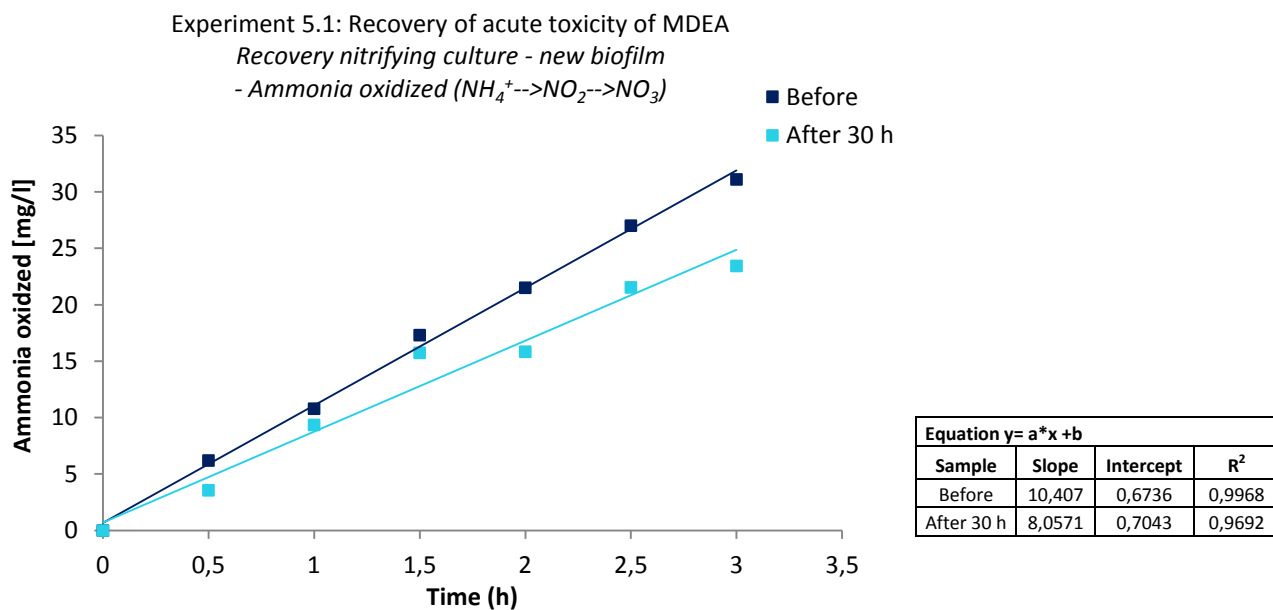


Figure 46 The nitrification activity after 30 hours of recovery of the acute toxicity of MDEA on the nitrifying culture represented as ammonia oxidized.

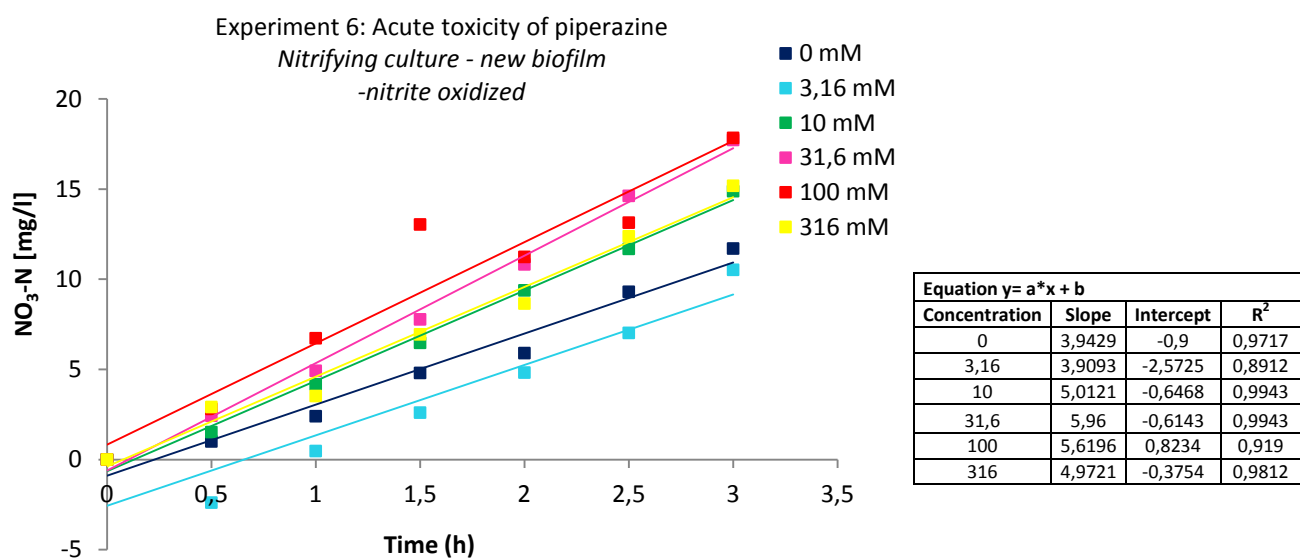


Figure 47 The nitrification activity in terms of nitrite oxidized during acute toxicity of piperazine on the nitrifying culture.

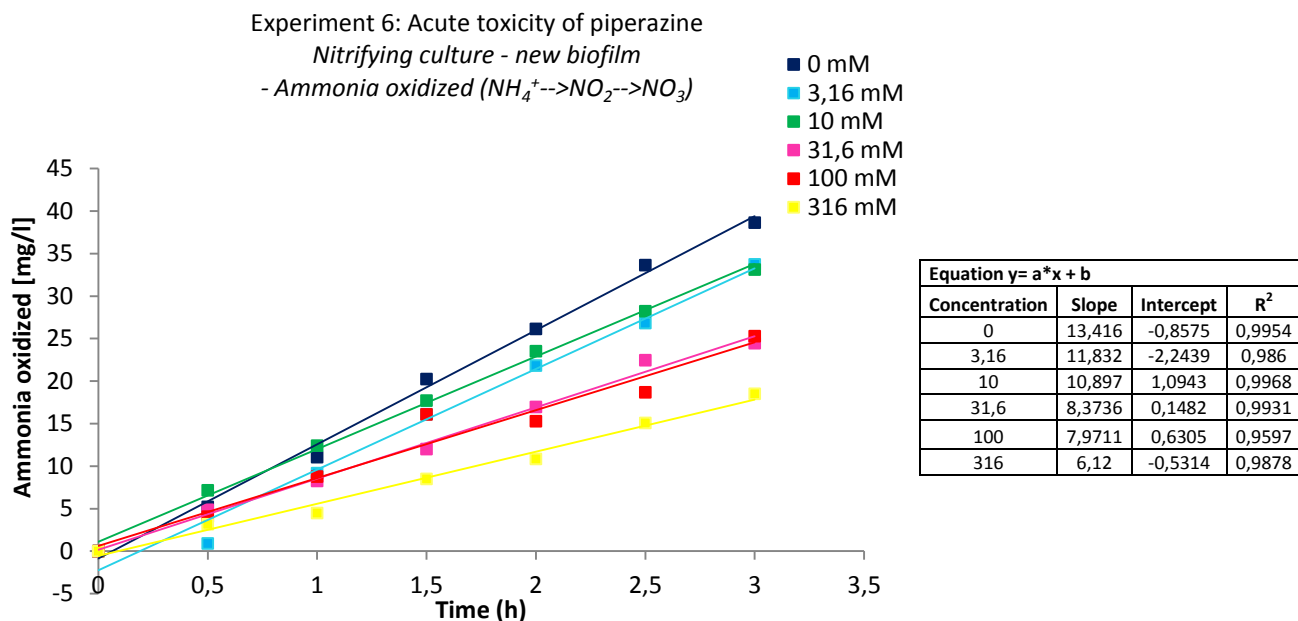


Figure 48 The nitrification activity in terms of ammonia oxidized during acute toxicity of piperazine on the nitrifying culture.

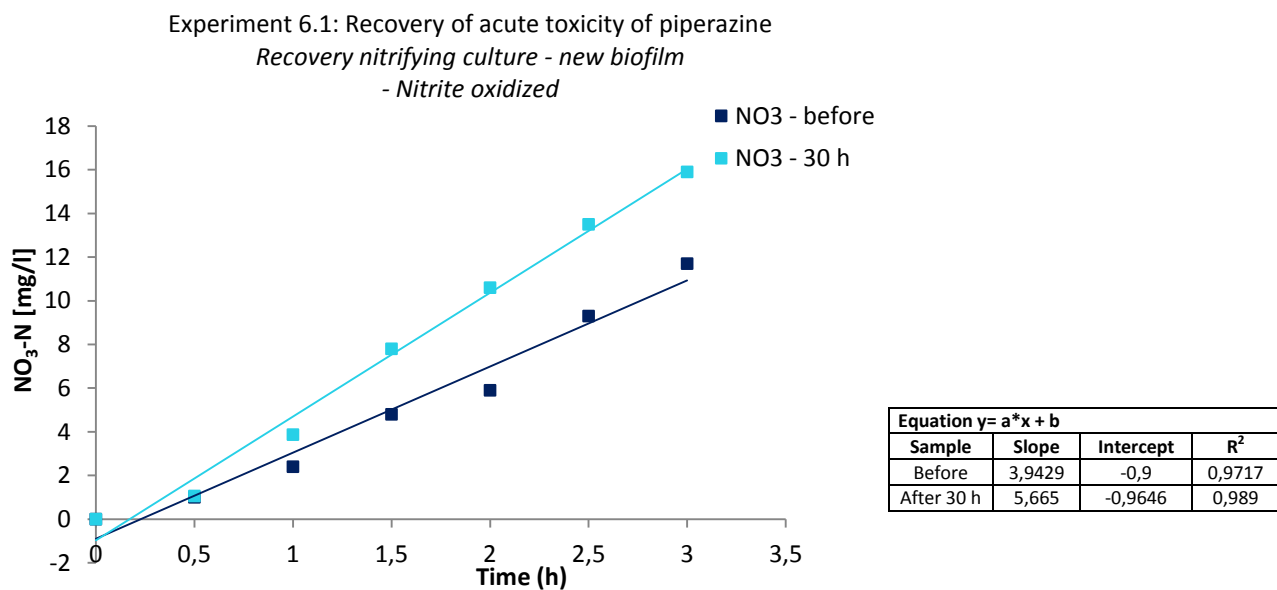


Figure 49 The nitrification activity after 30 hours of recovery of the acute toxicity of piperazine on the nitrifying culture represented as nitrite oxidized.

Experiment 6.1: Recovery of acute toxicity of piperazine
 Recovery nitrifying culture, new biofilm
 - Ammonia oxidized ($NH_4^+ \rightarrow NO_2^- \rightarrow NO_3^-$)

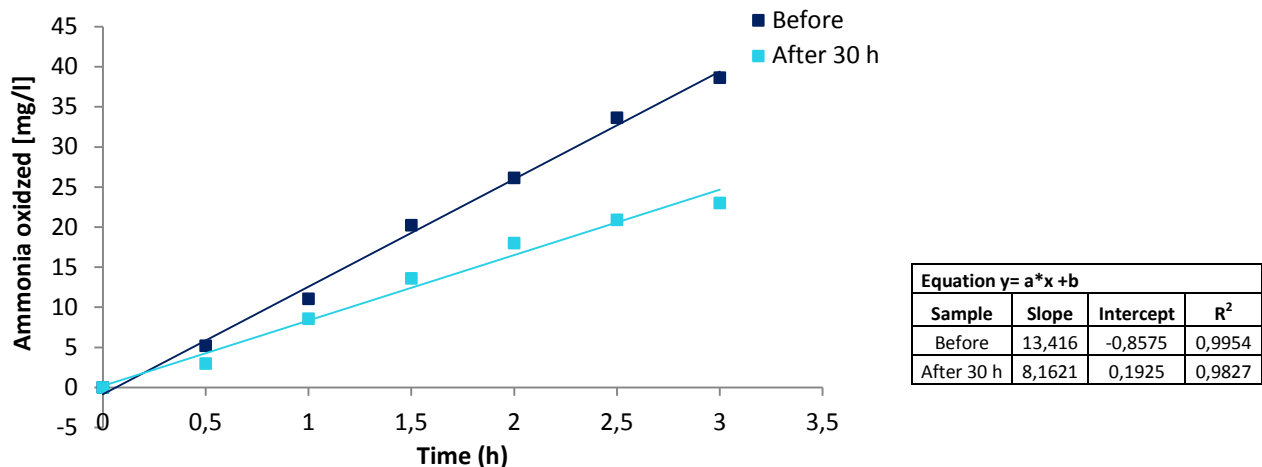


Figure 50 The nitrification activity after 30 hours of recovery of the acute toxicity of piperazine on the nitrifying culture represented as ammonia oxidized.

For estimating the EC₅₀, the calculated slope of each concentration was set relative to the slope of the initial activity without the test substance. Based on the calculated activity (%), a linear regression on Excel was applied to interpolate the concentration at 50 % activity for the nitrite oxidizing rate and the ammonia oxidizing rate. Figure 51 and Figure 52 shows the relative activity as a function of the logarithmic dose with the fitted curves and the estimated EC₅₀ for the amines AMP, DEA, MDEA and piperazine for the nitrite oxidizing rate and the ammonia oxidizing rate respectively. The estimated EC₅₀ and recovery kinetics for the nitrite oxidizing rate and the ammonia oxidizing rate are summarized in Table 13. The mass balance from the acute toxicity is shown in appendix D.

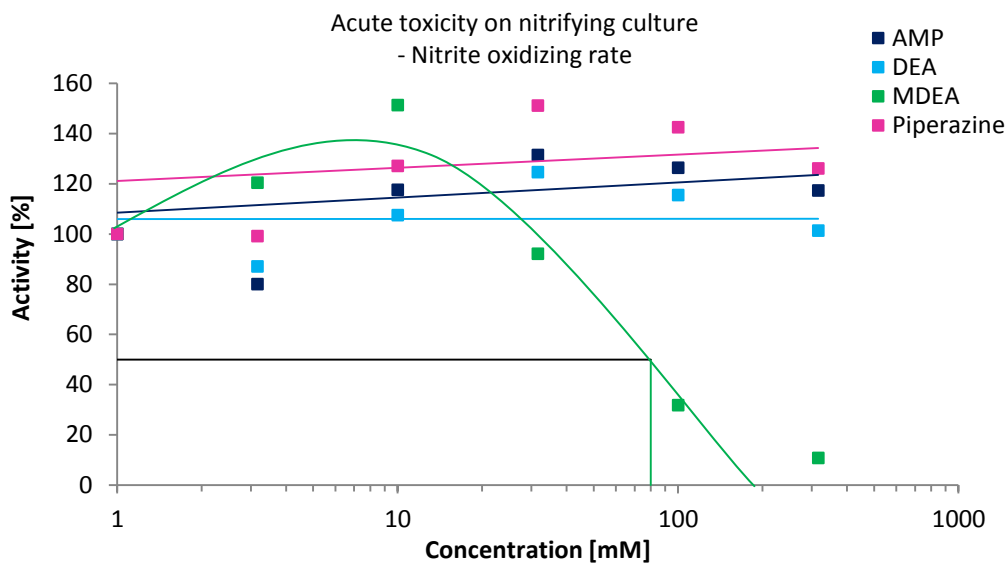


Figure 51 Acute toxicity of AMP, DEA, MDEA and piperazine on the nitrifying culture in terms of activity of the nitrite oxidizing rate. The estimated EC₅₀ of MDEA was 80 mM, based on a logistic model. All tests had a monitoring time range of 3 hours for each concentration.

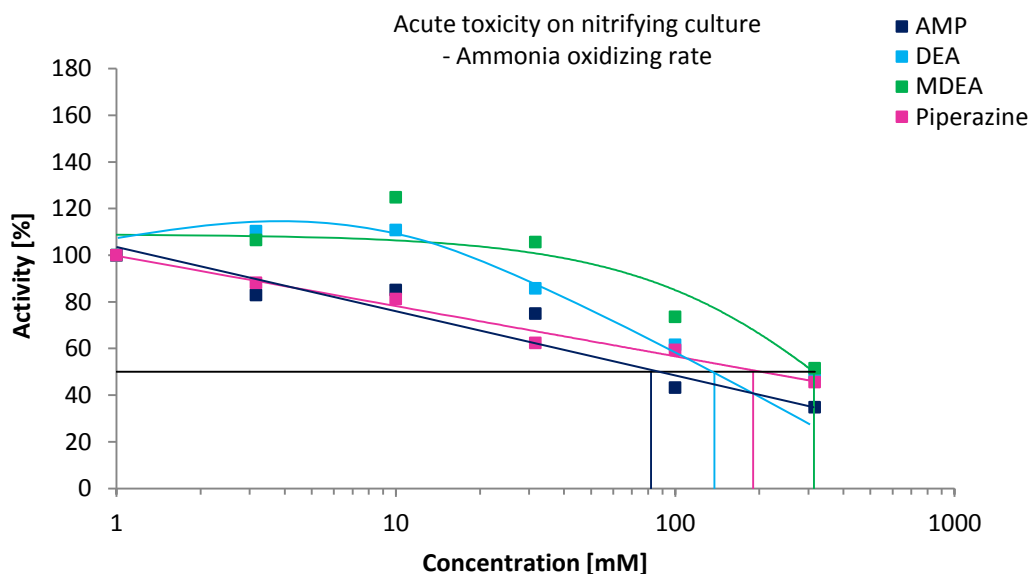


Figure 52 Acute toxicity of AMP, DEA, MDEA and piperazine on the nitrifying culture in terms of activity of the ammonia oxidizing rate. The estimated EC₅₀ of AMP, DEA, MDEA and piperazine was respectively 82 mM, 138 mM, 314 mM and 190 mM, based on a logistic model. All tests had a monitoring time range of 3 hours for each concentration.

Table 13 Summary of the acute toxicity of AMP, DEA, MDEA and piperazine on the nitrifying culture in terms of activity for the nitrite oxidizing rate (NOR) and the ammonia oxidizing rate (AOR).

Experiment	Amine	EC ₅₀ [mM]		Recovery 30 h [%]	
		NOR	AOR	NOR	AOR
3	AMP	-	82	88	66
4	DEA	-	138	122	82
5	MDEA	80	314	129	77
6	Piperazine	-	190	144	61

3.2.4.1 Total dry weight

Based on the average weight and SEM for 49 empty Kaldnes K1 carriers, being 153±1 mg, the total dry weight of the new biofilm, in terms of mg, before and after the acute toxicity of AMP were found. Table 14 shows the average and SEM of ten parallels before and after the acute toxicity of AMP.

Table 14 Total dry weight of the new biofilm in terms of mg, before and after the acute toxicity test with AMP, given as the average and standard error of mean of ten parallels.

Amine	Before	After
	Average (mg)	Average (mg)
AMP	4,4±3,0	6,5±2,3

3.2 Denitrification

Denitrification was promoted with excess NO₃⁻ until a steady-state was reached. The experimental timeline (in days) of the denitrification reactor is shown in Figure 53.

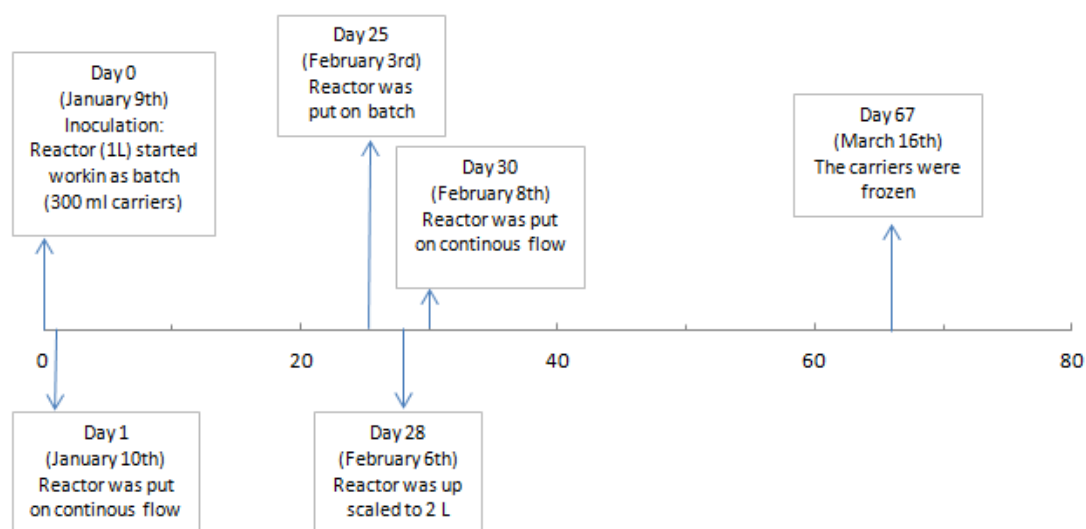


Figure 53 Timeline (in days) of the denitrification reactor

3.2.1 Stabilization

The development and stabilization of the denitrification reactor is shown in figure 54 and 55. Figure 54 shows the concentration of the components, $\text{NH}_4^+\text{-N}$, $\text{NO}_3\text{-N}$ and $\text{NO}_2\text{-N}$, in the denitrification process, from day zero, when the carriers were added to the reactor together with the denitrification medium (138 mg NO_3^-/l), until day 67. Figure 55 shows the reduction rate of the denitrifying activity represented as nitrate loading rate (NLR) and $\text{NO}_3\text{-N}$ reduction rate, starting on day 31 after the up scaling to a 2 l glass reactor when the reactor were on a continuous flow mode with a flow rate of 60 ml/h until day 67.

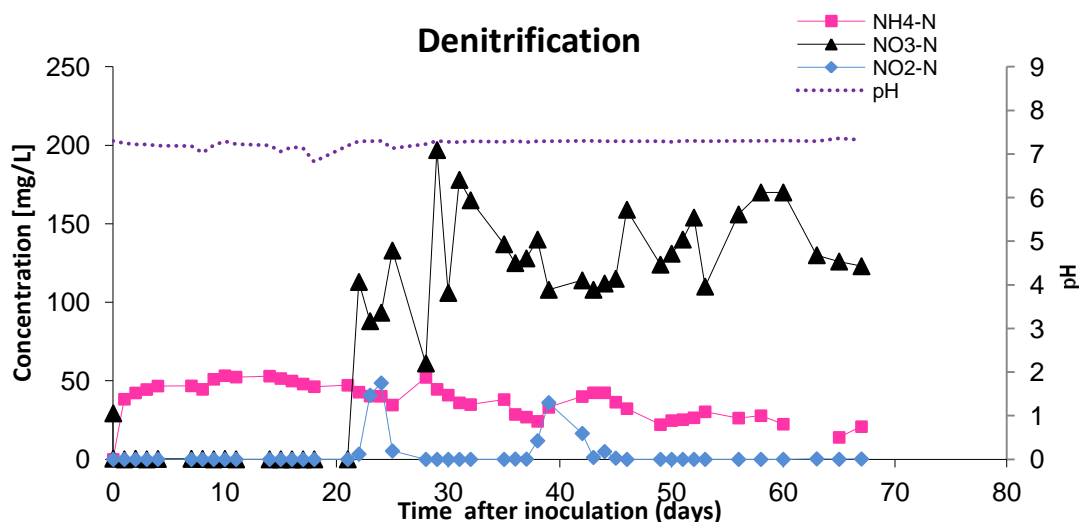


Figure 54 Measured activity [mg/l] of ammonium ($\text{NH}_4^+\text{-N}$), nitrite ($\text{NO}_2\text{-N}$) and nitrate ($\text{NO}_3\text{-N}$), and monitored pH in the denitrification reactor. The measurement started at day zero, when adding the Kaldnes K1 carriers, until day 67.

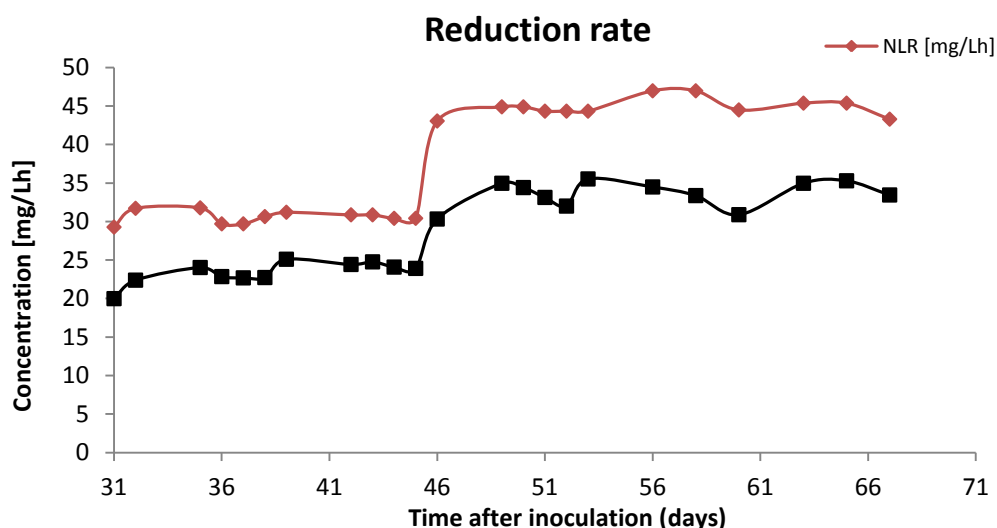


Figure 55 The reduction rate of the denitrifying activity represented as nitrate loading rate (NLR) and nitrate ($\text{NO}_3\text{-N}$) reduction rate, starting on day 31 after the up scaling to a 2 l glass reactor when the reactor were on a continuous flow mode with a flow rate of 60 ml/h until day 67.

During the start-up the continuous feeding started with a relatively low flow rate of 36 ml/h to avoid wash out. Because of a miscalculation in the medium concentration the reactor started up with a $\text{NO}_3\text{-N}$ concentration of 138 mg/l instead of 553 mg/l which were intended. Along the process there were some operational problems with some of the pumps (which were replaced) and therefore the $\text{NO}_3\text{-N}$ and the $\text{NO}_2\text{-N}$ concentrations was observed to be high around day 22 after the inoculation. The reactor was therefore put on batch on day 25, and on day 28 the reactor was up scaled to a 2 l glass reactor. On day 30 the reactor was put on continuous flow mode with a flow rate of 60 ml/h and $\text{NO}_3\text{-N}$ concentration of 553 mg/l. The flow rate was increased to a flow rate of 100 ml/h on day 45 in order to promote biofilm development. Previous studies have shown that the denitrifying culture is much more robust and almost unaffected by the acute toxicity of the amines MEA, AMP, DEA, MDEA and piperazine, compared to the nitrifying culture which has shown a higher sensitivity. Therefore the denitrifying biofilm was frozen on day 67.

4. Discussion

4.1 Nitrification

4.1.1 Stabilization

Along the process of developing the nitrifying culture there were some operational problems with pumps which were replaced, and a wash out was observed. The wash out may have been caused by a high flow rate in the start-up phase. The same start-up flow rate (100ml/h) was tried out by Hauser in 2011, but then the Kaldnes K1 carriers were pre-inoculated in a sludge-return before start-up. A pre-inoculation was not carried out in this work because of possible organic matter which could attach to surface of the carriers; the main goal was to develop a thin and evenly distributed biofilm. However, after setting up a sludge-trap to resuspend the sludge into the reactor the nitrifying culture regained activity and reached a steady NH_4^+ consumption around day 43 after inoculation, indicating that a well adjusted nitrifying culture was well developed.

4.1.2 Biofilm development

Because of the high COD value per empty Kaldnes K1 carrier, being (6040±269) mg/l, following the procedure described in section 2.2.1, compared to the COD value of the Kaldnes K1 carrier with develop biofilm, being (5246±225) mg/l on day 7 after inoculation following the same procedure, the development of the nitrifying biofilm on Kaldnes K1 carriers could not be successfully tracked by monitoring the gained COD per carrier. The empty Kaldnes K1 carriers were pre-treated in different solutions (see section 2.2.1), but the high COD value per Kaldnes K1 carrier did not decrease to the COD value measured on an empty Kaldnes K1 carrier by Hauser (Hauser, 2011), being (748±75) mg/l. The high COD value per Kaldnes K1 carrier indicates interference on the COD assay possibly from the polyethylene which the Kaldnes K1 carriers are made of.

4.2 Inhibition of nitrification

4.2.1 State of biofilm

Previous studies have indicated diversity between biofilms tested, it was therefore important to state the activity of the biofilm before carrying out the acute toxicity test. The state of the old and the new biofilm were found by plotting the measured concentration (mg/l) of NO_3^- -N, NO_2^- -N and NH_4^+ -N against time (h), before adding the test substances to the media. For the old biofilm the activity of the NO_3^- and NO_2^- activity were respectively 9,2 mg/h and 3,4 mg/h. The percentage oxidation of NH_4^+ to either NO_2^- or NO_3^- when comparing measurements at 0 hours and after 3 hours was 79 %.

For the new biofilm the activity of the NO_3^- and NO_2^- production was 4,5 mg/h and 11,3 mg/h respectively. The percentage oxidation of NH_4^+ to either NO_2^- or NO_3^- when comparing measurements at 0 hours and after 3 hours was 83 %.

The activity of the new and the old biofilm was significantly different. For the old biofilm the activity of produced NO_3^- (9,2 mg/h) was more than twice as high as the activity of produced NO_2^- (3,4 mg/h). Meanwhile, for the new biofilm the trend was opposite, the activity of produced NO_2^- (11,3 mg/h) was more than twice as high as the activity of produced NO_3^- (4,5 mg/h). However, the percentage NH_4^+ oxidized to either NO_2^- or NO_3^- was relatively equal for the both the old and the new biofilm.

4.2.2 Acute toxicity

The determination of the EC_{50} value is in several aspects a source of error. For example, prior to the acute toxicity the pH of the respective solutions had to be adjusted and could possibly lead to changes in the chemical properties of the test substances such as solubility and volatilization. Also, this could have an effect on the actual concentration in the reactor. The choice of a curve-fitting model, including all data points, could also be a source of error although evidently being the most un-biased calculation of the EC_{50} value.

4.2.2.1 Acute toxicity test on old biofilm

The acute toxicity of MEA unloaded and MEA loaded with 5 % CO_2 was tested on an old biofilm previously tested by Colaço (Colaço, 2009), Skjæran (Skjæran, 2010) and Hauser (Hauser, 2011). Before the acute toxicity tests the medium in the reactor contained 50 mg/l $\text{NH}_4^+\text{-N}$, and as a control the $\text{NH}_4^+\text{-N}$ concentration was measured at 0 hours and after 3 hours for every amine concentration added to the reactor. Interference was observed, but the values were corrected by the correction graph established by Colaço (Colaço, 2009) except for the highest concentration of MEA (100 mM and 316 mM) which were still over estimated even after the corrections were made. The main focus of this work was to establish an activity by the formation of NO_3^- and NO_2^- , because these two factors are a stronger evidence of the nitrification process than just the monitoring of the $\text{NH}_4^+\text{-N}$ concentration, therefore it was not crucial for this work that the measured $\text{NH}_4^+\text{-N}$ concentrations were not reliable.

Comparing the activity of the MEA unloaded and MEA loaded there were no big difference in the observed trend. However there were some differences when analyzing the percentage activity of the AOR (and NOR for the highest concentrations of MEA unloaded and MEA loaded), and the percentage recovery 30 hours after the acute toxicity; The percentage activity for the AOR showed a steeper slope for the MEA unloaded than for the MEA loaded, indicating that during the acute

toxicity the MEA unloaded had a stronger effect on the nitrifying culture than the MEA loaded, this was also the case for the percentage activity for the NOR for the highest concentrations of MEA unloaded and MEA loaded. The recovery 30 hours after the acute toxicity showed that the nitrifying culture recovered faster after the acute toxicity of MEA unloaded (65 %) compared with the MEA loaded which recovered poorly (19 %).

In general, the acute toxicity of MEA indicated that the NOR was inhibited at higher MEA concentrations, while the AOR was inhibited at low MEA concentrations.

Comparing the EC_{50} values for NOR of the acute toxicity of MEA unloaded (being 168 mM) with the previous EC_{50} values gained by Colaço (twice) (Colaço, 2009) (being 10 mM and 100 mM), and Hauser (Hauser, 2011) (being 86 mM) the EC_{50} values indicates that the nitrifying culture developed a stronger resistance towards MEA, needing a higher concentration before being inhibited. A reason for the varying EC_{50} of MEA could be found in the biofilm age and thereby the respectively thickness, decreasing diffusion over the carrier surface, change in the biofilm community as more resistant cultures could be developed and therefore showing a higher tolerance level.

In terms of recovery, the result is not consistent with Hauser (Hauser, 2011), being 109 % after 30 hours, meanwhile being 65 % for the MEA unloaded in this experiment.

4.2.2.1.1 Quantification of MEA with fluorescamine assay

The Fluorescamine assay was performed to quantify the concentration of MEA during the time course of the acute toxicity test with MEA unloaded and MEA loaded. A calibration curve was prepared to determine the concentration in the samples by interpolation, and the measured values of MEA unloaded and MEA loaded [mM] was plotted as a function of the theoretical MEA unloaded and MEA loaded concentration [mM]. The correlation between the measured and the theoretical MEA concentration was good with R^2 values being 0,9982 and 0,997 for the MEA unloaded and MEA loaded respectively, indicating a good accuracy of the fluorescamine assay relatively unaffected of the factor with or without 5 % CO_2 and no degradation of MEA during the experiment.

4.2.2.2 Acute toxicity test on new biofilm

The acute toxicity of the amines AMP, DEA, MDEA and piperazine were tested on the new developed nitrifying biofilm. Before the acute toxicity tests the medium in the reactor contained 50 mg/l NH_4^+ -N, and as a control the NH_4^+ -N concentration was measured at 0 hours and after 3 hours for every amine concentration added to the reactor. There were interferences observed; For AMP, there were an over estimation of the NH_4^+ -N concentration when adding the concentrations 31,6 mM, 100 mM and 316 mM of AMP. For DEA, there was a small over-estimation of the NH_4^+ -N concentration when

adding 10 mM, 31,6 mM and 100 mM. When adding 316 mM DEA a complete block was observed. For MDEA there was no significant interference observed. For piperazine no significant interference was observed except when adding the highest concentration (316 mM) a complete block was observed. As mentioned earlier, the main focus of this work was to establish an activity by the formation of NO_3^- and NO_2^- , because these two factors are a stronger evidence of the nitrification process than just the monitoring of the NH_4^+ -N concentration, therefore it was not crucial that the measured NH_4^+ -N concentration was not reliable.

When comparing the activity of produced NO_2^- and NO_3^- during the acute toxicity on the new nitrifying culture, the NO_3^- -N activity was stable, except for when adding the highest concentrations of MDEA. Meanwhile the NO_2^- -N activity decreased with increased concentration of AMP, DEA, MDEA and piperazine. The trend indicates that when the new nitrifying culture was exposed to the acute toxicity less NH_4^+ was being oxidized and therefore producing less NO_3^- .

The AOB seem to be more sensitive at lower concentrations of AMP, DEA, MDEA and piperazine, meanwhile the NOB seem to be more stable, except for when testing with MDEA. High concentrations of MDEA seem to inhibit the nitrite oxidizing bacteria.

When testing AMP, DEA or piperazine on the new biofilm, the NOR never reached 50 % of the activity. Only MDEA inhibited the NOR up to 50 % at a concentration of 80 mM. The EC_{50} value of the NOR of MDEA, and no observed 50 % inhibition by AMP, DEA and piperazine are in contrast to previous results. The estimated EC_{50} values of AMP on biofilm previously exposed to amines was 31,6 mM and 30 mM (Skjæran, 2010, Hauser, 2011). Furthermore, the EC_{50} values of AMP, DEA and piperazine were reported with 18 mM, 39 mM and 10 mM, respectively (Hauser, 2011).

A reason for the varying EC_{50} values of AMP, DEA, MDEA and piperazine could again be found in the biofilm age and thereby the respectively thickness and/or a shift in the biofilm community as more resistant cultures could be developed and therefore showing a higher tolerance level. The result indicates that the new nitrifying biofilm has a higher tolerance towards an increased amine concentration compared to the old biofilm which were inhibited at relatively low concentrations of AMP, DEA, MDEA and piperazine.

The tolerance in amine concentration represented by the EC_{50} values for the AOR in ascending order: AMP (82 mM) < DEA (138 mM) < piperazine (190 mM) < MDEA (314 mM).

Recent studies of ecotoxicity and biodegradation on skeletonema and algae focusing on inhibiting growth in respect to the marine environment showed that AMP, MDEA and piperazine would have

long persistence due to their low biodegradability, whereas DEA and MEA were found to be higher degradable. In terms of the ecotoxicity, all five amines were above the lowest acceptable value (10mg/l) for a chemical to be released in the marine environment (Eide-Haugmo et al., 2009). The following EC₅₀ values in ascending order: AMP (119mg/l) < MDEA (141mg/l) < MEA (198 mg/l) < DEA (357mg/l) < piperazine (472mg/l). Comparing these values to the EC₅₀ values for AOR in this present work, the EC₅₀ values for AMP and MEA were relatively consistent. However, the EC₅₀ values for DEA and piperazine were much higher, except for the EC₅₀ value for MDEA which was higher in this present work.

In terms of recovery for the NOR of the acute toxicity of AMP, DEA, MDEA and piperazine, the result is not consistent with Hauser (Hauser, 2011), being 41 %, 27 %, 84 % and 17 %, versus 88 %, 122 %, 129 % and 144 % in this experiment, respectively. However, the recovery for the NOR of the acute toxicity of AMP is relatively consistent with the result of Skjæran (Skjæran, 2010), being 100 %, versus 88 % in this experiment. For the recovery of the AOR of the acute toxicity of AMP, DEA, MDEA and piperazine there are no previous studies to compare with.

4.2.2.3 Total dry weight

Based on the average weight and standard error of mean (SEM) of 49 empty Kaldnes K1 carriers, being 153±1 mg, the total dry weight of the biofilm, in mg, before and after the acute toxicity of MEA unloaded were determined. The total dry weight was also determined before and after the acute toxicity of AMP on the new biofilm. However, the result did not give any indication of abundance of the nitrifying culture. A source of error in this procedure may possible be the variety in the weight of the empty Kaldnes K1 carrier (from 132,2 mg to 168,5 mg).

4.3 Denitrification

4.3.1 Stabilization

Along the process of developing and stabilizing the denitrifying culture, there were some operational problems with pumps which had to be replaced. However the culture regained activity and reached a steady-state indicating that the denitrifying biofilm was robust and well developed. Previous studies by Hauser (Hauser, 2011) have shown that the denitrifying culture is much more robust and almost unaffected to the acute toxicity of the amines MEA, AMP, DEA, MDEA and piperazine, compared to the nitrifying culture which has shown a higher sensitivity. Therefore the biofilm was frozen on day 67 after inoculation.

5. Conclusions

The main purpose of this work was to investigate the feasibility of applying biological Nitrogen removal to remove the ammonia from the process water from a CO₂ capture plant based on amine absorption, where the main concern is the possible toxicity of the high amine content in the process water to the nitrifying bacteria culture.

This work was based on previous studies done by Colaço (Colaço, 2009), Skjæran (Skjæran, 2010) and Hauser (Hauser, 2011) to try to reproduce the results gained from the acute toxicity test with MEA, AMP, DEA, MDEA and piperazine on an old biofilm and comparing the results to a new nitrifying biofilm, previously not exposed to amines.

Since the main focus of this work was to test the acute toxicity on a freshly developed biofilm, two reactors were built with nitrification process running in one reactor and denitrification running in the other. Based on previous results showing that the nitrifying culture is the limiting factor, being more sensitive towards amines compared to the denitrifying culture (almost unaffected response), the toxicity testing was focused on the nitrifying culture.

5.1 Nitrification

5.1.1 Stabilization

The activity of the nitrifying culture stabilized around day 43 after the inoculation and a well adjusted nitrifying culture was obtained. All the NH₄⁺ was oxidized to NO₃⁻, indicating that the AOB and the NOB were equally developed.

5.1.2 Biofilm development

Because of the high COD values per Kaldnes K1 carriers, being (5182±238) mg/l, the gained COD per Kaldnes K1 carrier in the start-up phase in the nitrification culture could not be tracked. The high COD value per Kaldnes K1 carrier indicates interference on the COD kit from the polyethylene which the carriers are made of.

5.2 Inhibition of nitrification

5.2.1 Acute toxicity

A total of five amines have been tested for the acute toxicity on an old and a new nitrifying culture.

For acute toxicity on the previously tested nitrifying biofilm for MEA unloaded and MEA loaded the EC₅₀ values for the NOR were respectively 168 mM and 210 mM, and EC₅₀ values for the AOR were respectively 58 mM and 82 mM.

For acute toxicity on the new nitrifying biofilm for DEA, AMP and piperazine the activity never reached 50 %, except for MDEA the EC₅₀ values for the NOR was 80 mM. However, the EC₅₀ values for the AOR were for AMP, DEA, MDEA, and piperazine respectively 82 mM, 138 mM, 314 mM and 190 mM.

The recovery 30 hours after the acute toxicity for the biofilm previously tested was 88 % and 26 % for the NOR tested with respectively MEA unloaded and MEA loaded, and 65 % and 19 % for the AOR tested with respectively MEA unloaded and MEA loaded.

For the new biofilm had the NOR recovered 88 %, 122 %, 129 % and 144 % tested with respectively AMP, DEA, MDEA and piperazine. And the AOR had recovered 66 %, 82 %, 77 % and 61 % tested with respectively AMP, DEA, MDEA and piperazine.

Comparing the acute toxicity of MEA unloaded with the acute toxicity of the MEA loaded the affect on the nitrifying culture are relative similar, except for when comparing the percentage recovery, which showed that the MEA unloaded recovers faster than the MEA loaded.

Overall the EC₅₀ values for the AOR were less than the EC₅₀ values for the NOR (except for MDEA, which showed had a higher EC₅₀ value for the AOR), indicating that the AOR was more sensitive to lower concentrations during the acute toxicity than the NOR. The activity of the nitrifying process varied during the toxicity tests, but it did not stop.

The EC₅₀ values can be used as an indication on how much the reclaimer waste has to be diluted when using biological degradation of the effluent from amine based CCS.

5.2.1.1 Quantification of MEA with fluorescamine assay

The Fluorescamine assay was performed to quantify the concentration of MEA during the time course of the acute toxicity test with MEA unloaded and MEA loaded. The correlation between the measured and the theoretical MEA concentrations were relative good with R² value being 0,9982 for the MEA unloaded and 0,997 for the MEA loaded, indicating that there was no degradation of MEA during the time period of the acute toxicity test.

5.2.1.2 Total dry weight

The total dry weight found by weighing the Kaldnes K1 carriers before and after the acute toxicity and subtracting the average weight found per Kaldnes K1 carrier were not optimal and did not give any indication of bacterial abundance during the acute toxicity.

5.3 Future work

Suggestions for future work

- Optimize a procedure to follow the development of the biofilm on the Kaldnes K1 carriers, without detecting interference from the carrier itself. The chemical analyses with Hach-Lange assays should be further tested especially the LCK 114 COD. The chemical analyses with Hach-Lange assays should also be further tested to optimize the measurement of $\text{NH}_4^+\text{-N}$, $\text{NO}_3\text{-N}$ and $\text{NO}_2\text{-N}$, as unidentified compounds during the acute toxicity with amines leads to cross-interference with these assays.
- Before and after the acute toxicity of the amines the carriers were fixated for FISH analysis and frozen, these samples could be used to characterize and quantify the biofilm before and after the acute toxicity of selected amines. And possible state if the microbial community died or was inhibited by the acute toxicity.
- Analyze the difference between AOR and NOR since the AOR seem to be more sensitive than the NOR when the new developed nitrifying biofilm was exposed for acute toxicity.
- Analyze the difference in terms of the recovery after the acute toxicity of MEA unloaded and MEA loaded. The result in this present work indicated that the loaded MEA recover more poorly than unloaded MEA, 19 % and 65 % recovery respectively.
- Also, there should be carried out more acute toxicity tests on new developed biofilms to compare reproducibility and to find a correlation between age and thickness of the biofilm.

6. Bibliography

- AHN, Y.-H. 2006. Sustainable nitrogen elimination biotechnologies: A review. *Process Biochemistry*.
- AMAP 2011. Snow, Water, Ice and Permafrost in the Arctic (SWIPA).
- BARIBEAU, H., KOZYRA, M. K. & BEHNER, B. 2006. Microbiology and isolation of nitrifying bacteria.
- BELLONA. 2012. Available: <http://bellona.org/ccs/technology.html> [Accessed April 25th 2012].
- BP 2011. Energy outlook 2030.
- CHEN, S., LING, J. & BLANCHETON, J.-P. 2006. Nitrification kinetics of biofilm as affected by water quality factors. *Aquacultural Engineering*.
- CHERCHI, C., ONNIS-HAYDEN, A., EL-SHAWABKEH, I. & GU, A. Z. 2009. Implication of Using Different Carbon Sources for Denitrification in Wastewater Treatments. *Water Environment Research*, 81.
- COLAÇO, A. B. 2009. *Biological water treatment for removal of ammonia from process water in a CO₂-capture plant*. Master thesis, Instituto Superior Tecnico, Lisboa.
- DEPARTMENT OF COMMERCE, U. S. 2009. Available: <http://www.esrl.noaa.gov/gmd/ccgg/trends/mlo.html#mlo> [Accessed 6. March 2012].
- EIDE-HAUGMO, I. 2011. *Environmental impacts and aspects of absorbents used for CO₂ capture*. Doctoral thesis, Norwegian University of Science and Technology - Trondheim.
- EIDE-HAUGMO, I., BRAKSTAD, O. G., HOFF, K. A., SØRHEIM, K. R., DA SILVA, E. F. & SVENDSEN, H. F. 2009. Environmental impact of amines. *Energy Procedia*, 1, 1297-1304.
- HACH-LANGE 2011a. LCK 014. *Working procedure LCK 014 COD cuvette* 2011-08-11 ed. Hach-Lange homepage: Hach-Lange.
- HACH-LANGE 2011b. LCK 114. *Working procedure LCK 114 COD cuvette test* 2011-08-11 ed. Hach-Lange homepage: Hach Lange.

- HACH-LANGE 2011c. LCK 303. *Working procedure LCK 303 Ammonium-Nitrogen cuvette test* 2011-08-12 ed. Hach-Lange homepage: Hach-Lange.
- HACH-LANGE 2011d. LCK 341. *Working procedure LCK 341 Nitrite cuvette test* 2011-08-16 ed. Hach-Lange homepage: Hach-Lange.
- HACH-LANGE 2011e. LCK 342. *Working procedure LCK 342 Nitrite cuvette test* 2011-08-16 ed. Hach-Lange homepage: Hach-Lange.
- HACH-LANGE 2012. LCK 339. *Working procedure LCK 339 Nitrate cuvette test* 2012-01-31 ed. Hach-Lange homepage: Hach-Lange.
- HAUSER, I. 2011. *Biological treatment of process water of an amine based CO₂ - capture plant*. Master thesis.
- HENZE, M., HARREMOES, P., ARVIN, E. & JANSEN, J. L. C. 2002. *Wastwater Treatment: Biological and Chemical Processes*. Springer.
- IEA, I. E. A. 2011. CO₂ emissions from fuel combustion, highlights 134.
- IPCC 2007. *Climate Change 2007: Synthesis Report*. In: ALLALI, A., BOJARIU, R., DIAZ, S., ELGIZOULI, I., GRIGGS, D., HAWKINS, D., HOHMEYER, O., JALLOW, B. P., KAJFEZ4-BOGATAJ, L., LEARY, N., LEE, H. & WRATT, D. (eds.).
- LIE, E. 1996. *Limiting factors in biological nutrient removal from wastewater*. PhD, Lund University.
- OKABE, S., SATOH, H., ITO, T. & WATANABE, Y. 2004. Analysis of microbial community structure and in situ activity of nitrifying biofilms. *Journal of Water and Environmental Technology*.
- REHM, H.-J., REED, G. & WINTER, J. 1999. Nitrogen removal during wastewater treatment. *Environmental Processes*, 1.
- REYNOLDS, A. J., VERHEYEN, T. V., ADELOJU, S. B., MEULEMAN, E. & FERON, P. 2012. Towards Commercial Scale Postcombustion Capture of CO₂ with Monoethanolamine Solvent: Key Considerations for Solvent Management and Environmental Impacts. *Environmental Science and Technology*.
- RITTMAN, B. E. & MCCARTY, P. L. 2001. Nitrification. *Environmental biotechnology: principles and applications*, 470-506.

ROGNE, E. 2010. *Characterization of biofouling in membrane nanofiltration (NF) systems by molecular biological techniques*. Norwegian University of Science and Technology (NTNU).

RUSTEN, B., EIKEBROKK, B., ULGENES, Y. & LYGREN, E. 2006. Design and operations of kaldnes moving bed biofilm reactors. *Aquacultural Engineering*.

SHAO, R., STANGELAND, A. & BELLONA 2009. Amines Used in CO₂ Capture - Health and Environmental Impacts. 49.

SINTEF. 2011. *CO₂ Innfangingsprosesser* [Online]. Available: <http://www.sintef.no/Materialer-og-kjemi/Prosessteknologi/CO2-Fangst/> [Accessed April 25th 2012].

SKJÆRAN, J. A. 2010. *Biologisk nitrogenfjerning fra prosessvann fra et CO₂-innfangingsanlegg*. Master thesis.

ZHU, G., PENG, Y., LI, B., GUO, J., YANG, Q. & WANG, S. 2008. Biological Remocal of Nitrogen from Wastewater. *Rev Environ Contam Toxicol* 192:159-195.

ZUMFT, W. G. 1997. Cell biology and molecular basis of denitrification. *MICROBIOLOGY AND MOLECULAR BIOLOGY REVIEWS*, 61, 533-616.

Appendix A

Biofilm development - gained COD per Kaldnes K1 carrier

The results of measured COD [mg/l] per empty Kaldnes K1 carrier, were the error bars represent the standard error of the mean (SEM).

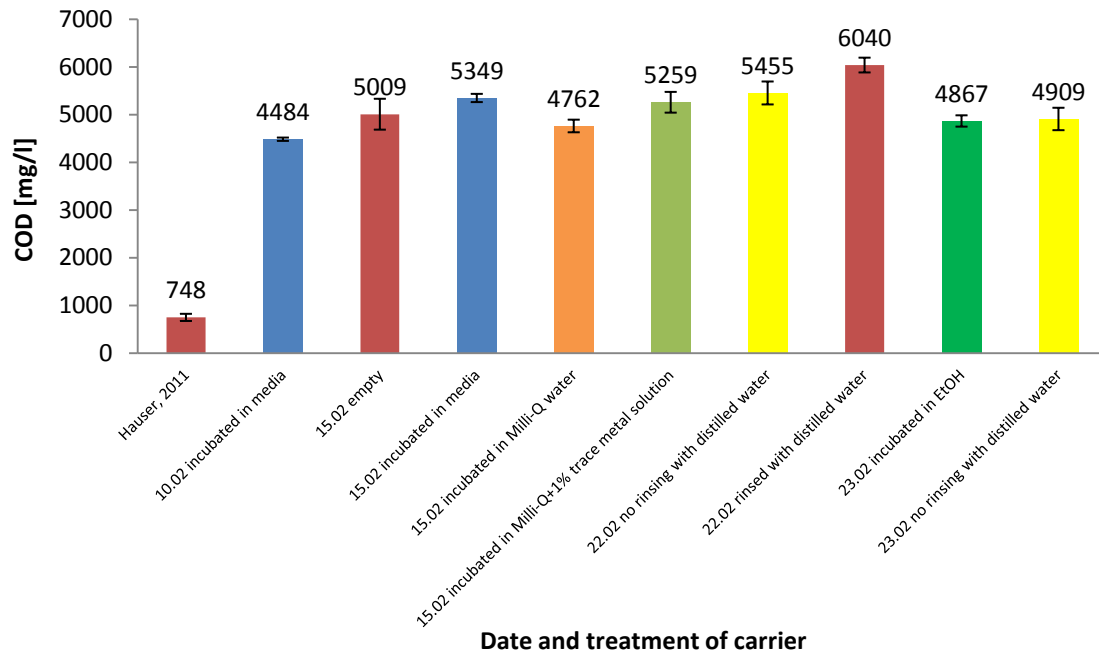


Figure A.1 The geometric mean of measured COD value per Kaldnes K1 carrier. The error bars represents the standard error of the mean (SEM).

Appendix B

State of the old biofilm and the new biofilm

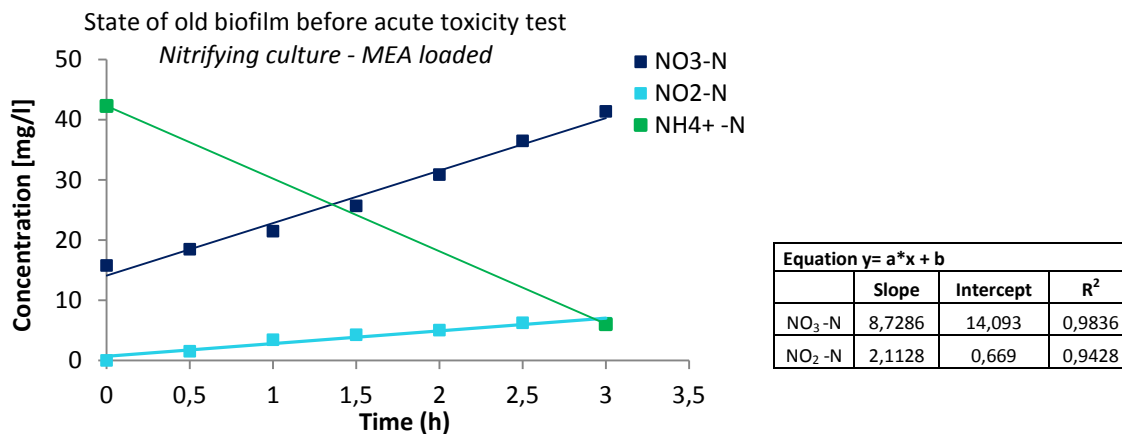


Figure B.1 The nitrification activity before the acute toxicity of loaded MEA on the nitrifying culture.

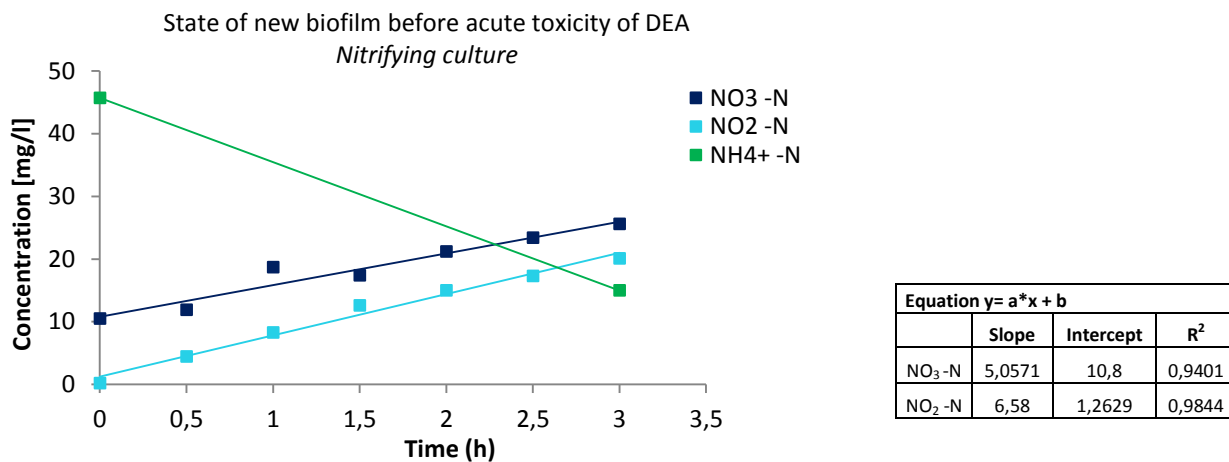


Figure B.2 The nitrification activity before the acute toxicity of DEA on the nitrifying culture.

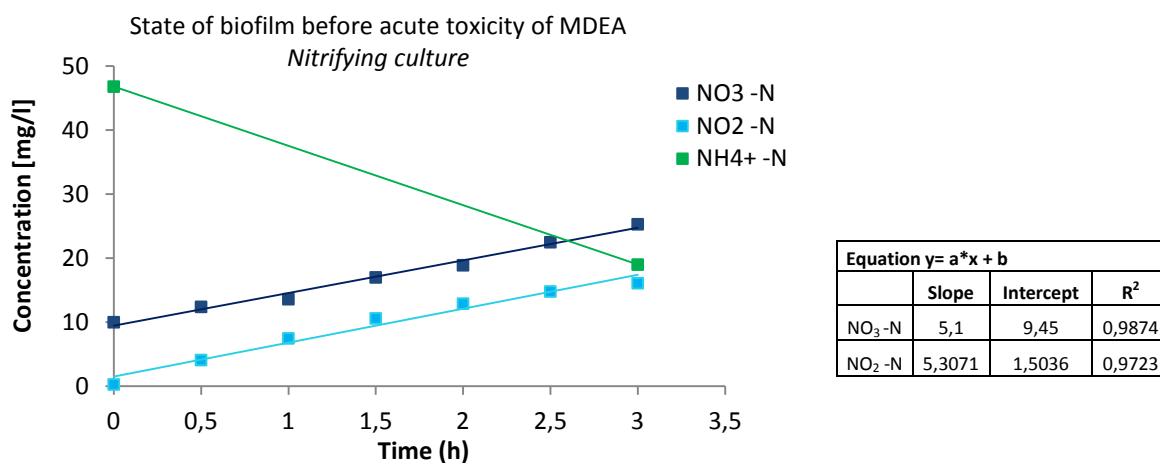


Figure B.3 The nitrification activity before the acute toxicity of MDEA on the nitrifying culture.

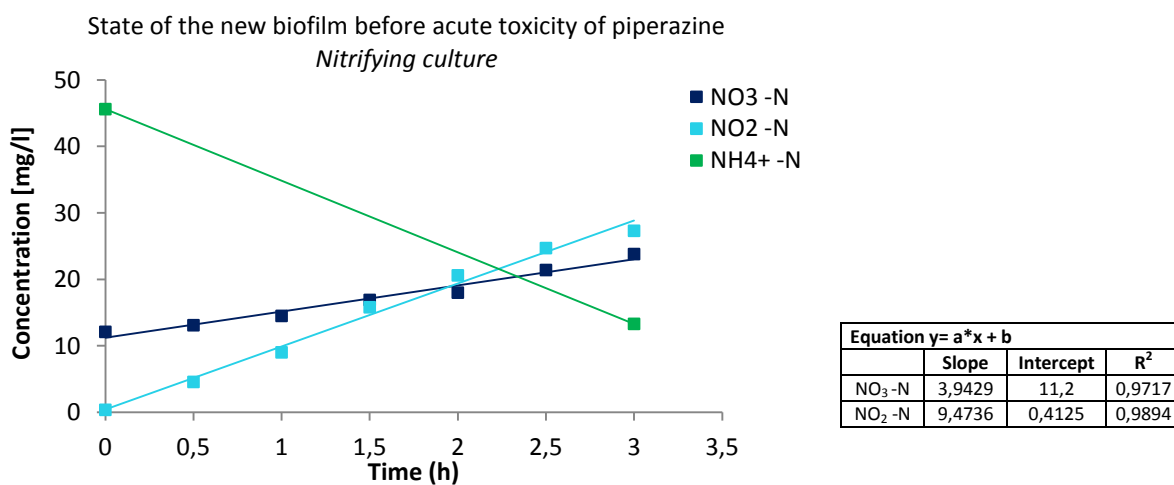


Figure B.4 The nitrification activity before the acute toxicity of piperazine on the nitrifying culture.

Appendix C

Acute toxicity test - Nitrifying culture

MEA unloaded – Experiment 1

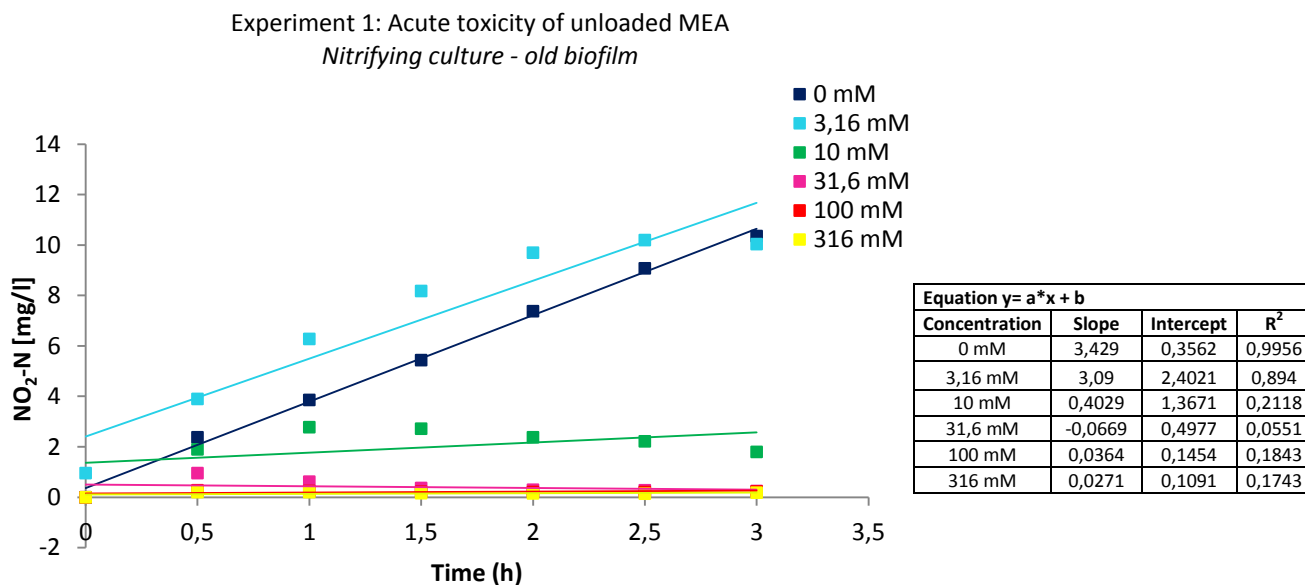


Figure C.1 The nitrification activity during the acute toxicity of MEA unloaded on the nitrifying culture represented as NO₂-N concentration.

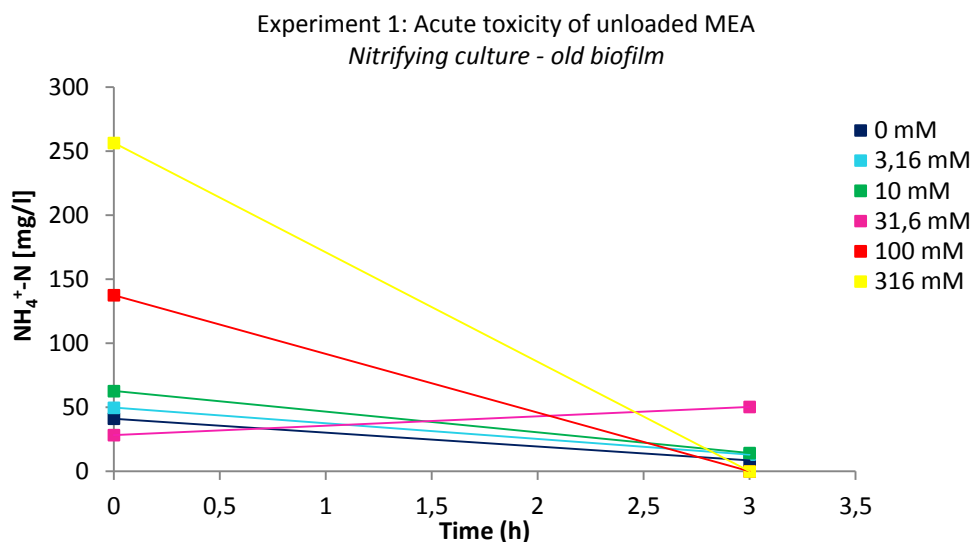


Figure C.2 The nitrification activity during the acute toxicity of MEA unloaded on the nitrifying culture represented as NH₄⁺-N concentration.

Experiment 1.1: Recovery of acute toxicity of unloaded MEA
Nitrifying culture - old biofilm

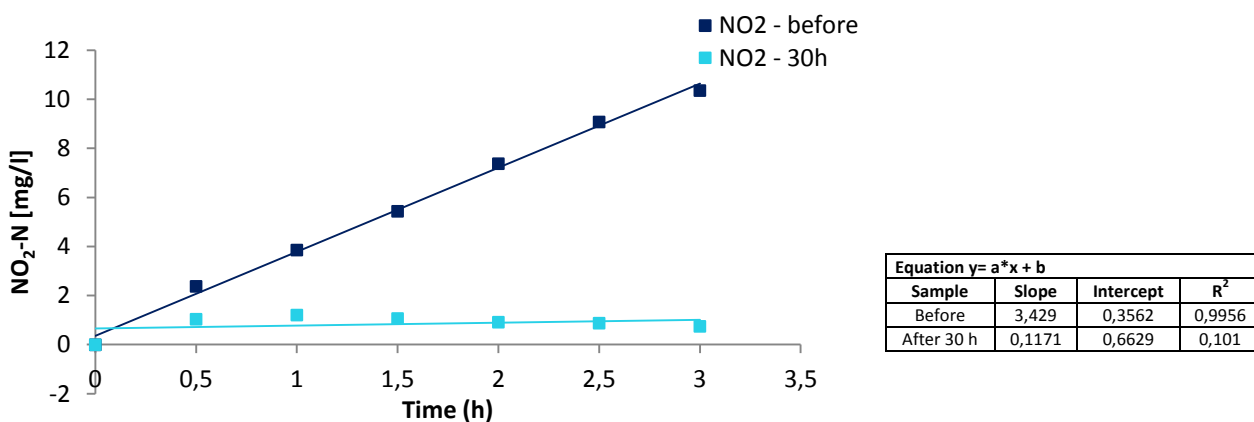


Figure C.3 The nitrification activity after 30 hours of recovery after the acute toxicity of MEA unloaded on the nitrifying culture represented as $\text{NO}_2\text{-N}$ concentration.

Experiment 1.1: Recovery of acute toxicity of unloaded MEA
Nitrifying culture - old biofilm

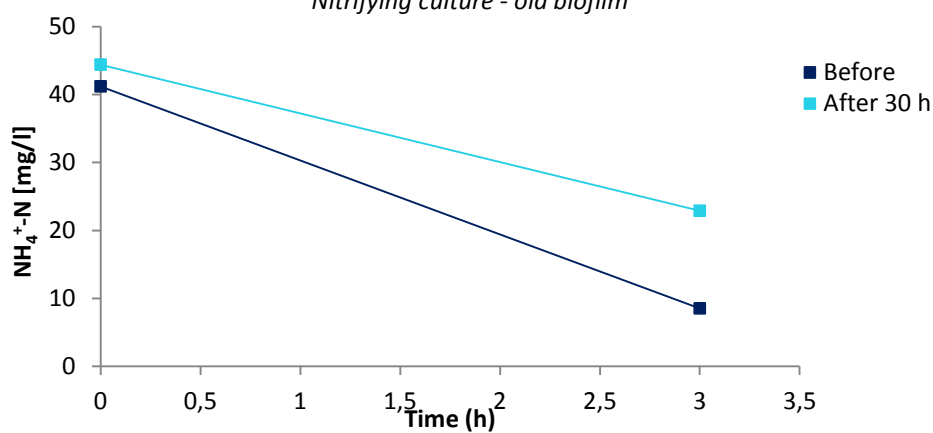


Figure C.4 The nitrification activity after 30 hours of recovery after the acute toxicity of MEA unloaded on the nitrifying culture represented as $\text{NH}_4^+\text{-N}$ concentration.

MEA loaded – Experiment 2

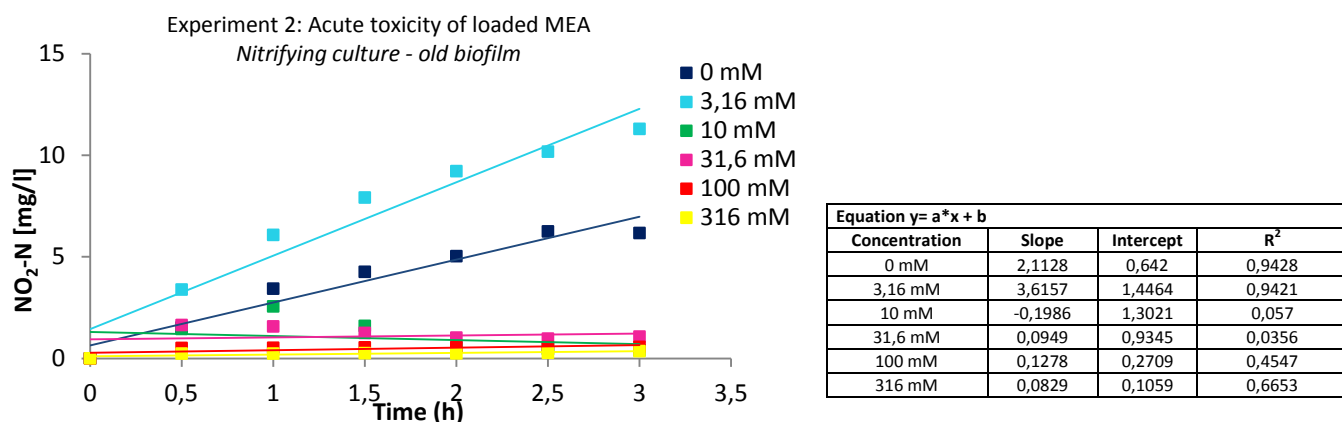


Figure C.5 The nitrification activity during the acute toxicity of MEA loaded on the nitrifying culture represented as NO₂-N concentration.

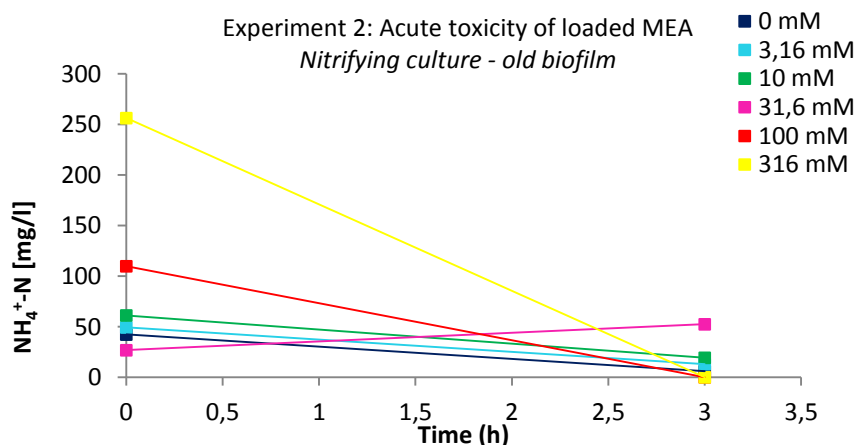


Figure C.6 The nitrification activity during the acute toxicity of MEA loaded on the nitrifying culture represented as NH₄⁺-N concentration.

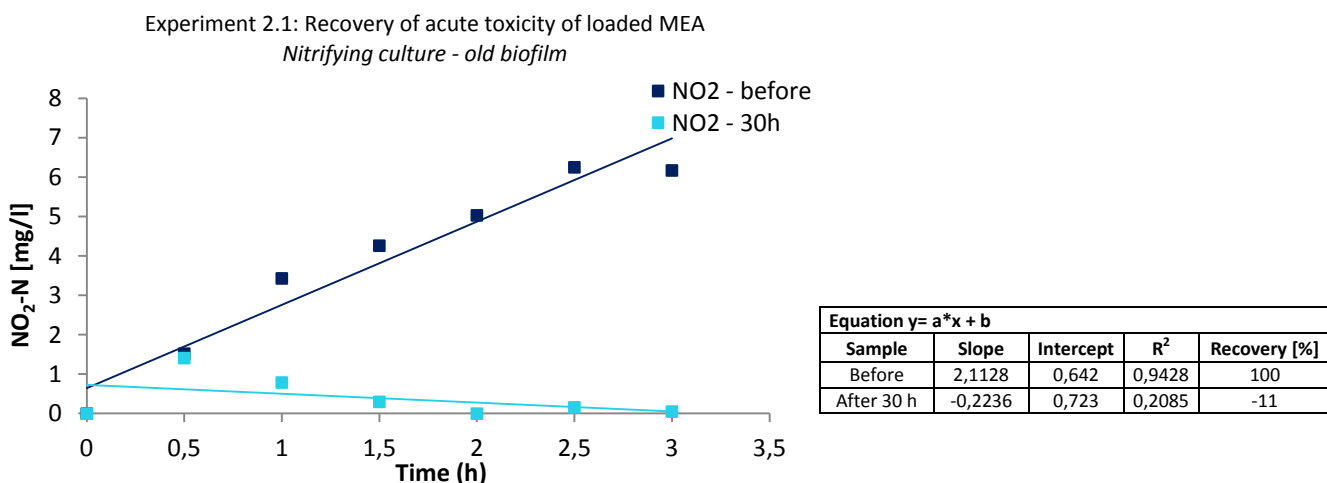


Figure C.7 The nitrification activity after 30 hours of recovery after the acute toxicity of MEA loaded on the nitrifying culture represented as NO₂-N concentration.

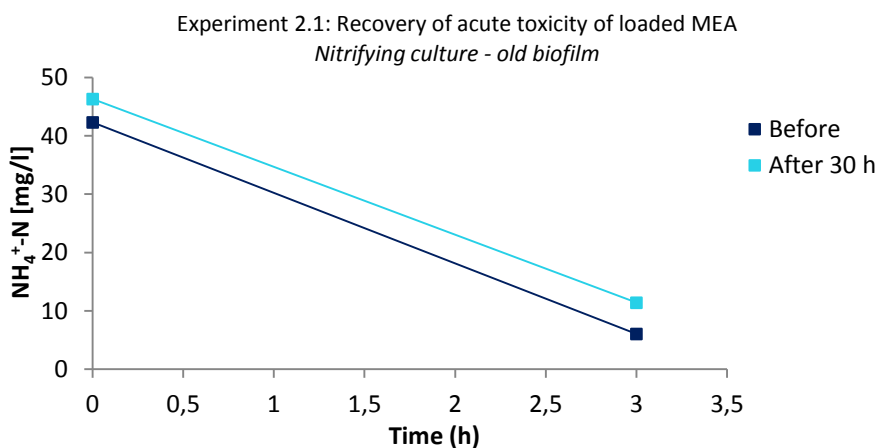


Figure C.8 The nitrification activity after 30 hours of recovery after the acute toxicity of MEA loaded on the nitrifying culture represented as NH₄⁺-N concentration.

AMP – Experiment 3

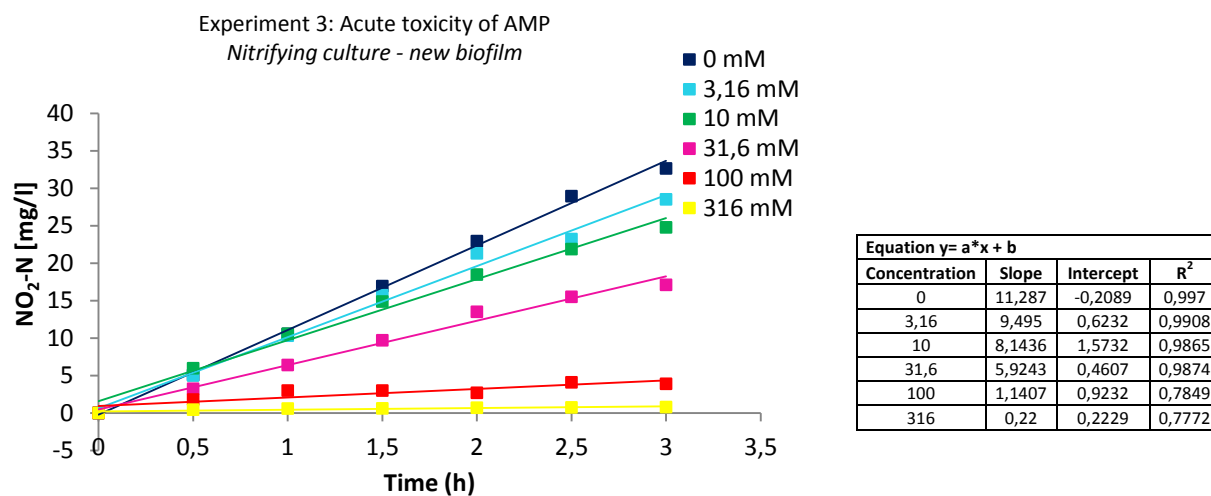


Figure C.9 The nitrification activity during the acute toxicity of AMP on the nitrifying culture represented as NO₂-N concentration.

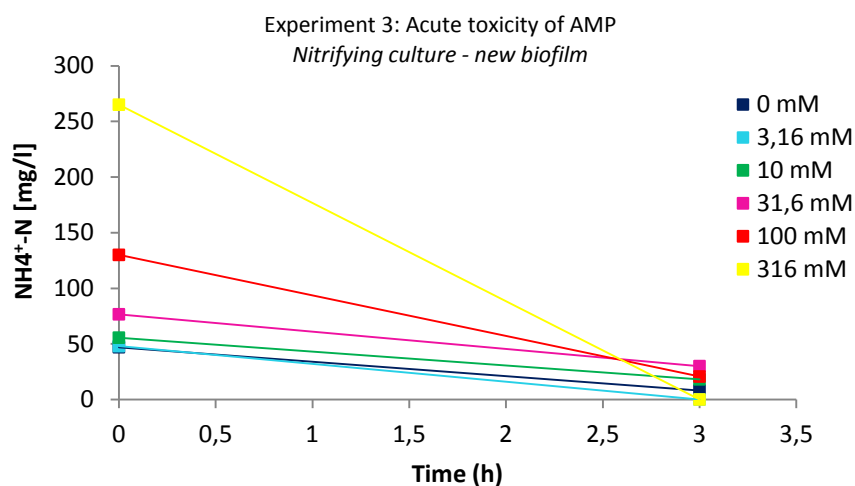


Figure C.10 The nitrification activity during the acute toxicity of AMP on the nitrifying culture represented as NH₄⁺-N concentration.

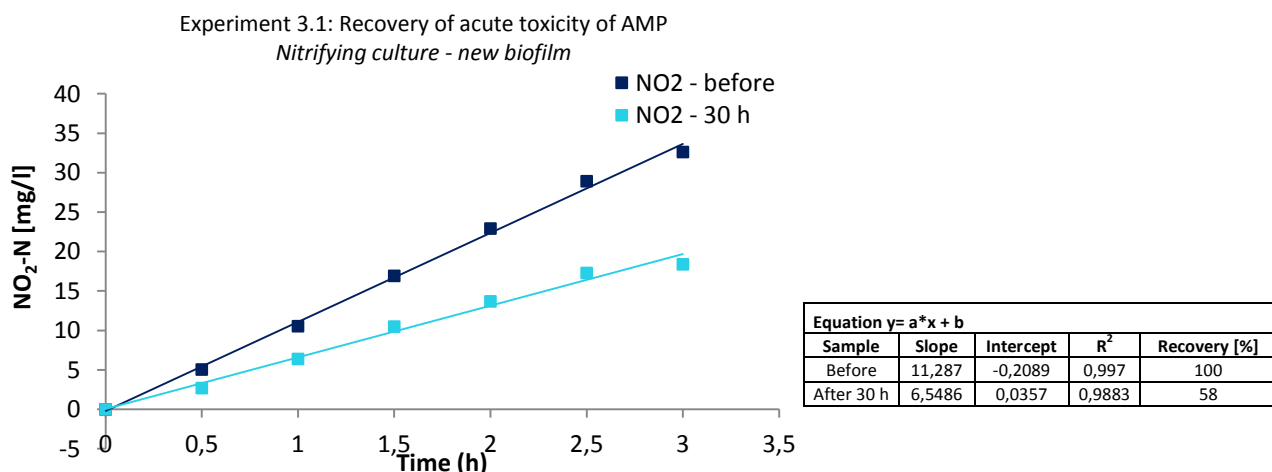


Figure C.11 The nitrification activity after 30 hours of recovery after the acute toxicity of AMP on the nitrifying culture represented as NO₂-N concentration.

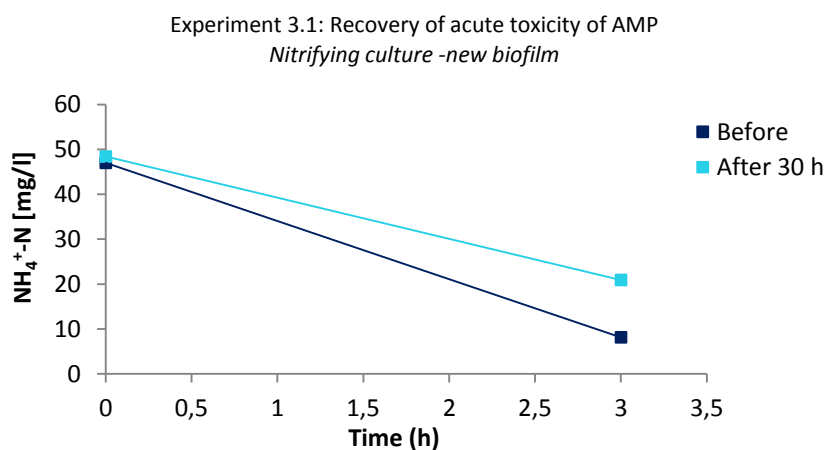


Figure C.12 The nitrification activity after 30 hours of recovery after the acute toxicity of AMP on the nitrifying culture represented as NH₄⁺-N concentration.

DEA – Experiment 4

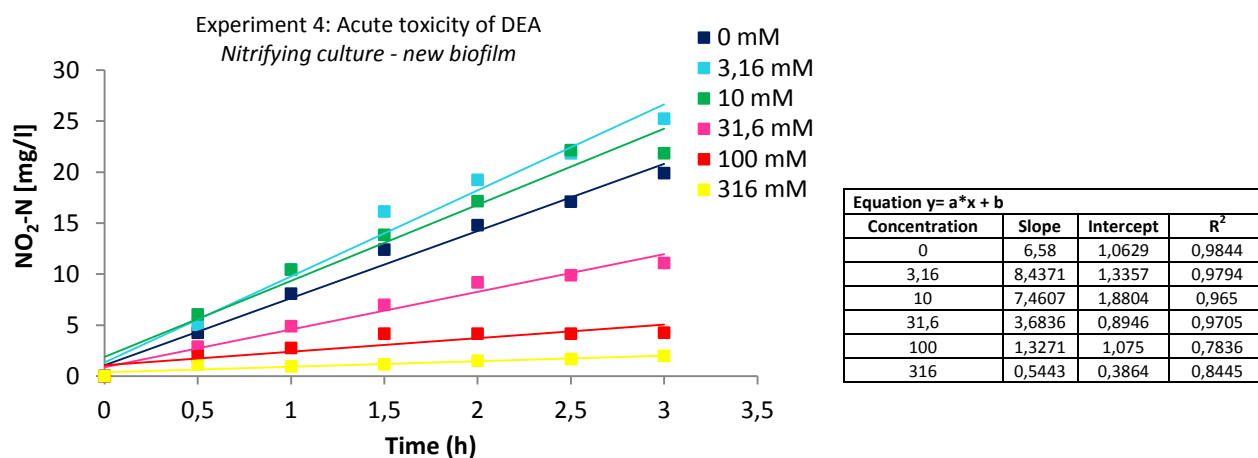


Figure C.13 The nitrification activity during the acute toxicity of DEA on the nitrifying culture represented as NO₂-N concentration.

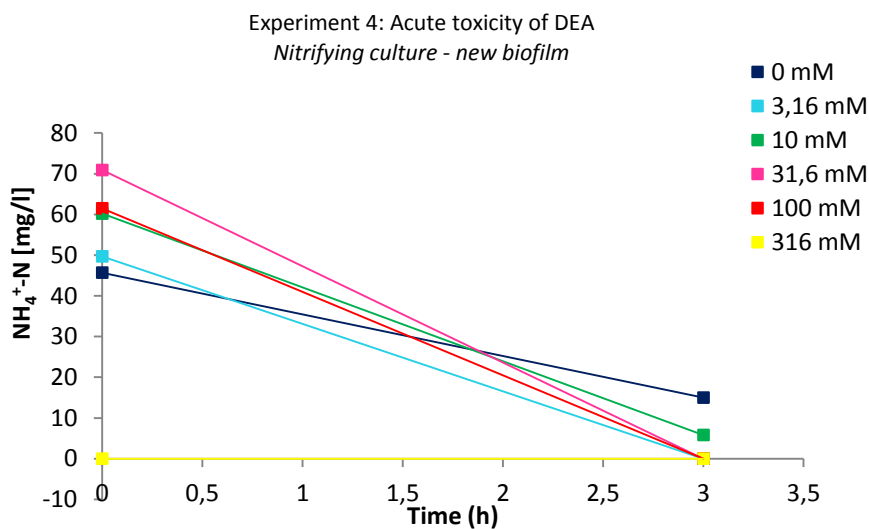


Figure C.14 The nitrification activity during the acute toxicity of DEA on the nitrifying culture represented as NH₄⁺-N concentration.

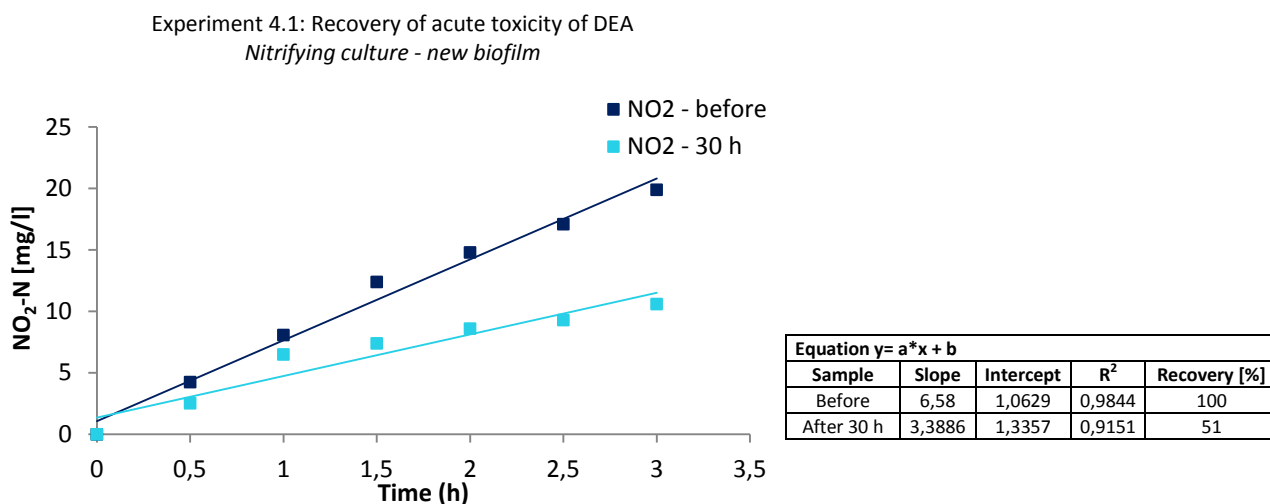


Figure C.15 The nitrification activity after 30 hours of recovery after the acute toxicity of DEA on the nitrifying culture represented as NO₂-N concentration.

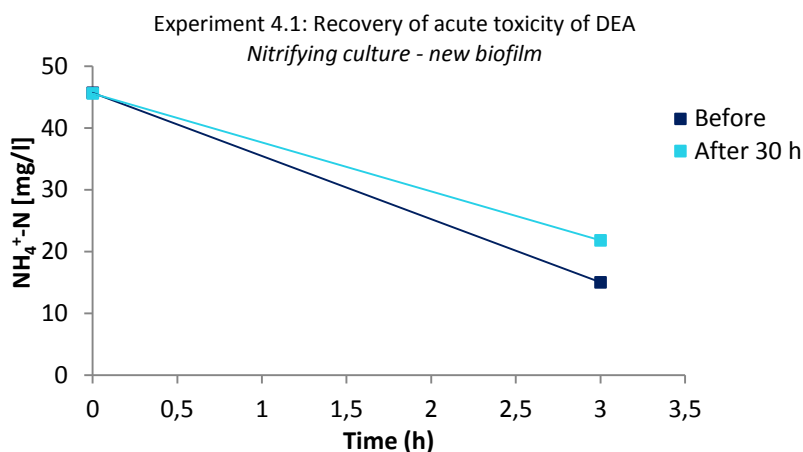


Figure C.16 The nitrification activity after 30 hours of recovery after the acute toxicity of DEA on the nitrifying culture represented as NH₄⁺-N concentration.

MDEA – Experiment 5

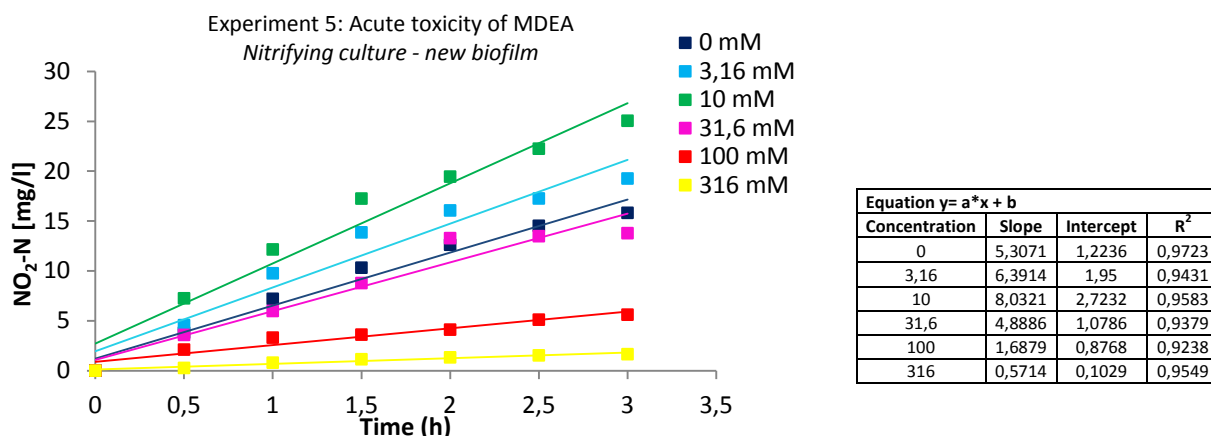


Figure 56 The nitrification activity during the acute toxicity of MDEA on the nitrifying culture represented as NO₂-N concentration.

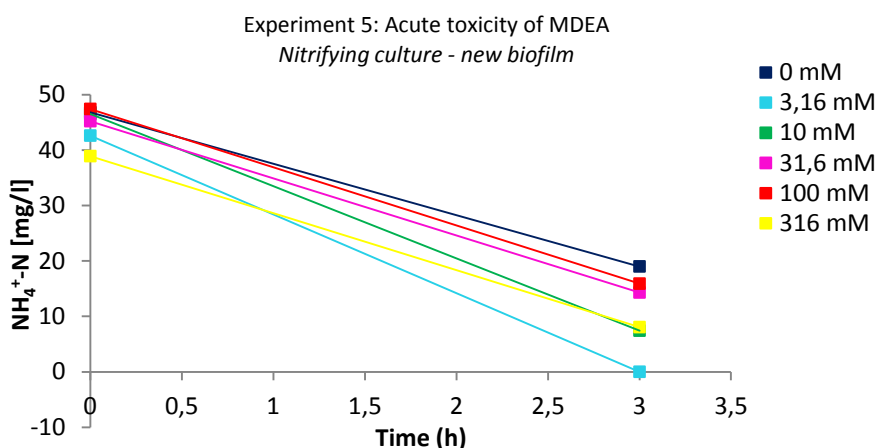


Figure C.18 The nitrification activity during the acute toxicity of MDEA on the nitrifying culture represented as NH₄⁺-N concentration.

Experiment 5.1: Recovery of acute toxicity of MDEA
Nitrifying culture - new biofilm

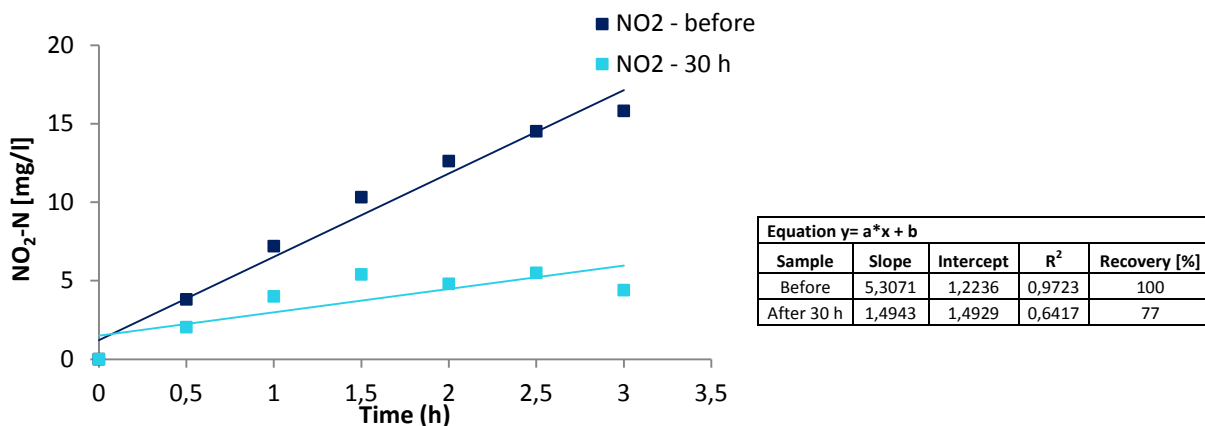


Figure C.19 The nitrification activity after 30 hours of recovery after the acute toxicity of MDEA on the nitrifying culture represented as NO₂-N concentration.

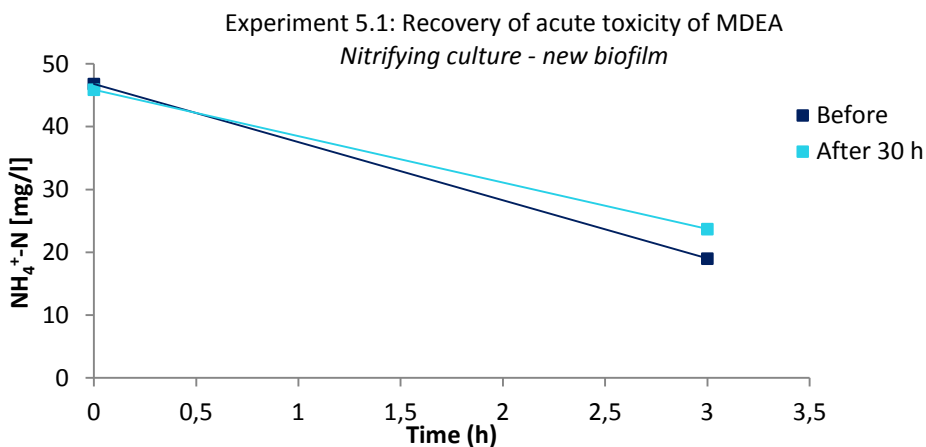


Figure C.20 The nitrification activity after 30 hours of recovery after the acute toxicity of MDEA on the nitrifying culture represented as NH₄⁺-N concentration.

Piperazine– Experiment 6

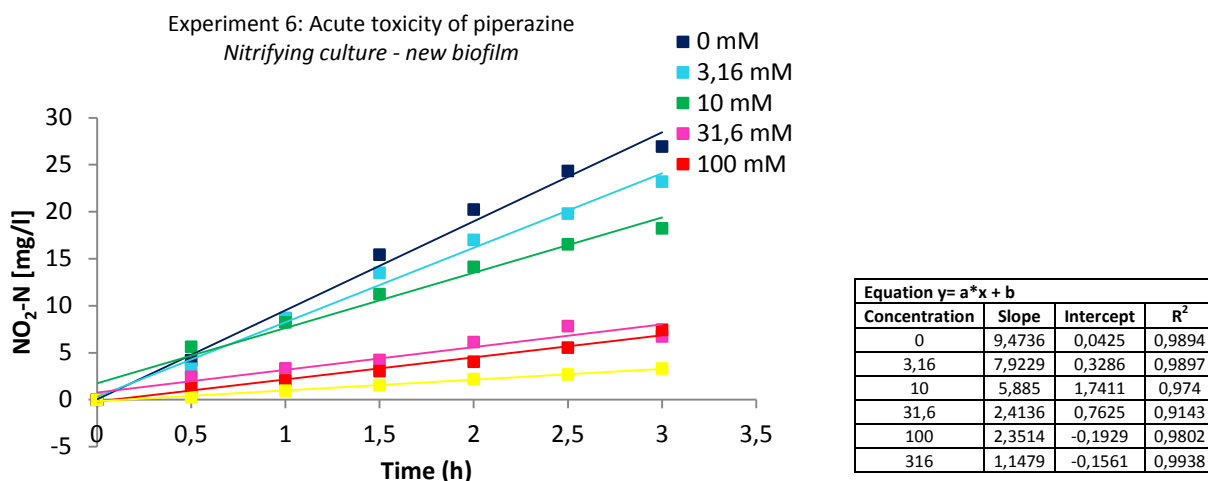


Figure C.21 The nitrification activity during the acute toxicity of piperazine on the nitrifying culture represented as NO₂-N concentration.

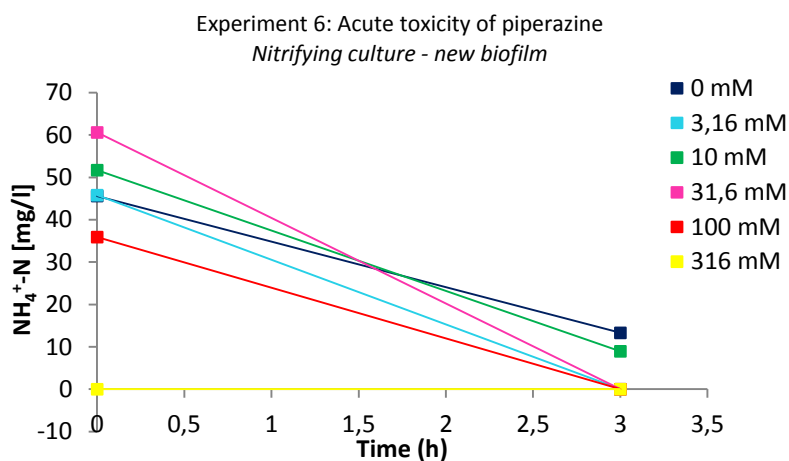


Figure C.22 The nitrification activity during the acute toxicity of piperazine on the nitrifying culture represented as NH₄⁺-N concentration.

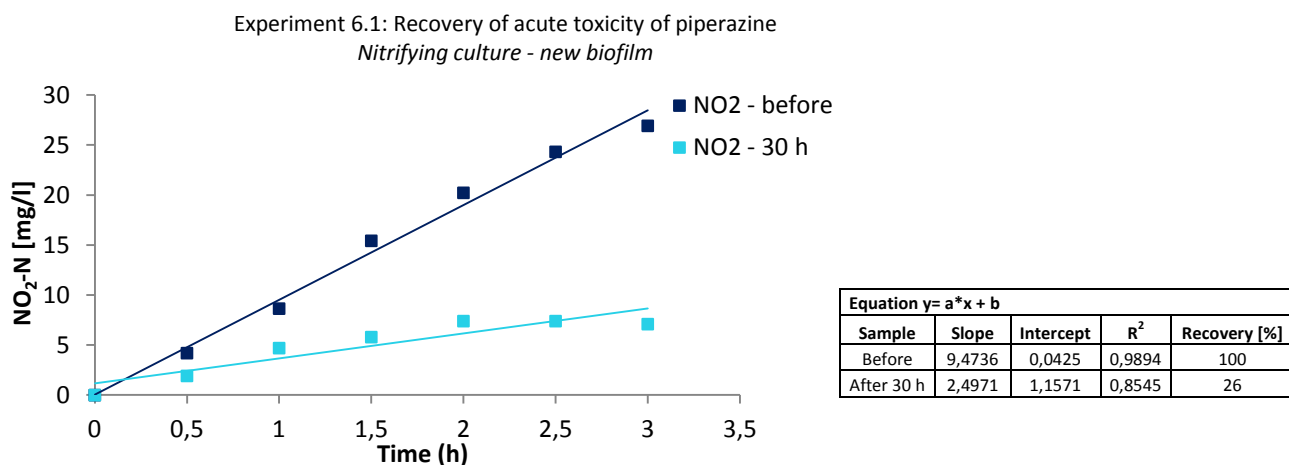


Figure C.23 The nitrification activity after 30 hours of recovery after the acute toxicity of piperazine on the nitrifying culture represented as NO₂-N concentration.

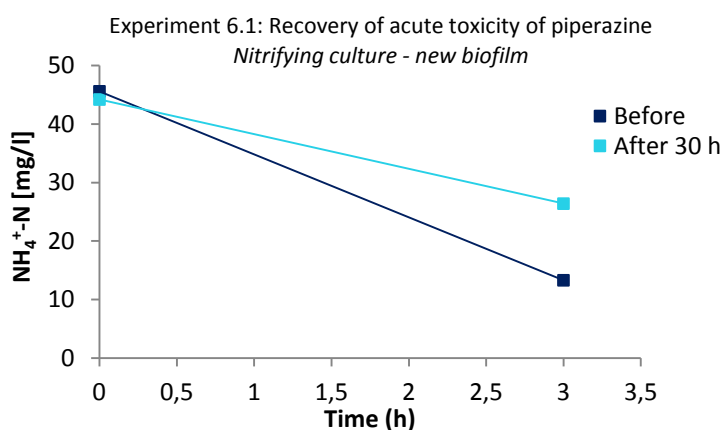


Figure C.24 The nitrification activity after 30 hours of recovery after the acute toxicity of piperazine on the nitrifying culture represented as NH₄⁺-N concentration.

Appendix D

Mass balance

- During the acute toxicity of MEA unloaded, MEA loaded, AMP, DEA, MDEA and piperazine.

Table D.1 Mass balance for the acute toxicity of MEA unloaded.

Concentration	N _{initial} (NH ₄ ⁺ --> NO ₂ ⁻ --> NO ₃ ⁻)				N _{out} (NH ₄ ⁺ --> NO ₂ ⁻ --> NO ₃ ⁻)				Δ	Recovery (%)
	NH ₄ ⁺	NO ₂ ⁻	NO ₃ ⁻	Σ N _{initial}	NH ₄ ⁺	NO ₂ ⁻	NO ₃ ⁻	Σ N _{out}		
0 mM	41,2	17,8	0,038	59	8,54	10,4	46,1	65	-6	110
3,16 mM	49,7	0,1	4,41	54	13,2	10,2	25,300	49	5	90
10 mM	62,7	0,94	3,87	68	14,4	2,7	29,90	47	20	70
31,6 mM	28,4	0,2	3,020	32	50,4	0,4	24,50	75	-44	238
100 mM	137,6	0,03	1,300	139	0	0,3	20,30	21	118	15
316 mM	256,4	0,027	0,903	257	256,4	0,21	9,03	266	-8	103
Recovery	44,4	0	4,09	48	22,9	0,75	28,9	53	-4	108

Table D.2 Mass balance for the acute toxicity of MEA loaded.

Concentration	N _{initial} (NH ₄ ⁺ --> NO ₂ ⁻ --> NO ₃ ⁻)				N _{out} (NH ₄ ⁺ --> NO ₂ ⁻ --> NO ₃ ⁻)				Δ	Recovery (%)
	NH ₄ ⁺	NO ₂ ⁻	NO ₃ ⁻	Σ N _{initial}	NH ₄ ⁺	NO ₂ ⁻	NO ₃ ⁻	Σ N _{out}		
0 mM	42,3	0,0	15,8	58	6,05	6,2	41,4	54	4	92
3,16 mM	49,3	0,48	2,91	53	13,0	11,8	23,10	48	5	91
10 mM	61,2	1,4	2,9	66	19,3	1,8	1,82	23	43	35
31,6 mM	26,8	0,2	1,9	29	52,4	1,2	23,40	77	-48	267
100 mM	109,9	0,097	1,3	111	0	0,7	16,30	17	94	15
316 mM	256,4	0,053	0,911	257	0	0,41	11,3	12	246	5
Recovery	46,3	0	4,39	51	11,4	0,053	11,7	23	28	46

Table D.3 Mass balance for the acute toxicity of AMP.

Concentration	N _{initial} (NH ₄ ⁺ --> NO ₂ ⁻ --> NO ₃ ⁻)				N _{out} (NH ₄ ⁺ --> NO ₂ ⁻ --> NO ₃ ⁻)				Δ	Recovery (%)
	NH ₄ ⁺	NO ₂ ⁻	NO ₃ ⁻	Σ N _{initial}	NH ₄ ⁺	NO ₂ ⁻	NO ₃ ⁻	Σ N _{out}		
0 mM	47	0,1	11,300	58	8,13	32,7	25,4	66	-8	113
3,16 mM	48	2,2	8,62	59	0	30,7	16,700	47	11	81
10 mM	55,6	0,23	1,28	57	18,1	25,0	16,80	60	-3	105
31,6 mM	76,6	2,5	1,810	81	30	19,6	18,0	68	13	84
100 mM	130	1,51	1,490	133	20,8	5,4	18,30	45	89	33
316 mM	265	0,42	0,943	266	0	1,21	17,2	18	248	7
Recovery	48,4	0	6,01	54	20,9	18,4	16,4	56	-1	102

Table D.4 Mass balance for the acute toxicity of DEA.

Concentration	$N_{\text{initial}} (\text{NH}_4^+ \rightarrow \text{NO}_2^- \rightarrow \text{NO}_3^-)$				$N_{\text{out}} (\text{NH}_4^+ \rightarrow \text{NO}_2^- \rightarrow \text{NO}_3^-)$				Δ	Recovery (%)
	NH_4^+	NO_2^-	NO_3^-	$\Sigma N_{\text{initial}}$	NH_4^+	NO_2^-	NO_3^-	ΣN_{out}		
0 mM	46,8	0,3	10,000	57	19	16,1	25,3	60	-3	106
3,16 mM	42,6	1,3	4,37	48	0	20,6	18,4	39	9	81
10 mM	46,5	0,15	1,64	48	7,42	25,2	22,7	55	-7	115
31,6 mM	45,2	2,1	1,90	49	14,3	15,9	20,2	50	-1	102
100 mM	47,4	0,99	1,09	49	15,9	6,6	19,3	42	8	84
316 mM	38,9	0,5	0,892	40	8,06	2,15	15,4	26	15	64
Recovery	45,9	0	2,55	48	23,7	4,4	21,6	50	-1	103

Table D.5 Mass balance for the acute toxicity of MDEA.

Concentration	$N_{\text{initial}} (\text{NH}_4^+ \rightarrow \text{NO}_2^- \rightarrow \text{NO}_3^-)$				$N_{\text{out}} (\text{NH}_4^+ \rightarrow \text{NO}_2^- \rightarrow \text{NO}_3^-)$				Δ	Recovery (%)
	NH_4^+	NO_2^-	NO_3^-	$\Sigma N_{\text{initial}}$	NH_4^+	NO_2^-	NO_3^-	ΣN_{out}		
0 mM	45,7	0,2	10,500	56	15	20,1	25,6	61	-4	108
3,16 mM	49,7	1,7	4,17	56	0	26,9	17,200	44	11	79
10 mM	60,2	0,15	1,19	62	5,82	22,0	17,40	45	16	73
31,6 mM	70,9	1,6	1,560	74	0	12,7	20,40	33	41	45
100 mM	51,5	0,94	1,720	54	0,0	5,2	19,30	25	30	45
316 mM	0,0	0,57	1,46	2	0	2,56	18,9	21	-19	1057
Recovery	45,6	0	2,62	48	21,8	10,6	21,5	54	-6	112

Table D.6 Mass balance for the acute toxicity of piperazine.

Concentration	$N_{\text{initial}} (\text{NH}_4^+ \rightarrow \text{NO}_2^- \rightarrow \text{NO}_3^-)$				$N_{\text{out}} (\text{NH}_4^+ \rightarrow \text{NO}_2^- \rightarrow \text{NO}_3^-)$				Δ	Recovery (%)
	NH_4^+	NO_2^-	NO_3^-	$\Sigma N_{\text{initial}}$	NH_4^+	NO_2^-	NO_3^-	ΣN_{out}		
0 mM	45,6	0,4	12,100	58	13,3	27,3	23,8	64	-6	111
3,16 mM	45,8	2,5	5,78	54	0	25,7	16,3	42	12	78
10 mM	51,7	0,17	1,52	53	8,95	18,4	16,4	44	10	82
31,6 mM	60,6	1,17	1,28	63	0	7,9	19,0	27	36	43
100 mM	35,9	0,46	0,765	37	0,0	7,9	18,6	27	11	71
316 mM	0	0,43	1,120	2	0	3,75	16,3	20	-19	1294
Recovery	44,2	0	3,40	48	26,4	7,1	19,3	53	-5	111

Appendix E

Calibration curve

- Quantification of MEA with Fluorescamine assay

Table E.1 Measured intensities of the calibration curve of fluorescamine assay in five parallels, the concentrations being 0, 0.2, 0.4, 0.6, 0.8 and 1.0 mM, and calculated average and standard deviation of the five parallels.

MEA [mM]	Parallell 1	Parallell 2	Parallell 3	Parallell 4	Parallell 5	Average	SD
0	5,994	4,957	5,964	6,207	4,881	5,6	0,63
0,2	51,210	56,561	53,348	57,207	66,278	56,9	5,77
0,4	119,322	83,383	100,213	129,072	103,44	107,1	17,72
0,6	163,577	165,808	174,083	141,363	156,653	160,3	12,28
0,8	215,867	218,157	181,858	215,918	196,904	205,7	15,88
1	269,612	282,654	289,751	240,748	262,676	269,1	19,08

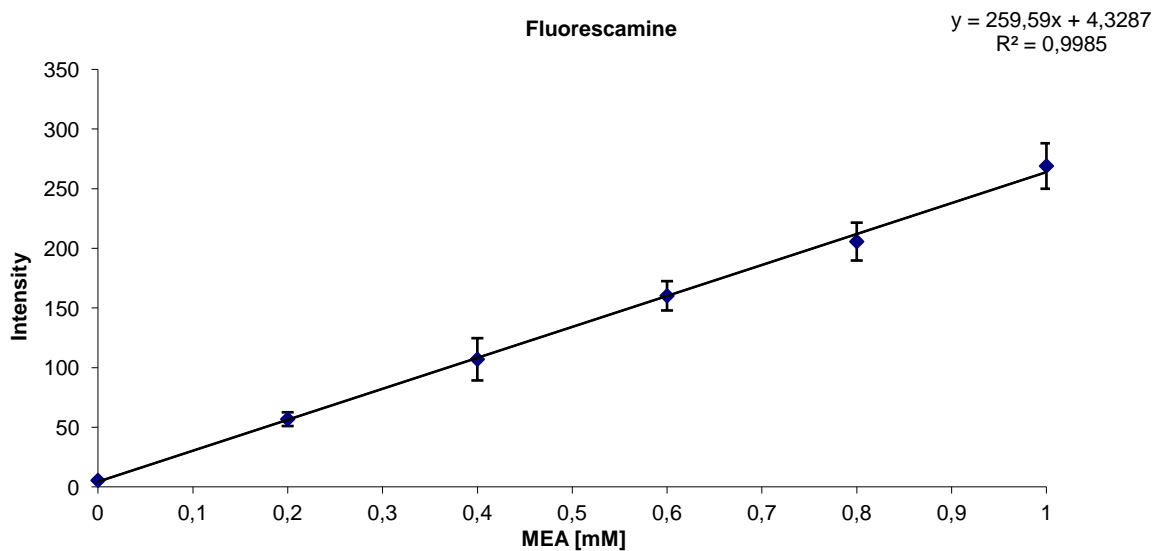


Figure E.1 Calibration curve, concentration of MEA [mM] plotted against measured intensity.